

INTEGER SUPERHARMONIC MATRICES ON THE F -LATTICE

AHMED BOU-RABEE

ABSTRACT. We prove that the set of quadratic growths achievable by integer superharmonic functions on the F -lattice, a periodic subgraph of \mathbb{Z}^2 with oriented edges, has the structure of an overlapping circle packing. The proof recursively constructs a distinct pair of recurrent functions for each rational point on a hyperbola. This resolves a conjecture of Smart (2013) and characterizes the scaling limit of the Abelian sandpile on the F -lattice.

1. INTRODUCTION

The F -lattice is a directed, periodic, planar graph (\mathbb{Z}^2, E) , where

$$\begin{cases} (x \pm e_1, x) \in E & \text{if } x_1 + x_2 \pmod{2} = 0 \\ (x \pm e_2, x) \in E & \text{otherwise ,} \end{cases}$$

and e_1, e_2 are the standard basis vectors in \mathbb{Z}^2 . A function $g : \mathbb{Z}^2 \rightarrow \mathbb{Z}$ is *integer superharmonic* if

$$(1) \quad \Delta g(x) := \sum_{(y,x) \in E} (g(y) - g(x)) \leq 0,$$

for all $x \in \mathbb{Z}^2$. Let S_2 denote the set of 2×2 symmetric matrices. The *quadratic growth* of g is specified by $A \in S_2$,

$$(2) \quad g(x) = \frac{1}{2}x \cdot Ax + o(1 + |x|^2).$$

When g is integer superharmonic and has quadratic growth A , we say that it is an *integer superharmonic representative* of A and A is an *integer superharmonic matrix*. Moreover, g is *recurrent* if whenever $f : \mathbb{Z}^2 \rightarrow \mathbb{Z}$ is integer superharmonic and $X \subset \mathbb{Z}^2$ is finite and strongly connected (with respect to E),

$$(3) \quad \sup_X (g - f) \leq \sup_{\partial X} (g - f),$$

where $\partial X = \{y \in \mathbb{Z}^2 : \text{there is } x \in X \text{ with } (y, x) \in E\}$. We call an integer superharmonic representative of A which is recurrent an *odometer* for A .

In this article we demonstrate an explicit characterization of integer superharmonic matrices on the F -lattice via a recursive construction of their odometers.

1.1. Background. Any periodic Euclidean directed graph, (V, E) , defines a set of integer superharmonic matrices. The study of these matrices was initiated by Pegden and Smart [PS13] in the context of the Abelian sandpile model of Bak, Tang and Wiesenfeld and Dhar [BTW87, Dha90]. We briefly describe the model, referring the interested reader to the surveys [Red05, HLM⁺08, Jár18] and books [Kli18, CP18].

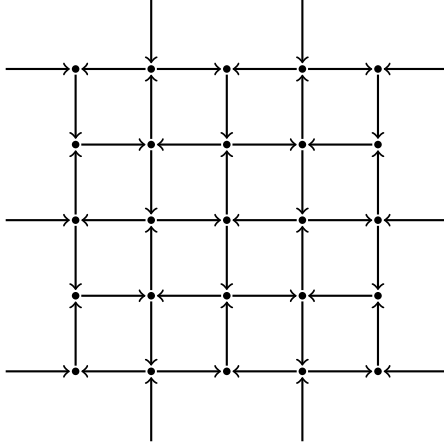


FIGURE 1. A 5×5 section of the F -lattice

The Abelian sandpile is a diffusion process on (V, E) , of which the following, the *single-source sandpile*, is a canonical example. Start with n chips at the origin (or the closest point to the origin) in V . When a vertex has at least as many chips as outgoing edges, it topples, sending one chip along each outgoing edge. When n is large, the final configuration of chips, $s_n : V \rightarrow \mathbb{Z}$, displays fascinating fractal structure. Pegden-Smart made it possible to study this structure by showing that s_n converges weakly-* to a limiting $s : \mathbb{R}^d \rightarrow \mathbb{R}$ which is described by the solution to a certain nonlinear partial differentiable equation, later called the *sandpile PDE*.

The sandpile PDE is characterized by the set of integer superharmonic matrices on (V, E) ; in particular, the fractal structure of large sandpiles is dependent on the graph upon which the sandpile is run. In a tour de force, Levine, Pegden, and Smart showed that the set of integer superharmonic matrices on the square lattice, \mathbb{Z}^2 with nearest neighbor edges, is the downwards closure of an Apollonian circle packing [LPS17]. This led to an understanding of the fractal patterns appearing in sandpile experiments, [LPS16, PS20], something which had evaded physicists and mathematicians for decades [LKG90, LBR02, Ost03].

Levine-Pegden-Smart's proof in [LPS17] involved explicitly constructing an odometer for each circle in an Apollonian band packing. Their construction mirrored the Soddy recursive generation of Apollonian circle packings - it pieced together later odometers from earlier ones. Our strategy in this article is similar but with several key differences which we detail in Section 2.

The patterns which appear in s_n on the F -lattice have also been investigated by mathematical physicists with notable contributions made by Caracciolo, Paoletti, and Sportiello [CPS08, Pao12] and Dhar, Sadhu, Chandra [DSC09, DS13, DS10, DS11]. This article provides a new perspective on their results. For example, the patterns which appear in their experiments correspond empirically to the Laplacians of our constructed odometers. In fact, an immediate consequence of Theorems 1.1 and 1.2 is that the weak-* limit of the sandpile identity on ellipsoidal domains is constant [Mel20]. We leave open, but expect that these results can also be used to construct more elaborate sandpile fractals as in [LPS16]. Moreover, it is a difficult open problem to construct the weak-* limit of the single-source sandpile on the square lattice. It would be interesting to see if the relatively simple structure of the sandpile PDE here can be used to make progress on this for the F -lattice.

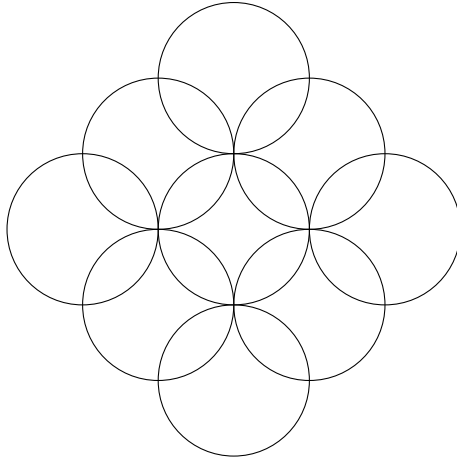


FIGURE 2. A few periods of the bases of cones in $\partial\Gamma_F$.

1.2. Main results. Our primary result is that the set of integer superharmonic matrices on the F -lattice is the downwards closure of an overlapping circle packing.

Theorem 1.1. *A $\in S_2$ is integer superharmonic if and only if the difference*

$$\frac{1}{2} \begin{bmatrix} s-t & s+t \\ s+t & t-s \end{bmatrix} - A$$

is positive semidefinite for some $s, t \in \mathbb{Z}$.

We explain the connection to circles. Denote the set of integer superharmonic matrices on the F -lattice by Γ_F . The boundary of Γ_F may be viewed as a surface by taking the parameterization $M : S_2 \rightarrow \mathbb{R}^3$,

$$M(a, b, c) := \frac{1}{2} \begin{bmatrix} c+a & b \\ b & c-a \end{bmatrix}.$$

In particular, Theorem 1.1 may be restated as

$$\partial\Gamma_F = \{M(a, b, \gamma_F(a, b)) : (a, b) \in \mathbb{R}^2\},$$

where

$$(4) \quad \gamma(x)_F := \max_{s,t \in \mathbb{Z}} -|x - (s-t, s+t)|.$$

Viewed from above, $\partial\Gamma_F$ is the union of identical slope-1 cones whose bases are the overlapping circle packing displayed in Figure 2.

One may check that the matrices, $M(s-t, s+t, 0)$ lie on $\partial\Gamma_F$ for all $s, t \in \mathbb{Z}$ (see Section 1.3 for the data to do so in a more general setting). This together with the downwards closure of Γ_F reduces the proof of Theorem 1.1 to verifying that the intersection curve of each pair of overlapping cones is in $\partial\Gamma_F$. Moreover, by symmetry, it suffices to check only one such hyperbola. Smart made these observations in [Sma13] and then conjectured the following, which we prove.

Theorem 1.2. *For each $0 \leq t \leq 1$, $M(t, 1-t, -\sqrt{t^2 + (1-t)^2})$ lies on the boundary of Γ_F .*



FIGURE 3. The first three iterations of the hyperbola recursion defined in Section 3. The two visible hyperbolas are outlined by dashed lines.

The set Γ_F is closed (Lemma 3.4 in [LPS17]), therefore, it suffices to prove Theorem 1.2 for all rational $0 \leq t \leq 1$ along the bottom branch of the hyperbola $\mathcal{H} := \{(t, c) \in \mathbb{R} \times \mathbb{R}^- : t^2 + (1-t)^2 = c^2\}$. We do this recursively. We start with explicit formulas for the odometers for $(0, -1)$ and $(1, -1)$ and then use those to construct odometers for all other rational points in between. Surprisingly, the recursion requires building not just one odometer for each such rational t , but *two* distinct odometers. This is a significant difference between the square lattice case which builds one odometer at a time; the square lattice odometers were also later shown to have a strong uniqueness property [PS20].

Another new challenge is in identifying the correct recursive structure. There is a well-known secant line sweep algorithm which produces (and parameterizes) the rational points on \mathcal{H} given a single rational point on \mathcal{H} (and generally any elliptic curve - see *e.g.*[Tan96]). For example, since $(0, -1) \in \mathcal{H}$, all other rational points can be enumerated by varying the rational slope of a secant line between $(0, -1)$ and \mathcal{H} . Unfortunately, the odometers lying on \mathcal{H} under this labeling do not have an apparent recursive structure.

The parameterization which we adopt in this article utilizes the geometry of two adjacent cones. Each rational point on \mathcal{H} is an intersection of two unique lines of rational slope starting at the apexes of the cones. These intersections are dense in \mathcal{H} so we may identify each such point by its rational slope. See Figure 3.

Specifically, each point in $\mathbb{Q}^2 \cap \mathcal{H}$ may be labeled by a reduced fraction $0 \leq n/d \leq 1$ with corresponding matrix

$$(5) \quad M(n, d) := \frac{1}{(d^2 + 2dn - n^2)} \begin{bmatrix} -n^2 & dn \\ dn & -d^2 \end{bmatrix}.$$

We construct odometers for each $M(n, d)$ which grow along the lattice of the matrix,

$$(6) \quad L(n, d) = \{x \in \mathbb{Z}^2 : M(n, d) \cdot x \in \mathbb{Z}^2\},$$

and which have periodic Laplacians. However, the F -lattice is not transitive. In particular, if $h : \mathbb{Z}^2 \rightarrow \mathbb{Z}$ is $L(n, d)$ periodic, then Δh may not be $L(n, d)$ periodic unless its period is even. To circumvent this, we must pass to a sub-lattice by doubling along the kernel of



FIGURE 4. One $L'(2, 5)$ period of $\Delta g_{2,5}$ and $\Delta \hat{g}_{2,5}$. White and black are values of 0 and 1 respectively. These are used to construct the odometers seen in Figure 7.

$M(n, d)$. We show in Section 3 that $L(n, d)$ is equal to the integer span of

$$(7) \quad v_{n/d,1} := \begin{bmatrix} d \\ n \end{bmatrix} \quad v_{n/d,2} := \begin{bmatrix} n-d \\ n+d \end{bmatrix},$$

and $v_{n/d,1}$ generates the kernel of $M(n, d)$. Our modified lattice is

$$(8) \quad L'(n, d) = \begin{cases} L(n, d) & \text{if } (n+d) \text{ is even} \\ 2\mathbb{Z}v_{n/d,1} + \mathbb{Z}v_{n/d,2} & \text{if } (n+d) \text{ is odd.} \end{cases}$$

We then derive Theorem 1.2 from the following.

Theorem 1.3. *For each reduced fraction $0 < n/d < 1$ there exists two distinct odometers $g_{n,d}, \hat{g}_{n,d}$ both of which satisfy the periodicity condition,*

$$(9) \quad g(x+v) = g(x) + x^t M(n, d)x + c_v$$

for all $v \in L'(n, d)$.

As in [LPS17], the periodicity condition (9) implies that $g_{n,d}$ and $\hat{g}_{n,d}$ are each integer superharmonic representatives for $M(n, d)$. Moreover, integer superharmonic matrices with odometers are on $\partial\Gamma_F$. Indeed, if g were recurrent but not on the boundary of Γ_F there would exist an integer superharmonic $f \geq g + \delta|x|^2$ for some $\delta > 0$. However, on the boundary of a ball of radius n , B_n , $\sup_{\partial B_n}(g - f) \leq -n\delta/2^2$ for all n sufficiently large, contradicting the definition of recurrent as $\sup_{B_n}(g - f) \geq g(0) - f(0)$, a constant.

1.3. $F^{(k)}$ lattices and Kleinian bugs. We briefly mention a connection and possible extensions of this work. The overlapping circle packing in Figure 2 is an example of an object recently coined as a *Kleinian bug* [KK21]. Kleinian bugs may be thought of as a generalization of Appolonian circle packings in which circles are allowed to have prescribed overlaps. In particular, the Appolonian band packing from [LPS17] is a Kleinian bug. An important aspect of [LPS17] is an analogue of Descartes rule for integer superharmonic functions - Kleinian bugs share a similar rule.

The symmetry group of the Kleinian bug for the F -lattice is trivial (the difficult aspect of the argument in this manuscript is in accounting for the intersections between adjacent

cones). However, numerical evidence suggests that the set of integer superharmonic matrices on other planar lattices may also be described by nontrivial symmetries of Kleinian bugs.

Levine-Pegden-Smart have derived a numerical algorithm which can determine the set of integer superharmonic matrices on periodic graphs up to arbitrary precision [LPS16] (see [Peg] for some high resolution outputs of this algorithm). We ran the Levine-Pegden-Smart algorithm on a family of lattices which generalize the F -lattice, what we call the $F^{(k)}$ lattices. For each $k \geq 2$, the $F^{(k)}$ -lattice is a directed, periodic, planar graph $(\mathbb{Z}^2, E^{(k)})$, where

$$\begin{cases} (x \pm e_1, x) \in E & \text{if } x_1 + x_2 \pmod k = 0 \\ (x \pm e_2, x) \in E & \text{otherwise.} \end{cases}$$

Computed sets of $\partial\Gamma_k$, the boundary of the set of integer superharmonic matrices for the the $F^{(k)}$ lattice, are in Figure 5.

Some basic structure of these sets for all $k \geq 2$ may be understood after verifying that

$$(10) \quad \begin{aligned} \Delta r_1(x, y) &= 1\{(x_1 + x_2) \pmod k \neq 0\} & \text{for } r_1(x_1, x_2) &= \frac{x_2(x_2 + 1)}{2} \\ \Delta r_2 &= \Delta r_1 & \text{for } r_2(x_1, x_2) &= q_k(x_1 + x_2) \\ \Delta r_3 &= 1 & \text{for } r_3(x_1, x_2) &= \frac{x_1(x_1 + 1) + x_2(x_2 + 1)}{2} \end{aligned}$$

where

$$q_k(n) = \frac{(k-1)}{2k}(n^2 - s^2) + \frac{s(s-1)}{2} \quad \text{where } s = n \pmod k,$$

(note the Laplacian is that of the $F^{(k)}$ lattice). In particular, $h_1 := r_1 - r_2$ is integer valued and harmonic, $\Delta h_1 = 0$. The function $h_2(x_1, x_2) = x_1 x_2$ is also harmonic. This together with (10) and the standard argument in Lemma 6.1 below can be used to show that $r_i + s \cdot h_1 + t \cdot h_2 - r_3$ are odometers for all $s, t \in \mathbb{Z}$ and $i \in \{1, 2\}$. These odometers lie on the hyperbolas between the largest cones in Figure 5 and the harmonic functions explain the apparent periodicity of Γ_k .

Remark 1. Interestingly, the function $q_k(n)$ also counts the number of edges in a k -partite Turán graph of order n . We note that $q_k(n)$ has a simple closed form when k is small,

$$q_k(n) = \lfloor \frac{(k-1)}{2k} n^2 \rfloor \quad \text{only for } k \leq 7,$$

but this is false for $k \geq 8$.

The general characterization of Γ_k seems to require both a recursive construction of the odometers for all circles in a Kleinian bug as in [LPS17] and all rational points on an infinite family of distinct hyperbolas. For example, we have explicitly computed in Figure 6 odometers for some of the largest circles appearing in $\partial\Gamma_3$. Each pair of overlapping circles generates a new hyperbola which we must check contains a dense family of odometers.

We leave the possibility of more detailed investigations of Γ_k for future work. From here onwards, we focus solely on Γ_2 and omit the sub/superscripts.

1.4. Supplementary materials. Code which produces tile odometers will be uploaded on the arXiv.

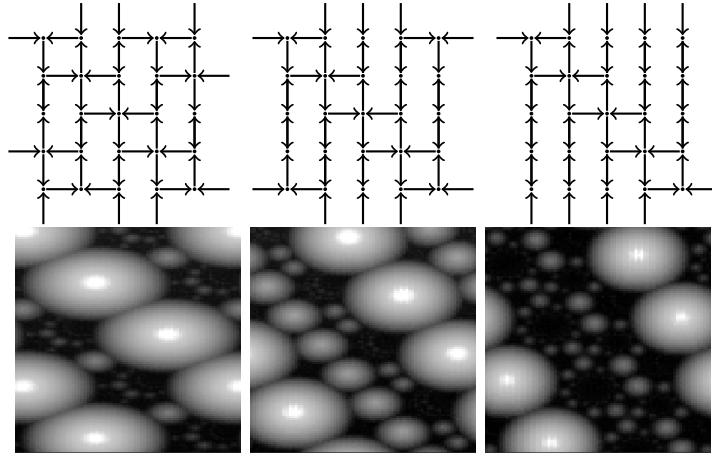


FIGURE 5. The $F^{(k)}$ lattices for $k = 3, 4, 5$ and computed $\partial\Gamma_k$.

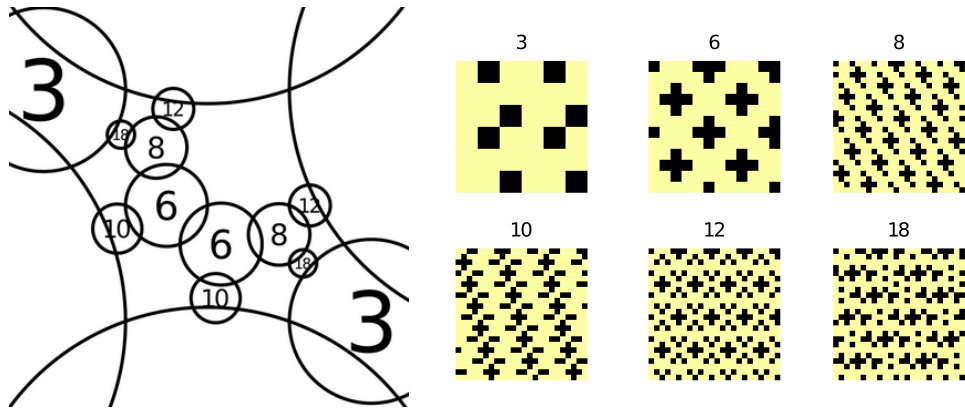


FIGURE 6. The seven largest circles in a period of $\partial\Gamma_3$. Periods of the Laplacians of odometers for the indicated circles on the left are displayed on the right, black is -1 and yellow is 0. Note that the four bordering largest circles have Laplacian identically 0 and correspond to harmonic functions built from (10).

Acknowledgments. Thank you to Charles K. Smart for valuable feedback throughout this project.

2. PROOF OUTLINE AND COMPARISON TO PREVIOUS WORK

Our method at a high level follows the outline of [LPS16]: the proof recursively constructs odometers which then identify Γ_F . The implementation of this outline, however, requires several new ideas, the most significant being the recursive algorithm itself.

In order to make the comparison, we briefly recall Levine-Pegden-Smart's construction in [LPS16]. On the square lattice, odometers were built by first specifying a *tile odometer*, a function with a finite domain, and then extending that function via a periodicity condition like (9) above. Levine-Pegden-Smart's construction associates tile odometers to circles in an Apollonian band packing. Recall that Apollonian packings can be drawn by starting with a triple of mutually tangent circles and then recursively filling in Soddy circles [GLM⁺05].

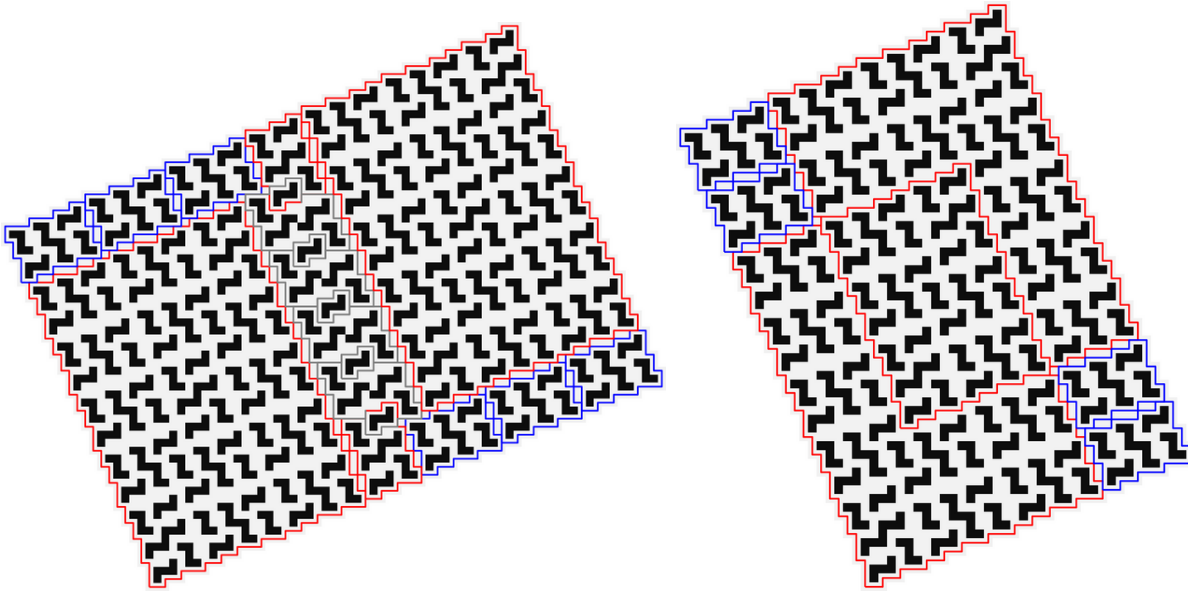


FIGURE 7. The Laplacian of two standard tile odometers corresponding to the Farey pair $(13/32, 15/37)$; the left and right displays are the odd and even child respectively. Gray is 0 and black is -1. The Laplacian of the standard odd-even ancestor odometers and alternate odometers are outlined in blue, red, and gray respectively. The even odometer decomposes perfectly into four-two copies of the odd-even standard odometers for the parent Farey pair, $(2/5, 11/27)$. In particular, two copies of the even parent overlap perfectly on a copy of an even grandparent. The odd odometer does not have a perfect decomposition into parents or grandparents; the decomposition requires multiple copies of the standard and alternate odometers of the distant ancestor pair $(2/5, 3/7)$.

Each circle in a packing is then part of a *Descartes quadruple* of pair-wise mutually tangent circles - thus every circle (other than the initial three) has a unique triple of parent circles. Levine-Pegden-Smart build tile odometers following this - the recursion starts with a simple formula for the largest circles in a band packing and then builds each child odometer by gluing together two copies each of the three parent odometers in a specified way.

In our setting, the Apollonian band packing is replaced by reduced rationals $0 \leq t \leq 1$ lying on a hyperbola $\mathcal{H} = \{(t, c) \in \mathbb{R} \times \mathbb{R}^- : t^2 + (1-t)^2 = c^2\}$. The rational recursion is Farey-like but parity aware. That is, all *odd* and *even* reduced rationals - those whose numerator and denominator sum to an odd and even integer respectively - are grouped together into unique odd-even *Farey pairs*. The initial Farey pair is $(0/1, 1/1)$ and subsequent pairs are produced via a modification of the mediant operation and parent-child rotation; the rational recursion produces a ternary tree of unique *Farey quadruples*, a grouping of child and parent Farey pairs. We use this tree structure to recursively produce tile odometers.

A major difference beyond this is that we build for each reduced rational in a Farey pair not one but *two* distinct odometers. If the recursive algorithm attempted to use only one of the two odometers, it would get stuck - see Figure 7. (This can be thought of as coupling one odometer to each of the two intersecting downwards paths in Figure 3.) The construction also requires ancestor odometers which are arbitrarily far up the recursive tree. Moreover,

although the function domains, the *tiles*, constructed are 180-degree symmetric, the tile odometers are not even centrally symmetric, leading to a blow-up in the the number of cases the algorithm must consider.

For these reasons and more, proving correctness of the recursive algorithm presents new technical challenges. A notable one being distant ancestor dependence precludes a finite step inductive proof. We address this by augmenting the recursion and associating a binary *boundary string* to each odometer. These strings encapsulate certain compatibility properties across the recursive tree and show it is possible to glue distinct tile odometers together in a well-defined way.

Our proof that the functions which we construct are recurrent also differs from the corresponding proof on the square lattice. There, the odometers were shown to be *maximal*, a property strictly stronger than recurrent. Roughly, an integer superharmonic function is maximal if no other integer superharmonic function grows faster than it. Levine-Pegden-Smart showed that their constructed odometers were maximal using the fact that their Laplacians have a ‘web of 0s’, an infinite connected subgraph of 0s. In our case, there is no such web (which uses F -lattice edges) and no hyperbola odometer is maximal. Another technical difference is that the tiles which we construct do not tile \mathbb{Z}^2 - they ‘almost’ do but this is fortunately sufficient for our arguments.

To summarize, our proof proceeds as follows.

- (1) Identify a Farey-like recursion on reduced fractions $t = n/d$ which is dense on a hyperbola and tracks the parity of $(n + d)$.
- (2) Pair each reduced fraction with a binary word which records how it was generated.
- (3) Associate to each such word a *boundary string* which carries additional function and domain data.
- (4) Augment the rational recursion to produce two distinct tile odometers, a standard and an alternate by piecing together combinations of earlier standard and alternate odometers.
- (5) Show the recursion is well-defined by reducing every interface into a pair of boundary strings.
- (6) Prove that the functions constructed are recurrent and have the correct growth.

We start in Section 3 by precisely defining the modified Farey recursion on the hyperbola. We then prove a technical ‘almost’ tiling lemma in Section 4; this is later used to show that tile odometers extend periodically to cover space. Then in Section 5, we introduce and analyze a recursion on binary words which supplements the hyperbola recursion. There we also associate degenerate function and tile data, boundary strings, to each such word.

Then, in Section 6 we prove Theorem 1.3 for a special family of reduced fractions. In particular, this family is simple enough that we are able to provide explicit formulas for the tile odometers. This forms the base case for the general recursion. In Section 7 we then introduce a weak form of the recursion which builds essentially just the boundary of the tile odometers. We show that these boundaries consist of exactly the boundary strings from Section 5. The full recursion is completed in Section 8 where we show the interior of tile odometers can be filled in either by immediate parents or by a chain of distant ancestors. We conclude in Section 9 by showing that both standard and alternate tile odometers can be extended in a way that give the desired growth and recurrence.

3. HYPERBOLA RECURSION

We specify a modified Farey recursion for rational matrices lying on the hyperbola $\mathcal{H} := \{(t, c) \in [0, 1] \times \mathbb{R}^+ : t^2 + (1-t)^2 = c^2\}$. We also prove that the recursion is invariant with respect to a certain rotation of matrix space. As is later shown, this rotational invariance is maintained in the general recursion and can be leveraged to simplify the proofs of correctness.

3.1. Matrix and lattice parameterization. Recall the map $M : S_2 \rightarrow \mathbb{R}^3$

$$(11) \quad M(a, b, c) = \frac{1}{2} \begin{bmatrix} c+a & b \\ b & c-a \end{bmatrix}$$

and the hyperbola matrices in the statement of Theorem 1.2, $M(t, 1-t, -\sqrt{t^2 + (1-t)^2})$. By solving for the intersection point of rank 1 perturbations of two adjacent cones and then subtracting a harmonic matrix, we can label $(t, c) \in \mathbb{Q} \cap \mathcal{H}$ by

$$(12) \quad f(n, d) := \frac{1}{T(n, d)} \cdot ((d^2 - n^2), -(d^2 + n^2)),$$

which has corresponding matrix

$$M(n, d) := \frac{1}{T(n, d)} \begin{bmatrix} -n^2 & dn \\ dn & -d^2 \end{bmatrix},$$

where $T(n, d) := (d^2 + 2dn - n^2)$. Another computation shows that $(n, d) \rightarrow (d-n, n+d)$ is a rotation of S_2 by: $(a, b) \rightarrow (b, a)$. We return to these rotations in Section 3.3 once we have defined the rational recursion.

As indicated in the introduction, we consider the lattice

$$(13) \quad L'(n, d) = \begin{cases} \mathbb{Z}v_{n/d,1} + \mathbb{Z}v_{n/d,2} & \text{if } (n+d) \text{ is even} \\ 2\mathbb{Z}v_{n/d,1} + \mathbb{Z}v_{n/d,2} & \text{if } (n+d) \text{ is odd.} \end{cases}$$

where

$$(14) \quad v_{n/d,1} := \begin{bmatrix} d \\ n \end{bmatrix} \quad v_{n/d,2} := \begin{bmatrix} n-d \\ n+d \end{bmatrix}.$$

Setting $a_i := M(n, d) \cdot v_i$, we note

$$(15) \quad a_1 := \begin{bmatrix} 0 \\ 0 \end{bmatrix} \quad a_2 := \begin{bmatrix} n \\ -d \end{bmatrix}.$$

We first observe that $v_{n/d,1}$ and $v_{n/d,2}$ generate the lattice of the matrix $M(n, d)$.

Lemma 3.1. *For each reduced fraction $t = n/d$,*

$$L(n, d) := \{v \in \mathbb{Z}^2 : M(n, d) \cdot v \in \mathbb{Z}^2\} = \mathbb{Z}v_{n/d,1} + \mathbb{Z}v_{n/d,2}.$$

Proof. Suppose $M(n, d) \cdot x = y$ for $x, y \in \mathbb{Z}^2$. For convenience, write $v_{n/d,i} =: v_i$. Since $\mathbb{R}^2 = \mathbb{R}v_1 + \mathbb{R}v_2$, we may write

$$x = cv_1 + c'v_2$$

for $c, c' \in \mathbb{Q}$. We show that c, c' must be in \mathbb{Z} , starting with c' . By (15),

$$M(n, d) \cdot x = cM(n, d) \cdot v_1 + c'M(n, d) \cdot v_2 = c'a_2$$

where by supposition

$$c'a_2 := \begin{bmatrix} z_1 \\ z_2 \end{bmatrix},$$

for integers z_1, z_2 . Since $\gcd(n, -d) = 1$, by Bézout's identity, there exists $w_1, w_2 \in \mathbb{Z}$ so that

$$w_1n - w_2d = 1.$$

Multiplying the above expression by c' ,

$$w_1z_1 + w_2z_2 = c',$$

in particular, since the left-hand side is integer-valued, $c' \in \mathbb{Z}$. The exact same argument then shows that $c \in \mathbb{Z}$ once we observe $cv_1 = x - c'v_2$ is integer valued. \square

We then check that the map in (12) is indeed dense in \mathcal{H} by noting it is dense in the first output.

Lemma 3.2. $\frac{d^2-n^2}{d^2+2dn-n^2}$ is dense in $[0, 1]$ for reduced fractions $0 \leq n/d \leq 1$.

Proof. Suppose $0 < n/d < 1$ and rewrite

$$\frac{d^2 - n^2}{d^2 + 2dn - n^2} = 1 - \frac{1}{1 + \frac{1}{2}(\frac{d}{n} - \frac{n}{d})}.$$

Conclude after observing that $\frac{d}{n} - \frac{n}{d}$ is dense in $[0, \infty)$. \square

3.2. Modified Farey recursion. As evident from (13), the recursion which we specify must be parity-aware. To that end, we say a reduced fraction p_n/p_d is *even* if $p_n + p_d$ is even and otherwise is *odd*. We exhibit a modified Farey recursion which generates all rationals in $[0, 1]$ and associates to each rational a unique set of odd-even parents and a sibling of the opposite parity.

An odd reduced fraction $p =: o_n/o_d$ and an even reduced fraction $q =: e_n/e_d$ produce an odd-even child pair by

$$(16) \quad \mathcal{C}(p, q) := \left(\frac{e_n + o_n}{e_d + o_d}, \frac{2 \cdot o_n + e_n}{2 \cdot o_d + e_d} \right).$$

A quadruple of reduced rationals, (p_1, q_1, p_2, q_2) is a *Farey quadruple* if $p_1, q_1 = \mathcal{C}(p_2, q_2)$, p_2 is odd, and q_2 is even. Each odd-even pair in a Farey quadruple is a *Farey pair*, the second pair are the *Farey parents* of each child in the first pair. A Farey quadruple (p_1, q_1, p_2, q_2) produces three children

$$(17) \quad \begin{aligned} \text{Type 1: } & \mathcal{C}_1 & (\mathcal{C}(p_1, q_1), p_1, q_1) \\ \text{Type 2: } & \mathcal{C}_2 & (\mathcal{C}(p_1, q_2), p_1, q_2) \\ \text{Type 3: } & \mathcal{C}_3 & (\mathcal{C}(p_2, q_1), p_2, q_1). \end{aligned}$$

The *modified Farey recursion* begins with the base quadruple

$$(18) \quad \mathbf{q}_0 = \left(\frac{1}{2}, \frac{1}{3}, \frac{0}{1}, \frac{1}{1} \right),$$

and generates descendants which are labeled by *recursion words* in the free monoid F_3^* generated by $\{1, 2, 3\}$. The empty word $\{\}$ corresponds to the base quadruple. Each letter

in a recursion word corresponds to the type of the child chosen in each step. For example $\mathbf{q}_{(123)}$ refers to the quadruple taking the Type 1 child of the root, then the Type 2 child of that child, then the Type 3 child of that child.

Here is the connection to the usual, vanilla Farey recursion. Recall that the vanilla Farey sequence of order n consists of all reduced fractions of denominator at most n between 0 and 1. If a/b and c/d are neighboring terms in a vanilla Farey sequence of order n , then the first term which appears between them in a later sequence of order $m > n$ is the mediant, $p = \frac{a+c}{b+d}$. We refer to $(a/b, c/d)$ as the *vanilla Farey parents* of p while p is the *vanilla Farey child* of *vanilla Farey neighbors* $(a/b, c/d)$. We then observe that (16) is simply two steps of the vanilla Farey recursion.

Lemma 3.3. *The modified Farey recursion generates unique Farey quadruples in reduced form*

$$\mathbf{q} = (p_1, q_1, p_2, q_2) = \left(\frac{e_n + o_n}{e_d + o_d}, \frac{2 \cdot o_n + e_n}{2 \cdot o_d + e_d}, \frac{o_n}{o_d}, \frac{e_n}{e_d} \right),$$

in particular, p_1, p_2 are odd, q_1, q_2 are even and \mathbf{q} is a Farey quadruple.

Proof. This follows once we inductively check that (p_2, q_2) are vanilla Farey neighbors with vanilla Farey child p_1 and (p_1, p_2) are vanilla Farey neighbors with vanilla Farey child q_1 . That is, by induction, (p_1, q_1) , (p_1, q_2) , and (p_2, q_1) are each pairs of neighbors in some vanilla Farey sequence and thus each child has a unique set of Farey parents. \square

Lemma 3.3 shows that the recursion defines a ternary tree of Farey quadruples. Each node in the tree has 3 outgoing edges corresponding to the three types of children. For later reference let \mathcal{T}_n , denote the set of all Farey quadruples associated to words of length exactly n and denote the full tree by

$$(19) \quad \mathcal{T} = \bigcup \mathcal{T}_n.$$

3.3. Rotational symmetry reduction. As noted previously in Section 3.1, the following operator

$$(20) \quad \mathcal{R}(n, d) = (d - n, n + d)$$

rotates $\partial\Gamma_F$. The goal of this section is to show that an extension of \mathcal{R} to Farey quadruples preserves the depth of the modified Farey recursion. We start by observing a parity flipping property of \mathcal{R} .

Lemma 3.4. *If $0 \leq n/d \leq 1$ is even then $\gcd((d-n)/2, (n+d)/2) = 1$, otherwise $\gcd(d-n, n+d) = 1$. Therefore, in the even case, the reduction of $\frac{d-n}{n+d}$ is odd and vice versa.*

Proof. We split the proof into two steps.

Step 1. We check the first claim. By the Euclidean algorithm,

$$\gcd(n, d) = \gcd(d - n, n) = 1,$$

and,

$$\begin{aligned} \gcd(n + d, d - n) &= \gcd((n + d) - (d - n), d - n) \\ &= \gcd(2n, d - n). \end{aligned}$$

If $(n+d)$ is even or odd, then $(d-n)$ is respectively even or odd. By Bézout's identity, there exist integers a_i, b_i so that

$$\begin{aligned} a_1(d-n) + b_12 &= c \\ a_2(d-n) + b_2n &= 1 \end{aligned}$$

where c is 1 if $(d-n)$ is odd and 2 otherwise. Multiplying the above two expressions together shows that $\gcd(2n, d-n) = c$. If $c = 1$, we are done, otherwise, another application of Bézout's identity shows that there is a_3, b_3 so that

$$a_3(n+d) + b_3(d-n) = 2$$

and if we divide by 2 then

$$a_3(n+d)/2 + b_3(d-n)/2 = 1$$

which concludes this step.

Step 2. If $(n+d)$ is odd, then Step 1 shows $\frac{d-n}{d+n}$ is in reduced form and therefore is even. Otherwise, reduce $\frac{d-n}{d+n} = \frac{(d-n)/2}{(d+n)/2}$ and note $(d-n+d+n)/2 = d$. Since $(n+d)$ is even and $\gcd(n, d) = 1$, both n and d must be odd, concluding the proof. \square

In light of Lemma 3.4, we extend \mathcal{R} to act on reduced fractions n/d by:

$$(21) \quad \mathcal{R}(n, d) = \begin{cases} (d-n, d+n) & \text{if } n+d \text{ is odd} \\ (\frac{d-n}{2}, \frac{n+d}{2}) & \text{otherwise.} \end{cases}$$

In an abuse of notation, we sometimes write $\mathcal{R}(n/d) = n'/d'$ instead. We extend \mathcal{R} to Farey pairs by $\mathcal{R}(p, q) = (\mathcal{R}(q), \mathcal{R}(p))$ and then component-wise to Farey quadruples. Our next two lemmas verify that this is well-defined.

Lemma 3.5. *If (p, q) is a Farey pair, $\mathcal{R}(\mathcal{C}(p, q)) = \mathcal{C}(\mathcal{R}(p, q))$.*

Proof. This is a direct computation. \square

We then show $\mathcal{R}(p)$ is a parent preserving bijection of the recursive tree \mathcal{T}_n .

Lemma 3.6. *The following holds for each word of length $n \geq 0$, $\mathbf{q}_{(w)} = (p_1, q_1, p_2, q_2) \in \mathcal{T}_n$.*

(1) *Rotations flip Type 2 and Type 3 children and preserve Type 1 children,*

$$\mathcal{R}(\mathbf{q}_{(w1)}) = \mathcal{R}(\mathbf{q}_{(w)})_1 \quad \mathcal{R}(\mathbf{q}_{(w2)}) = \mathcal{R}(\mathbf{q}_{(w)})_3 \quad \mathcal{R}(\mathbf{q}_{(w3)}) = \mathcal{R}(\mathbf{q}_{(w)})_2.$$

In particular,

$$\mathcal{R} \circ \mathcal{C}_1 = \mathcal{C}_1 \circ \mathcal{R} \quad \mathcal{R} \circ \mathcal{C}_2 = \mathcal{C}_3 \circ \mathcal{R} \quad \mathcal{R} \circ \mathcal{C}_3 = \mathcal{C}_2 \circ \mathcal{R}.$$

- (2) p_1 is the Farey child of (p_2, q_2) and $\mathcal{R}(q_1)$ is the Farey child of $\mathcal{R}(p_2, q_2)$
- (3) The rotation preserves depth $\mathcal{R}(\mathcal{T}_n) = \mathcal{T}_n$.

Proof. We prove the claims by induction on n , the depth of the tree; the base case $n = 0$ can be checked directly.

Proof of (1). Let

$$\mathbf{q}_{(w)} = (p'_1, q'_1, p'_2, q'_2)$$

so that

$$\begin{aligned}\mathbf{q}_{(w1)} &= (\mathcal{C}(p'_1, q'_1), p'_1, q'_1) \\ \mathbf{q}_{(w2)} &= (\mathcal{C}(p'_1, q'_2), p'_1, q'_2) \\ \mathbf{q}_{(w3)} &= (\mathcal{C}(p'_2, q'_1), p'_2, q'_1)\end{aligned}$$

By Lemma 3.5,

$$\begin{aligned}\mathcal{R}(\mathbf{q}_{(w)})_1 &= (\mathcal{C} \circ \mathcal{R}(p'_1, q'_1), \mathcal{R}(p'_1, q'_1)) \\ &= (\mathcal{R} \circ \mathcal{C}(p'_1, q'_1), \mathcal{R}(p'_1, q'_1)) \\ &= \mathcal{R}(\mathbf{q}_{(w1)}).\end{aligned}$$

For the other cases, we use the induction hypothesis together with the Lemma. Recall

$$\mathcal{R}(\mathbf{q}_{(w)}) = (\mathcal{R}(q_1), \mathcal{R}(p_1), \mathcal{R}(q_2), \mathcal{R}(p_2)),$$

hence

$$\begin{aligned}\mathcal{R}(\mathbf{q}_{(w)})_2 &= (\mathcal{C}(\mathcal{R}(q'_1), \mathcal{R}(p'_2)), \mathcal{R}(q'_1), \mathcal{R}(p'_2)) \\ &= (\mathcal{C} \circ \mathcal{R}(p'_2, q'_1), \mathcal{R}(p'_2, q'_1)) \\ &= (\mathcal{R} \circ \mathcal{C}(p'_2, q'_1), \mathcal{R}(p'_2, q'_1)) \\ &= \mathcal{R}(\mathbf{q}_{(w3)}).\end{aligned}$$

The other case is symmetric.

Proof of (2). By the inductive hypothesis (6), (p_2, q_2) are vanilla Farey neighbors therefore p_1 is the vanilla Farey child by definition. Also, by (6) and (3) $\mathcal{R}(p_2, q_2)$ are also vanilla Farey neighbors. Moreover, by Lemma 3.5, $\mathcal{C} \circ \mathcal{R}(p_2, q_2) = \mathcal{R}(p_1, q_1) = (\mathcal{R}(q_1), \mathcal{R}(p_1))$, meaning $\mathcal{R}(q_1)$ is also a Farey child.

Proof of (3).

By the inductive hypothesis, $\mathcal{R}(T_{n-1}) = T_{n-1}$ and by definition, $T_n = \bigcup_{i=1}^3 \mathcal{C}_i \circ T_{n-1}$. Hence, by part (1),

$$\mathcal{R} \circ T_n = \bigcup_{i=1}^3 \mathcal{R} \circ \mathcal{C}_i \circ T_{n-1} = \bigcup_{i=1}^3 \mathcal{C}_i \circ \mathcal{R} \circ T_{n-1} = \bigcup_{i=1}^3 \mathcal{C}_i \circ T_{n-1} = T_n,$$

concluding the proof. □

We conclude the section by observing that \mathcal{R} is also a rotation of the lattice vectors (14). By identifying \mathbb{Z}^2 with $\mathbb{Z}[i]$ we may write

$$(22) \quad v_{n/d,1} = d + ni \quad v_{n/d,2} = (n - d) + (n + d)i$$

and

$$(23) \quad a_{n/d,1} = 0 \quad a_{n/d,2} = n - di$$

Lemma 3.7. *For even p and odd q ,*

$$(24) \quad v_{\mathcal{R}(p),1} = -i \cdot v_{p,2} \quad v_{\mathcal{R}(p),2} = i \cdot 2v_{p,1}$$

and

$$(25) \quad 2v_{\mathcal{R}(q),1} = -i \cdot v_{q,2} \quad v_{\mathcal{R}(q),2} = i \cdot v_{q,1}$$

Proof. Write $p = n/d$ and note

$$\begin{aligned} v_{\mathcal{R}(p),1} &= (n+d) + (d-n)i \\ &= -i \cdot v_{p,2} \end{aligned}$$

and

$$\begin{aligned} v_{\mathcal{R}(p),2} &= (d-n) - (n+d) + (d-n+n+d)i \\ &= 2(-n+di) \\ &= i \cdot 2v_{p,1}. \end{aligned}$$

The equation for q follows once we recall \mathcal{R} is an involution, $\mathcal{R} \circ \mathcal{R}(q) = q$ \square

For the remainder of the paper write

$$(26) \quad v_{n/d,1} = \begin{cases} 2v_{n/d,1} & \text{if } n/d \text{ is odd} \\ v_{n/d,1} & \text{otherwise} \end{cases}$$

unless n/d is explicitly specified as odd or even.

4. ALMOST PSEUDO-SQUARE TILINGS

In this section we prove a technical tiling lemma which will allow us to show that the tiles which we define in the subsequent sections cover \mathbb{Z}^2 periodically.

We identify \mathbb{Z}^2 with $\mathbb{Z}[i]$. A *cell* is a unit square $s_x = \{x, x+1, x+i, x+1+i\} \subset \mathbb{Z}[i]$ and a *tile* is a simply connected union of cells whose boundary is a simple closed curve. The *vertices* of a tile are the Gaussian integers on its boundary. Let $(F_2, *)$ be the free group generated by $\{1, i\}$. For $w \in F_2$, let \hat{w} denote its involution, *i.e.*, $\hat{w} * w = \{\}$. Let $\mathbf{rev}(w)$ denote the reversal of $w \in F_2$, $w[i]$ the i th letter of w , and $|w|$ the number of letters in w . The *boundary word* of a tile is a word $w \in F_2$ which represents a vertex walk around the boundary of the tile. In particular, $\sum w = 0$ and $\sum w' \neq 0$ for any non-empty sub-word w' of w , where \sum denotes the abelianization of F_2 .

A *tiling* of the plane is an infinite set of translations of a tile T where every cell is contained in exactly one copy of T . A tiling of T is (v_1, v_2) -regular if every tile T' in the tiling can be expressed as $T + kv_1 + k'v_2$ for $k, k' \in \mathbb{Z}$ and $v_1, v_2 \in \mathbb{Z}[i]$. That is, the translations of T by (v_1, v_2) generate the tiling.

Beauquier-Nivat [BN91] have a simple criteria for determining if a tile generates a regular tiling. Their criteria is expressed in terms of the boundary words of a tile, but can be interpreted geometrically as: a tile generates a regular tiling if it can be perfectly surrounded by copies of itself. We refer to a tiling satisfying the conditions in Proposition 4.1 as a *pseudo-square tiling*.

Proposition 4.1 ([BN91]). *If the boundary word of a tile, $w \in F_2$, can be expressed as*

$$w = w_1 * w_2 * \hat{w}_1 * \hat{w}_2,$$

then the tile generates a $(\sum w_1, \sum w_2)$ -regular tiling.

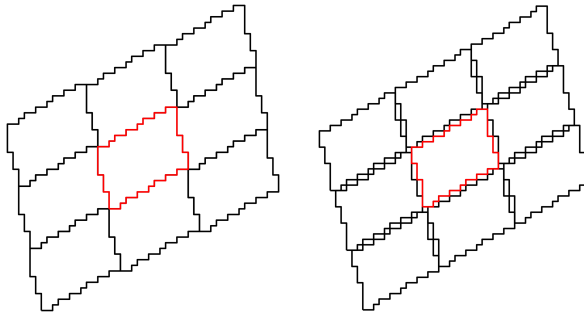


FIGURE 8. A surrounding of a pseudo-square tiling and an almost pseudo-square tiling as defined in Proposition 4.1 and Lemma 4.1 respectively.

In our main argument, we require a technical modification of the notion of tiling in which bounded gaps are allowed. That is, we cannot use Proposition 4.1 and are thus forced to modify it. An *almost* tiling, \mathcal{T} , is an infinite set of translations of a tile T where every cell is contained in at most one tile and every $x \in \mathbb{Z}^2$ is a vertex of a cell in \mathcal{T} , i.e., there is $s_y \in \mathcal{T}$ with $x \in s_y$. The notion of regular with respect to a lattice is also extended to almost tilings.

We now give a sufficient condition for generating almost tilings. Roughly, this condition allows for slight gaps between cells in the surrounding of a tile. We will refer to the almost tiling from Lemma 4.1 as an *almost pseudo-square tiling*. See Figure 8 for an illustration of this.

Lemma 4.1. *Suppose $w = w_1 * w_2 * \widehat{\text{rev}(w_1)} * \widehat{\text{rev}(w_2)}$ is the boundary word of a tile T . Further suppose the following conditions on $w \in \{w_1, -i \cdot w_2\}$.*

- (1) *Monotonicity:* $\{-1, -i\} \notin w$ and $w[1] = w[|w|] = 1$
- (2) *At least one of the following three cases concerning the form of w and its reversal is satisfied:*
 - (a) w is a palindrome, $w = \text{rev}(w)$
 - (b) $w = (1 * 1 * i) * \tilde{w} * 1$, where \tilde{w} is a palindrome. Moreover, every i in w is followed by at least one 1.
 - (c) $w = 1 * \tilde{w} * (1 * 1 * 1)$ where \tilde{w} is a palindrome. Moreover, every i in w is followed by at least three 1s.

Then, T generates a $(\sum w_1 + i, \sum w_2 - 1)$ -regular almost tiling. Moreover, the only tiles in the tiling which share edges with T are $T \pm (\sum w_1 + i)$ and $T \pm (\sum w_2 - 1)$.

Proof. Let $(v_1, v_2) = (\sum w_1, \sum w_2)$. To show that T generates a $(v_1 + i, v_2 - 1)$ -regular almost tiling, by periodicity, it suffices to analyze one surrounding of T ,

$$S := \bigcup_{|k_1| \leq 1, |k_2| \leq 1} \{T + k_1(v_1 + i) + k_2(v_2 - 1)\},$$

see Figure 8. Specifically we show that the closure,

$$\bar{S} = \{s_x : x \in S \cap \mathbb{Z}^2\}.$$

is simply connected and no two cells in the decomposition of S overlap.

Observe that the boundary word of T implies it is 180-degree symmetric. Hence, S is 180-degree symmetric and we may reduce to analyzing the interfaces between T and its lower, right, and lower-right neighbors,

$$\begin{aligned} T_h &:= T + v_1 + i \\ T_v &:= T - v_2 + 1 \\ T_d &:= T + v_1 - v_2 + 1 + i. \end{aligned}$$

We show that the conditions imply no two pairs of edges cross and that every gap in the interface borders a cell of T .

Step 1: The bottom interface

We start with the bottom interface, T and T_v . Designate the origin as the lower-left vertex of T so that cells along the bottom of T can be labeled by a w_1 walk. By the definition and the translation offsets, vertices along the top edge of T_v can then be labeled by $\text{rev}(w_1) + 1$. For $j \leq |w_1|$, let $x_j = \sum w_1[1:j]$ and $y_j = 1 + \sum(\text{rev}(w_1)[1:j])$, where $w[1:j]$ represents the first j letters of w . In particular, $x_0 = 0$ and $y_0 = 1$.

We now split the argument into three cases depending on the form of w_1 as dictated by (2).

Case (a): $w_1 = \text{rev}(w_1)$

In this case, $y_j = 1 + \sum w_1[1:j]$ and so

$$(27) \quad \text{Im}(x_j) = \text{Im}(y_j) \quad \text{and} \quad \text{Re}(x_j) = \text{Re}(y_j) - 1.$$

Therefore, any vertex y_j along the top edge of T_v is distance at most one from x_j , the lower left-corner of a cell in T .

To see that the top edge of T_v does not cross above the bottom edge of T , we use monotonicity. Suppose for sake of contradiction a crossing occurs. Since $w_1 = 1$, $x_1 = y_0$ and therefore there is a first j at which $y_j = x_{j+1}$ and $y_{j+1} = x_{j+2} + i$. Since $y_j = x_{j+1}$, by (27)

$$\text{Im}(y_j) = \text{Im}(x_{j+1}) = \text{Im}(y_{j+1}) \quad \text{and} \quad \text{Re}(y_j) = \text{Re}(x_{j+1}) = \text{Re}(y_{j+1}) - 1,$$

which implies by monotonicity that $y_{j+1} = y_j + 1$, a contradiction.

Case (b):

In this case

$$\begin{aligned} w_1 &= (1 * 1 * i) * \tilde{w} * 1 \\ \text{rev}(w_1) &= 1 * \tilde{w} * (i * 1 * 1) \end{aligned}$$

Therefore, (after remembering the offset of T_v)

$$\begin{aligned} x_0 &= 0 & x_1 &= 1 & x_2 &= 2 & x_3 &= 2 + i \\ y_0 &= 1 & y_1 &= 2 & y_2 &= 2 + \tilde{w}[1] & y_3 &= 2 + \tilde{w}[1] + \tilde{w}[2]. \end{aligned}$$

also by the moreover clause, $y_2 = 3$ and

$$\begin{aligned} x_{3+|\tilde{w}|} &= (2 + i) + \sum \tilde{w} & x_{4+|\tilde{w}|} &= (3 + i) + \sum \tilde{w} \\ y_{1+|\tilde{w}|} &= (2) + \sum \tilde{w} & y_{2+|\tilde{w}|} &= (2 + i) + \sum \tilde{w} \\ y_{3+|\tilde{w}|} &= (3 + i) + \sum \tilde{w} & y_{4+|\tilde{w}|} &= (4 + i) + \sum \tilde{w} \end{aligned}$$

thus it suffices to consider $1 \leq j \leq 1 + |\tilde{w}|$ for which

$$(28) \quad x_{j+2} = y_j + i.$$

It remains to show this implies there are no crossings. Suppose for contradiction $y_j = x_{j'}$ and $y_{j+1} = y_j + i$ but $x_{j'+1} = x_{j'} + 1$. for some $1 \leq j \leq 1 + |\tilde{w}|$. By (28), $y_{j+1} = x_{j+2} = x_{j'} + i$. By monotonicity, $j' = j + 1$ and so $x_{j'+1} = x_{j'} + i$, a contradiction.

Case (c):

In this case,

$$w_1 = 1 * \tilde{w} * (1 * 1 * 1)$$

$$\mathbf{rev}(w_1) = (1 * 1 * 1) * \tilde{w} * 1$$

and so

$$\begin{aligned} x_0 &= 0 & x_1 &= 1 & x_2 &= 1 + \tilde{w}[1] \\ y_0 &= 1 & y_1 &= 2 & y_2 &= 3 & y_3 &= 4 \end{aligned}$$

and

$$\begin{aligned} x_{1+|\tilde{w}|} &= 1 + \sum \tilde{w} & x_{1+|\tilde{w}|+z} &= (1+z) + \sum \tilde{w} && \text{for } z \leq 3 \\ y_{3+|\tilde{w}|} &= 4 + \sum \tilde{w} & y_{4+|\tilde{w}|} &= 5 + \sum \tilde{w}. \end{aligned}$$

We note that for all $2 \leq j \leq |\tilde{w}| + 3$,

$$(29) \quad y_j = x_{j-2} + 3.$$

Indeed, $x_{1+z} = 1 + \sum \tilde{w}[1 : z]$ and $y_{3+z} = 4 + \tilde{w}[1 : z]$ for $z \leq |\tilde{w}|$.

We claim that this together with the moreover clause implies no gaps of size larger than 1. Indeed, if $y_j = x_{j-2} + 3$, then $x_j = x_{j-2} + 1 + (1 \text{ or } i)$. In the first case, we are done. In the second case, $x_{j+2} = x_{j-2} + 1 + i + 2$.

(29) also implies no crossings. Indeed, suppose for contradiction $y_j = x_{j'}$ and $y_{j+1} = y_j + i$ but $x_{j'+1} = x_{j'} + 1$. for some $2 \leq j \leq 2 + |\tilde{w}|$. We have $y_j = x_{j-2} + 3$ and $y_{j+1} = x_{j-1} + 3$. This implies $x_{j-1} = x_{j-2} + i$ and hence the moreover clause implies $x_{j+2} = x_{j-1} + 3 = x_{j-2} + 3 + i = y_j + i = y_{j+1}$. Monotonicity then implies $x_{j+1} = x_{j'} = y_j$, but this then contradicts $x_{j'+1} = x_{j'} + 1$.

Step 2: Conclude

After rotating, the arguments in Step 1 apply to the interface between T and T_h . We then check T and T_d . Let $z_0 = \sum w_1$ and note that the top left vertex of T_d is $z_0 + 1 + i$. By the assumption on the first and last letter of w_2 , the next vertices on the top and left edges of T_d are $z_0 + 2 + i$ and $z_0 + 1$ respectively while the next vertex on the right edge of T is $z_0 + i$. This implies that no cell of T overlaps one of T_d and that the gap between the two tiles is of unit size.

Finally, by monotonicity, for any other pair of cells in S to overlap, there must first be a crossing on the horizontal or vertical edges which we have just shown to be impossible. \square

5. ZERO-ONE BOUNDARY STRINGS

In this section we begin to associate additional data to the hyperbola recursion.

5.1. A recursion on binary words. We associate to the each reduced fraction in the modified Farey recursion a binary word, and expose some basic properties. Specifically, given any initial Farey pair (p, q) we associate each descendant to a *binary word*, a word in the alphabet generated by the two letters, $\{p, q\} \in F_2^*$, by augmenting the recursion.

Given a recursion word $w \in F_3^*$ and two binary words $p_t, q_t \in F_2^*$ we extend the child operator in (16) to pairs of binary words by

$$(30) \quad \mathcal{C}_{(w)}(p_t, q_t) = \begin{cases} (q_t q_t p_t, q_t p_t) & \text{if } \sum 1\{w_j = 1\} \text{ is even} \\ (p_t q_t q_t, p_t q_t) & \text{otherwise.} \end{cases}$$

Let $w_0 \in F_3^*$ describe the Farey pair (p, q) and $\mathbf{Q}_{(w_0)} = (\mathcal{C}_{w_0}(p, q), p, q)$ be the initial binary word quadruple in F_2^* . Then, recursively, given $w \in F_3^*$ and $\mathbf{Q}_{(w)} = (p, q, p', q')$, each child binary word quadruple is defined by

$$(31) \quad \begin{aligned} \mathbf{Q}_{(w*1)} &= (\mathcal{C}_{(w*1)}(p, q), p, q) \\ \mathbf{Q}_{(w*2)} &= (\mathcal{C}_{(w*2)}(p, q'), p, q') \\ \mathbf{Q}_{(w*3)} &= (\mathcal{C}_{(w*3)}(p', q), p', q). \end{aligned}$$

Recall that a palindrome $\tilde{w} \in F_2^*$ is a word that is equal to its reversal, $\tilde{w} = \mathbf{rev}(\tilde{w})$. An *almost palindrome* is a word $w = s_1 * \tilde{w} * s_2$, where $s_1, s_2 \in \{p, q\}$ are two letters and \tilde{w} is a palindrome. Write $w[a : b]$ for the first subword starting at the a -th letter of w and ending at the b -th letter.

Lemma 5.1. *The following hold for every subsequent pair of binary words (p_t, q_t) produced by (31).*

- (1) *Both p_t and q_t are almost palindromes*
- (2) *If $\sum 1\{w_{0j} = 1\}$ is even then all subsequent binary words begin with q and end with p and otherwise begin with p and end with q .*
- (3) *Let $n = \min(|p_t|, |q_t|)$ and $m = \min(|p_t|, 2|q_t|)$. Then,*

$$p_t[2 : n] = \mathbf{rev}(q_t)[2 : n] \quad p_t[2 : m] = \mathbf{rev}(q_t q_t)[2 : m].$$

Proof. We may suppose without loss of generality that $\sum 1\{w_{0j} = 1\}$ is even, otherwise, reverse the subsequent statements.

Let $\mathbf{Q}_{(w)} = (p_{t+1}, q_{t+1}, p_t, q_t)$ be given and we will verify claims (1) and (2) for the child Farey pair and claim (3) for the parent Farey pair in the quadruple

$$\mathbf{Q}_{(w')} = (p_{t+2}, q_{t+2}, p'_{t+1}, q'_{t+1})$$

defined by (31). To do so, we must eliminate the degenerate cases $p'_{t+1} = p$ or $q'_{t+1} = q$. Fortunately, these can only occur if $w' = 3^k$ or $w' = 2^k$ for $k \geq 0$ respectively. An induction shows that

$$(32) \quad \begin{aligned} \mathbf{Q}_{(3^k)} &= (qp^k qp^{k+1}, qp^{k+1}, p, qp^k) \\ \mathbf{Q}_{(2^k)} &= (q^{2(k+1)} p, q^{2k+1} p, q^{2k} p, q), \end{aligned}$$

and we can verify the claim directly in these cases by inspection. We can then use (32) to also handle the cases $w' = 3^k\{1, 2\}$ or $w' = 2^k\{1, 3\}$.

Hence, we may assume none of $p_t, q_t, p_{t+1}, q_{t+1}$ are singletons, that is the induction hypotheses hold for each of them. We also suppose $\sum 1\{w_j = 1\}$ is even. By the induction hypotheses

$$p_t = qw^1p \quad q_t = qw^2p$$

for palindromes w^1 and w^2 and so

$$(33) \quad \begin{aligned} p_{t+1} &= qw^2pqpw^2pqpw^1p \\ q_{t+1} &= qw^2pqpw^1p. \end{aligned}$$

Since p_{t+1} and q_{t+1} are almost palindromes and w^i are palindromes this implies the reversal relations

$$(34) \quad \begin{aligned} w^2pqpw^1 &= w^1qpw^2 \\ w^2pqpw^2pqpw^1 &= w^1qpw^2qpw^2, \end{aligned}$$

since w^i are palindromes. We can use this to check claim (3). Using (34) and that w^i are palindromes,

$$\begin{aligned} \mathbf{rev}(q_{t+1}) &= pw^1qpw^2q \\ p_{t+1} &= qw^1qpw^2qpw^2p \\ \mathbf{rev}(q_{t+1}q_{t+1}) &= pw^1qpw^2qpw^2pqpw^1q, \end{aligned}$$

For claim (2), the possible decompositions of (p_{t+2}, q_{t+2}) are

$$\begin{aligned} (p_{t+1}q_{t+1}q_{t+1}, p_{t+1}q_{t+1}) &\quad \text{Type 1} \\ (q_tq_tp_{t+1}, q_tp_{t+1}) &\quad \text{Type 2} \\ (q_{t+1}q_{t+1}p_t, q_{t+1}p_t) &\quad \text{Type 3}. \end{aligned}$$

The reversal(34) relations together (33) show that each of the decompositions are almost palindromes. We show only the odd Type 1 case as the rest are similar. First, write using (33)

$$p_{t+1}q_{t+1}q_{t+1} = qw^2pqpw^2pqpw^1pqpw^2pqpw^1pqpw^2pqpw^1p,$$

and then use (34) to check

$$\begin{aligned} \mathbf{rev}(w^2pqpw^2pqpw^1pqpw^2pqpw^1pqpw^2pqpw^1) &= [w^1qpw^2]qp[w^1qpw^2]qp[w^1qpw^2qpw^2] \\ &= [w^2pq(w^1)qp[w^2)pq(w^1qp[w^2)pqpw^2pqpw^1] \\ &= w^2pq(w^2pqpw^1)pq(w^2pqpw^1)pqpw^2pqpw^1. \end{aligned}$$

□

5.2. Basic definitions. We next associate tile and function data to the binary word recursion. But in order to do so, we must recall and modify some definitions from [LPS16]. A *tile* T is now, depending on the context, either a finite subset of \mathbb{Z}^2 or a finite union of simply connected cells. Let $c(T)$ denote the coordinate-wise minimum T , (geometrically the

lower-left vertex). A *partial odometer* is a function $h : T \rightarrow \mathbb{Z}$. The domain of h is $T(h)$ and $s(h) \in \mathbb{C}$ is the *slope* of T , the average of

$$(35) \quad \begin{aligned} & \frac{1}{2} (h(x+1) - h(x) + h(x+1+\mathbf{i}) - h(x+\mathbf{i})) + \\ & \frac{\mathbf{i}}{2} (h(x+\mathbf{i}) - h(x) + h(x+1+\mathbf{i}) - h(x+1)) \end{aligned}$$

for $x \in T$. Two partial odometers o_1 and o_2 are *translations* of one another if

$$(36) \quad T(o_1) = T(o_2) + v \quad \text{and} \quad o_1(x) = o_2(x+v) + a \cdot x + b$$

for some $v, a \in \mathbb{Z}^2$ and $b \in \mathbb{Z}$.

Partial odometers o_1 and o_2 are *compatible* if $o_1 - o_2 = c$ on $T(o_1) \cap T(o_2)$ for some *offset constant* $c \in \mathbb{Z}$. As in [LPS16], if the offset constant is 0 or the tiles do not overlap then $o_1 \cup o_2$ is the common extension to $T(o_1) \cup T(o_2)$. We recall for later reference the following lemma which will allow us to construct global odometers from pairwise compatible partial odometers.

Lemma 5.2 (Lemma 9.2 in [LPS16]). *If $\mathcal{S} = \{o_i\}$ is a collection of pairwise compatible partial odometers such that $\{T(o_i)\}$ forms an almost pseudo-square tiling then there is a function $g : \mathbb{Z}^2 \rightarrow \mathbb{Z}$ unique up to adding a constant that is compatible with every $o_i \in \mathcal{S}$.*

5.3. Even-odd boundary strings. We now associate additional data to each binary word constructed in the first subsection. The result in this subsection will form a key tool in verifying correctness of the subsequent tile and odometer recursion.

We first adapt the notion of *boundary string* from [LPS16] to our setting. Suppose T_p and T_q are tiles which generate $(v_{p,1}, v_{p,2})$ and $(v_{q,1}, v_{q,2})$ regular almost pseudo-square tilings respectively. A *q-p boundary string* is a collection of tiles $T_i \in \{T_q, T_p\}$ such that

$$(37) \quad c(T_i) - c(T_{i-1}) = \begin{cases} v_{p,j} & \text{if } T_{i-1} = T_p \\ v_{q,j} & \text{if } T_{i-1} = T_q, \end{cases}$$

for fixed $j \in \{1, 2\}$. A *q-p reversed boundary-string* is also a collection of tiles $T_i \in \{T_q, T_p\}$ but with different offsets:

$$(38) \quad c(T_i) - c(T_{i-1}) = \begin{cases} v_{p,j} + (v_{p,j'} - v_{q,j'}) & \text{if } pq \\ v_{p,j} & \text{if } pp \\ v_{q,j} + (v_{q,j'} - v_{p,j'}) & \text{if } qp \\ v_{q,j} & \text{if } qq, \end{cases}$$

where $(j, j') \in \{(1, 2), (2, 1)\}$ is fixed and the right column denotes the tile tuple, *e.g.*, the first row is $(T_{i-1}, T_i) = (T_p, T_q)$. When $j = 1$, a boundary string is *horizontal* and otherwise is *vertical*. We label a boundary string by a binary word $w \in F_2$, \mathcal{B}_w where a superscript r indicates it is reversed.

A horizontal or vertical *stacked boundary string* for $w \in F_2$ is a union of $\{T_i^+\} := \mathcal{B}_w$ and $\{T_i^-\} := \mathcal{B}_{\text{rev}(w)}^r$ both oriented in the same direction. The first tiles T_1^+ and T_1^- in each string and the shared direction dictate the relative positions,

$$(39) \quad c(T_1^+) - c(T_1^-) = v_{n/d', j'}$$

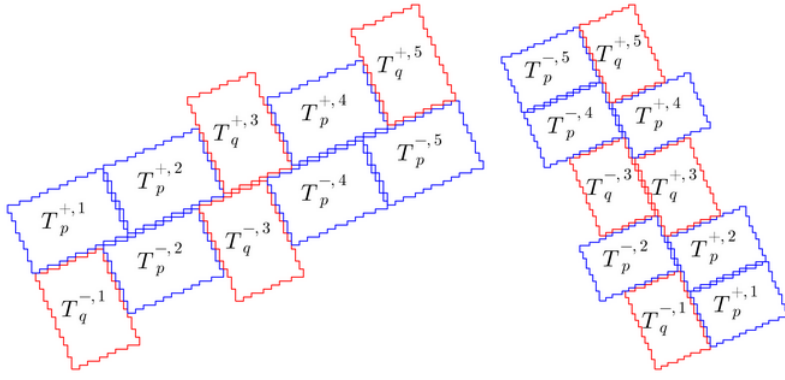


FIGURE 9. Stacked horizontal and vertical boundary strings. The superscripts $+$, $-$ denote the non-reversed and reversed strings respectively. Here the tiles are outlined in the dual lattice.

where $j' \in \{1, 2\}$ is the perpendicular direction and $n/d' \in \{p, q\}$ is the type of T_1^- . See Figure 9.

We now observe that tile offsets between perpendicular adjacent tiles in a stacked boundary string are given by a simple formula if the binary word describing the string is an almost palindrome.

Lemma 5.3. *If w is an almost palindrome, then for all $1 < i \leq |w|$*

$$c(T_i^+) - c(T_i^-) = v_{n/d', j'} + (v_{a,j} - v_{b,j})$$

where $j' \in \{1, 2\}$ is the perpendicular direction, $n/d', a, b \in \{p, q\}$ is the type of T_i^- , T_1^+ and T_1^- respectively.

Proof. For concreteness and since w is an almost palindrome, take $j = 1$, $T_1^+ = T_p$ and $T_1^- = T_q$. If T_2^- and T_2^+ are both of type p , then

$$\begin{aligned} c(T_2^+) - c(T_2^-) &= (c(T_2^+) - c(T_1^+)) + (c(T_1^+) - c(T_1^-)) + (c(T_1^-) - c(T_2^-)) \\ &= v_{p,1} + v_{q,2} - (v_{q,1} + (v_{q,2} - v_{p,2})) \\ &= v_{p,2} + (v_{p,1} - v_{q,1}). \end{aligned}$$

If T_2^- and T_2^+ are both of type q , then

$$c(T_2^+) - c(T_2^-) = v_{p,1} + v_{q,2} - v_{q,1}.$$

Conclude by similar computations together with an induction on $1 < i \leq |w|$. □

5.4. A degenerate boundary string. We now examine a degenerate boundary string which we will show completely describes the recursion. Due to the degenerate nature of the tiles in the string, the offsets in the definition of boundary string must be modified slightly. Let $p, q = 0/1, 1/1$ and the lattice vectors be as defined in Section 3:

$$v_{p,1} = 2 \quad v_{p,2} = -1 + i$$

$$v_{q,1} = 1 + i \quad v_{q,2} = 2i.$$

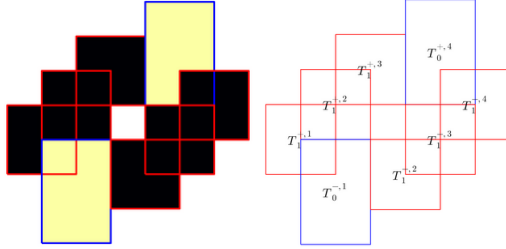


FIGURE 10. A gap inside a zero-one horizontal stacked boundary string corresponding to the word $qqqp$. Here we are outlining tiles on a square grid where each $x \in \mathbb{Z}[i]$ is in the center of a square. On the left, points in the stacked string are filled in with either black ($T_{0/1}$) or yellow ($T_{1/1}$). On the right the outlines and annotations are displayed; the superscripts $+$, $-$ denote the non-reversed and reversed strings respectively.

The *zero-tile* is $T_{0/1} = \{0, i, 2i, 1, 1+i, 1+2i\}$ and the *one-tile* is $T_{1/1} = \{0, i, 1, 1+i\}$. A *zero-one horizontal* boundary string is a collection of tiles $T_i \in \{T_{0/1}, T_{1/1}\}$ with offsets given by

$$(40) \quad c(T_i) - c(T_{i-1}) = \begin{cases} v_{q,1} & \text{if } T_i = T_q \\ v_{p,1} & \text{if } T_i = T_p, \end{cases}$$

and in the reversed case

$$(41) \quad c(T_i) - c(T_{i-1}) = \begin{cases} v_{q,1} + 1 & \text{if } pq \\ v_{p,1} & \text{if } pp \\ v_{p,1} - 1 & \text{if } qp \\ v_{q,1} & \text{if } qq. \end{cases}$$

We further impose that every (reversed) horizontal zero-one boundary string begins with $T_{1/1}$ ($T_{0/1}$).

A *zero-one stacked horizontal* boundary string is a union of a horizontal zero-one boundary string and its reversal where

$$(42) \quad c(T^{+,1}) - c(T^{-,1}) = v_{p,2} + i.$$

Unfortunately, in this case the stacked boundary strings may leave gaps which are too large. This occurs for exactly one particular interface, qq , which we have displayed in Figure 10. To fix this, we fill the gap by requiring that whenever $T_{1/1}$ follows a $T_{1/1}$, the subsequent tile is replaced by an enlarged version:

$$(43) \quad T_{1/1}^d = T_{1/1} \cup \{i-1, 1-i\},$$

but there are no other changes, *i.e.*, we impose $c(T_{1/1}^d) = c(T_{1/1})$. See Figure 11.

To define vertical strings, we simply rotate each of the above conditions by 90 degrees but exclude the doubled tiles. To be specific, a *zero-one vertical* boundary string is also a collection of tiles $T_i \in \{T_{0/1}, T_{1/1}\}$ but with rotated offsets:

$$(44) \quad c(T_i) - c(T_{i-1}) = \begin{cases} v_{q,2} & \text{if } T_i = T_q \\ v_{p,2} & \text{if } T_i = T_p \end{cases}$$

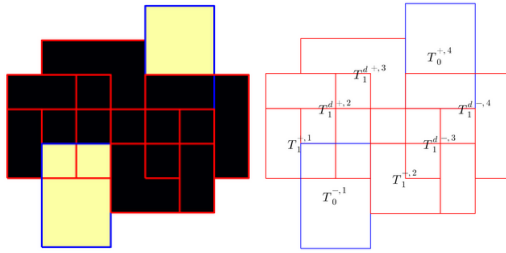


FIGURE 11. As Figure 10 but with gap fixed by $T_{1/1}^d$.

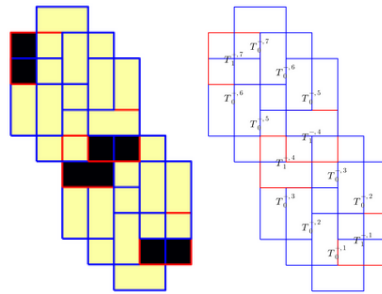


FIGURE 12. A vertical stacked zero-one boundary string with the same labeling scheme as Figure 10.

and in the reversed case

$$(45) \quad c(T_i) - c(T_{i-1}) = \begin{cases} v_{p,2} + i & \text{if } pq \\ v_{p,2} & \text{if } pp \\ v_{q,2} - i & \text{if } qp \\ v_{q,2} & \text{if } qq. \end{cases}$$

A *zero-one stacked vertical* boundary string is a union of a vertical even-odd boundary string and its reversal where

$$(46) \quad c(T^{+,1}) - c(T^{-,1}) = -v_{q,1}.$$

In the vertical case, we do not use doubled tiles and we further impose that every (reversed) vertical zero-one boundary string begins with $T_{0/1}$ ($T_{1/1}$). See an example of a stacked vertical zero-one boundary string in Figure 12. In both horizontal and vertical cases we label boundary strings by binary words in F_2^* and we also label stacked boundary strings by the non-reversed word.

We conclude with a similar counterpart to Lemma 5.3.

Lemma 5.4. *If w is an almost palindrome beginning with q and ending with p then the offsets between perpendicular tiles in the zero-one stacked string are fixed: in the horizontal*

DRAFT 9/16/21

FIGURE 13. Twelve possible overlaps in a stacked zero-one horizontal boundary string with labeling as Figure 10.

case

$$\begin{aligned}
 c(T_1^{+,1}) - c(T_1^{-,1}) &= -1 + 2i = v_{p,2} + i & qp \\
 c(T_{1/1}^+) - c(T_{1/1}^-) &= 2i - 2 = v_{p,2} + i - 1 & qq \\
 c(T_{0/1}^+) - c(T_{0/1}^-) &= 2i - 1 = v_{p,2} + i & pp \\
 c(T_{|w|}^+) - c(T_{|w|}^-) &= 1 - i = (v_{p,1} - v_{q,1}) + (v_{p,2} + i - 1) & pq
 \end{aligned}$$

and in the vertical case

$$\begin{aligned}
 c(T_1^{+,1}) - c(T_1^{-,1}) &= -(i + 1) = -v_{q,1} & pq \\
 c(T_{1/1}^+) - c(T_{1/1}^-) &= -(i + 1) = -v_{q,1} & qq \\
 c(T_{0/1}^+) - c(T_{0/1}^-) &= -(2 + i) = v_{p,2} - v_{q,2} + i - v_{q,1} & pp \\
 c(T_{|w|}^+) - c(T_{|w|}^-) &= -1 = -v_{q,1} + i & qp.
 \end{aligned}$$

In particular, there are finitely many types of pairwise intersecting tiles in such stacked strings. See Figures 13 and 14 respectively. This finite check implies every stacked zero-one boundary string is simply connected.

□

25

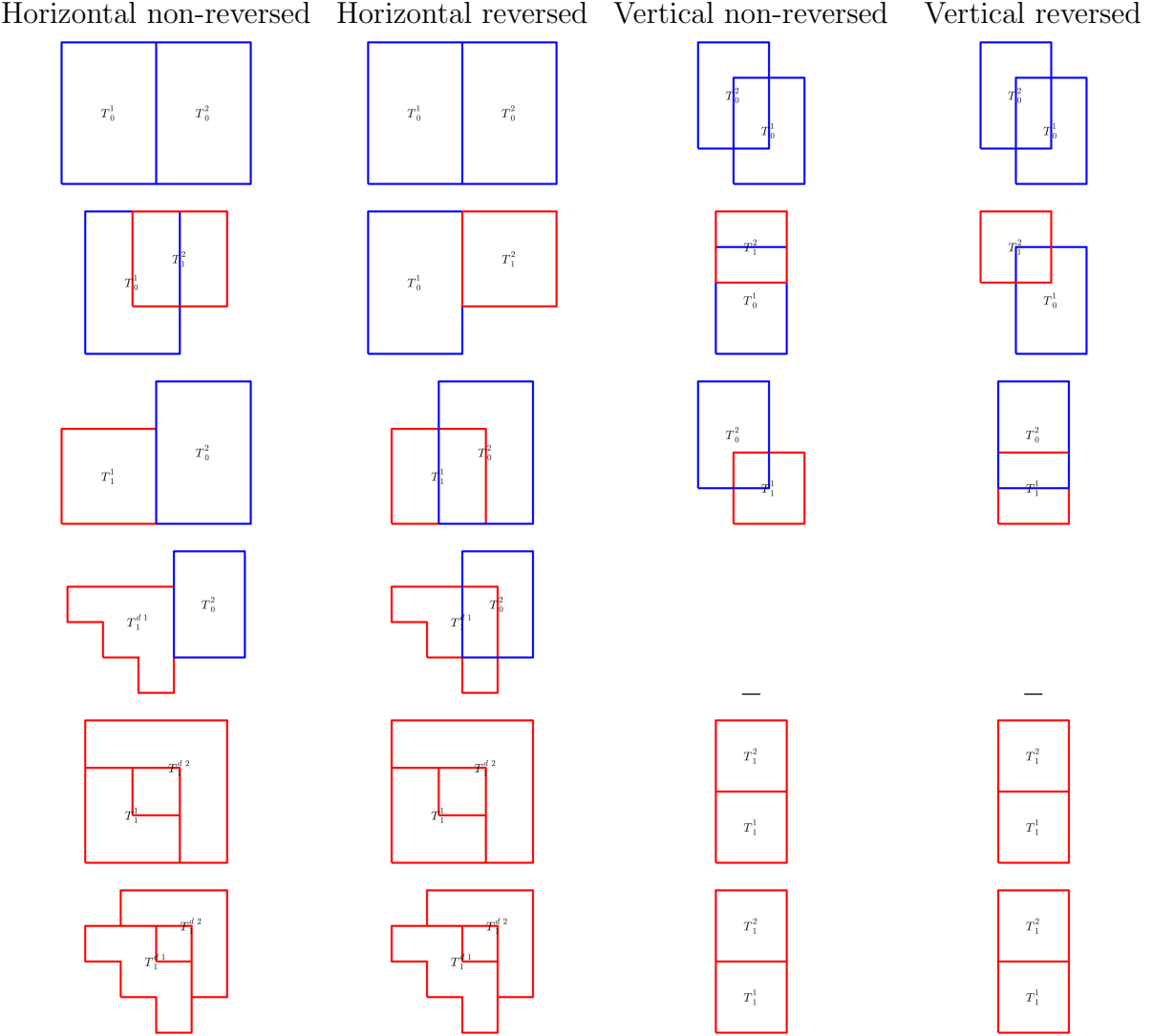


TABLE 1. Possible pairwise overlaps in a zero-one boundary string with labeling as Figure 10.

5.5. Function data. We now associate function data to zero-one boundary strings. Recall the affine offsets associated to the hyperbola bases,

$$\begin{aligned} a_{p,1} &= 0 & a_{p,2} &= -i \\ a_{q,1} &= 0 & a_{q,2} &= 1 - i, \end{aligned}$$

for $p, q = 0/1, 1/1$.

The *zero-odometer* is any translation of $o_{0/1} : T_{0/1} \rightarrow \mathbb{Z}$, defined by $o_{0/1}(0) = o_{0/1}(1) = o_{0/1}(i) = o_{0/1}(1+i) = 0$ and $o_{0/1}(2i) = o_{0/1}(1+2i) = -1$. The *one-odometer* is any translation of $o_{1/1} : T_{1/1} \rightarrow \mathbb{Z}$, defined by $o_{1/1}(0) = o_{1/1}(1) = o_{1/1}(1+i) = 0$ and $o_{1/1}(i) = -1$. The *enlarged one-odometer* is any translation of $o_{1/1}^d : T_{1/1}^d \rightarrow \mathbb{Z}$ defined by $o_{1/1}^d = o_{1/1}$ on T_1 and $o_{1/1}^d(i-1) = -2$, $o_{1/1}^d(1-i) = 0$.

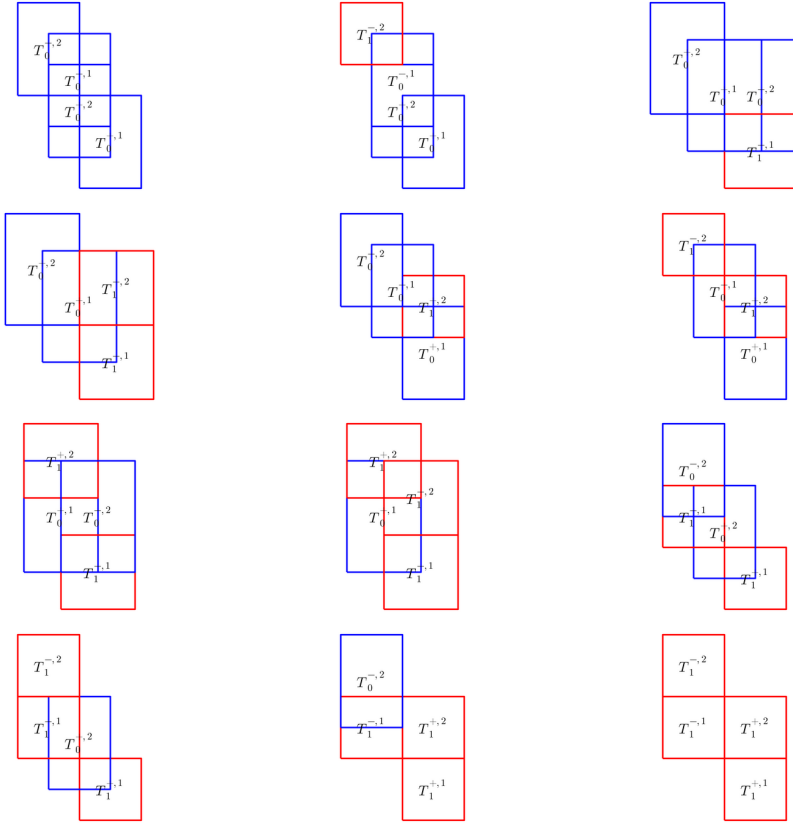


FIGURE 14. Twelve possible overlaps in a stacked zero-one vertical boundary string with labeling as Figure 10.

A sequence of zero/one-odometers $\{o_i\}$ respects a zero-one boundary string $\{T_i\}$ if each successive tile T_i is the domain of o_i and

$$(47) \quad \begin{aligned} s(o_{i+1}) - s(o_i) &= a_{i,j} && \text{not reversed case} \\ s(o_{i+1}) - s(o_i) &= a_{i,j} + (a_{i,j'} - a_{i+1,j'}) && \text{reversed case,} \end{aligned}$$

where $(j, j') \in \{1, 2\}$ are the direction and perpendicular direction respectively.

From Figure 13, one can see some consecutive pairs of tiles do not overlap. This means odometers corresponding to such tiles may blow up across the boundary. We fix this by requiring a further compatibility relation between pairs of non-overlapping tiles. We assume that if T_1, T_2 are a consecutive sequence of horizontal tiles that do not overlap then, after a shared translation, o_i and o_{i+1} are constant across the shared boundary. That is, after the translation, $o_i(x) = o_{i+1}(y)$ for all $|y - x| = 1$. In the vertical case, if T_i and T_{i+1} do not overlap, then they must both be type 1/1; we assume that after a shared translation, $o_{i+1}(y) - o_i(x) = -1$ for $|y - x| = 1$.

We now check existence, using Lemma 5.4.

Lemma 5.5. *Given any word w , a sequence of zero-one odometers with a common extension which respects its boundary string or its reversal exists. Moreover, if w is an almost palindrome, then there exists a sequence of odometers $\{o_i^+\}$, and $\{o_i^-\}$ respecting $\mathcal{B}_w = \{T_i^+\}$ and a sequence $\{o_i^-\}$ respecting the reversed string $\mathcal{B}_{\text{rev}(w)}^r$ which have a common extension to the*

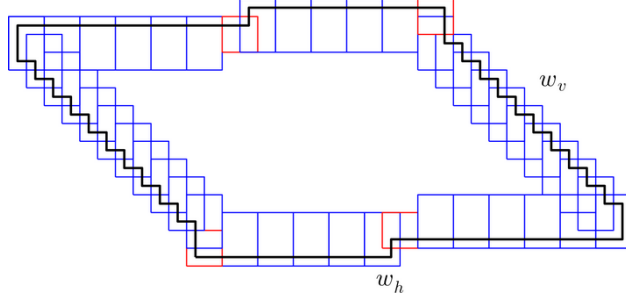


FIGURE 15. The boundary of a (w_h, w_v) -pseudo-square tile where w_h is the horizontal word qp^kqp^{k+1} and w_v is the vertical word $p^{2k+1}q$ for $k = 5$. The boundary word is outlined in the dual lattice in black.

stacked string where $s(o_{1/1}^+) - s(o_{1/1}^-) = 0$ in the vertical case and $s(o_{1/1}^+) - s(o_{1/1}^-) = a_{p,2}$ in the horizontal case.

Proof. From the definitions, one can see that no three consecutive pairs of tiles in a boundary string can overlap - only two consecutive pairs can. Therefore, existence of a sequence of zero/one odometers respecting a boundary string reduces to checking compatibility between partial odometers for pairwise consecutive tiles. Since compatibility is an affine invariant relationship, we can translate so that the first odometer is exactly $o_{1/1}$ or $o_{0/1}$. This then reduces the compatibility check to a finite one, see Table 1.

The existence problem for a stacked string is similar - by Lemma 5.4, there are only twelve possible cases for overlaps between tiles in a stacked string. We have enumerated these cases in Figures 13 and 14. \square

5.6. Pseudo-square tiles and boundary strings. We now associate horizontal and vertical boundary strings to tiles and partial odometers. Let (w_h, w_v) denote almost palindromes which define zero-one horizontal and vertical boundary strings respectively.

Definition 1. A (w_h, w_v) -pseudo-square is a tile, T , which can be decomposed along its boundary into a sequence of subtiles

$$\mathcal{T}_{h,v} := \{T_{i,h}^+\} \cup \{T_{i,h}^-\} \cup \{T_{i,v}^+\} \cup \{T_{i,v}^-\}$$

each of which respectively form a w_h , $\text{rev}(w_h)$, w_v , and $\text{rev}(w_v)$ zero-one horizontal, reversed horizontal, vertical, and reversed vertical boundary string. That is, $\mathcal{T}_{h,v} \subset T$, $c(T_{1,h}^+) = c(T_{1,v}^-) = c(T)$ and $\partial T \cap \mathcal{T}_{h,v} = \partial T$.

A partial odometer $o : T \rightarrow \mathbb{Z}$ respects (w_h, w_v) if its restrictions to $\mathcal{T}_{h,v}$ respect w_h -horizontal, w_v -vertical, and $\text{rev}(w_h)$ -reversed-horizontal and $\text{rev}(w_v)$ -reversed-vertical zero-one boundary strings respectively.

We will overload notation and also refer to the word describing the boundary string as a set of tiles.

We now extend the rotation operator to pseudo-square tiles. For a binary word w , let $\mathcal{F}(w)$ denote the *flipping operator* which flips every p to a q and vice versa. Then,

$$(48) \quad \mathcal{R}(w_h, w_v) = (\mathcal{F}(w_v), \mathcal{F}(w_h))$$

sends a pair of proper almost horizontal/vertical strings to a rotated pair. We now extend this to tiles. If T is a (w_h, w_v) -pseudo-square then

$$(49) \quad \mathcal{R}(T) = T_r,$$

where T_r is a $\mathcal{R}(w_h, w_v)$ -pseudo-square with $c(T_r) = c(T)$.

We now define a map $G(w_h, w_v) \in F_2^*$ to $(w_1, w_2) \in F_2$. We start by defining it for pairs of horizontal zero-one tiles (strings),

$$(50) \quad \begin{cases} g(p * q) & \rightarrow 1 * i \\ g(q * p) & \rightarrow 1 * 1 \\ g(q_d * p) & \rightarrow i * 1 \\ g(p * p) & \rightarrow 1 * 1 \\ g(q * q) & \rightarrow i * 1 \\ g(q_d * q) & \rightarrow i * 1, \end{cases}$$

where q_d indicates a $T_{1/1}^d$ tile. Next extend the map to w_h by,

$$(51) \quad G(w_h) = g(w_h[1 : 2]) * g(w_h[2 : 3]) * \dots * g(w_h[|w_h| - 1, |w_h|]) * 1$$

and extend this to w_v by

$$(52) \quad G(w_v) = i \cdot G(\mathcal{F}(w_h)),$$

where $i \cdot w_1$ denotes component multiplication (for example, $i \cdot (i * 1) = -1 * i$). And finally, extend the map pairwise $G(w_h, w_v) = (G(w_h), G(w_v))$.

Our next lemma uses this to express (w_h, w_v) pseudo-squares using the boundary words from Section 4. See Figures 16 and 15 for an illustration of this.

Lemma 5.6. *The boundary word of (w_h, w_v) -pseudo-square T can be written as $w_1 * w_2 * \widehat{\text{rev}}(w_1) * \widehat{\text{rev}}(w_2)$ where $(w_1, w_2) = G(w_h, w_v)$. This implies T is 180-degree symmetric, and $\mathcal{R}(T)$ is a 90-degree rotation of T .*

Proof. We first check that $G(w_h)$ traces out the lower boundary of w_1 . By checking Table 1, we see that the (50) does traces out the lower boundary for each pair of tiles. Indeed, if neither tile in the pair (T^1, T^2) is $T_{1/1}^d$, the path starts at $c(T^1)$ and ends at $c(T^2)$. Otherwise, the path starts or ends at $c(T_{1/1}^d) + (1 - i)$. The extra $*1$ in (51) ensures the path ends at the lower right corner of $T_{0/1}$. The lower right corner of $T_{0/1}$, after a 90-degree clockwise rotation maps to the lower-left corner of $T_{1/1}$. In general, the lower boundary of every pair of horizontal tiles in Table 1 maps to the right boundary of the flipped pair of vertical tiles. We can also use the table to check that the reversed string $\text{rev}(w_h)$ is a 180-degree rotation of w_h , thus $\text{rev}(w_1)$ traces the top boundary of $\text{rev}(w_h)$.

□

This next lemma shows that if a partial odometer respects a pseudo-square, then it has a common extension to the plane.

Lemma 5.7. *Let T be a (w_h, w_v) -pseudo-square, $(w_1, w_2) = G(w_h, w_v)$, and suppose $o : T \rightarrow \mathbb{Z}$ respects (w_h, w_v) . If the conditions in Lemma 4.1 are met, then, T generates a $(v_1, v_2) := (\sum w_1 + i, \sum w_2 - 1)$ regular almost-tiling.*

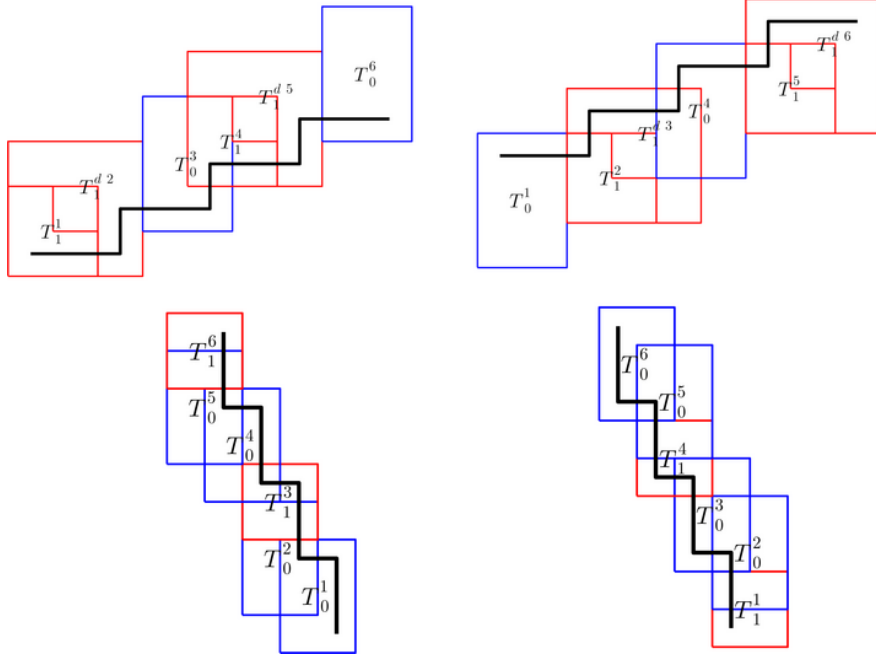


FIGURE 16. From top left to bottom right, $w_h = q^2pq^2p$, reversed $\text{rev}(w_h)$, $w_v = \mathcal{F}(w_h)$, reversed $\text{rev}(w_v)$. The boundary words, $G(w_h, w_v)$ are drawn in black.

Further suppose $(v_1, v_2) = v_{n/d,1}, v_{n/d,2}$ for some reduced fractions $0 < n/d < 1$. Then, the surrounding of T with respect to $(v_{n/d,1}, v_{n/d,2})$ consists of two stacked zero-one horizontal and two vertical boundary strings and

$$(53) \quad o(x \pm v_{n/d,i}) = o(x) \pm a_{n/d,i} \cdot x + k_{n/d,\pm i} \quad \text{for } x \in \mathbb{Z}^2,$$

where $k_{n/d,\pm i}$ are constants and $i \in \{1, 2\}$ selects the lattice vector, is a common extension of $o : T \rightarrow \mathbb{Z}$ to the plane.

Proof. The first claim follows from Lemmas 5.6 and 4.1. We next check that the interfaces $(T, T \pm v_{n/d,2})$ and $(T, T \pm v_{n/d,1})$ are stacked horizontal or vertical zero-one boundary strings respectively.

Let A be the horizontal string for T and B the reversed horizontal string for $T - v_{n/d,2}$. By Lemma 5.6, the first tile in B is located at $c(T) - v_{n/d,2} + v_{n/d,2} - (2i - 1)$. Thus, the offset between the first tile in B and the first tile in A is $2i - 1 = v_{0/1,2} + i$, the correct initial offset for a stacked string.

Similarly if C is the vertical string for T and D the reversed vertical string for $T + v_{n/d,1}$, then the offset between the respective first tiles in C and D is $(i + 1) = -v_{1/1,1}$. The other two interfaces are stacked strings by the above arguments for $T - v_{n/d,1}$ and $T + v_{n/d,2}$.

Let $\mathcal{T} = \{T + i \cdot v_{n/d,1} + j \cdot v_{n/d,2}\}$ denote the almost tiling of T and for $T_{i,j} \in \mathcal{T}$, let $o_{i,j} : T_{i,j} \rightarrow \mathbb{Z}$ denote the translations of o by $(i \cdot v_{n/d,1} + j \cdot v_{n/d,2}, i \cdot a_{n/d,1} + j \cdot a_{n/d,2})$. By definition, each $o_{i,j}$ respects (w_h, w_v) on $T_{i,j}$. Restrict the $o_{i,j}$ to the stacked boundary strings and check, by repeating the above argument, that the slope difference between the first two perpendicular tiles in the stacked horizontal strings are $-a_{p,2}$. Similarly, the slope

difference for the stacked vertical strings is $a_{q,1} = 0$. Therefore, by Lemma 5.5, each pair of odometers is compatible. This together with Lemma 9.1 implies there is a common extension of $o : T \rightarrow \mathbb{Z}$ to the plane as (53). \square

We also require the notion of a tile odometer respecting only a horizontal boundary or vertical boundary string.

Definition 2. A $w_{h/v}$ -pseudo-square is a tile, T , whose boundary contains (but may not be equal to)

$$\mathcal{T}_{h,*} = \{T_{i,h}^+\} \cup \{T_{i,h}^-\}$$

or

$$\mathcal{T}_{*,v} = \{T_{i,v}^+\} \cup \{T_{i,v}^-\},$$

where T are as in Definition 1 and either $c(T) = c(T_{1,h}^+)$ or $c(T) = c(T_{1,v}^-)$

A partial odometer $o : T \rightarrow \mathbb{Z}$ respects $w_{h/v}$ if its restriction to $\mathcal{T}_{h,*}$ are w_h -horizontal and $\text{rev}(w_h)$ -reversed-horizontal strings or its restriction to $\mathcal{T}_{*,v}$ are w_v and and $\text{rev}(w_v)$ -reversed-vertical zero-one boundary strings respectively.

5.7. Explicit formulas for zero-one boundary strings. We collect in this section some explicit formulas for zero-one boundary strings. In particular, these will correspond to the degenerate base cases in (32). At first read, this section may be skipped.

5.7.1. Horizontal boundary strings. We first note the form of the odometers after a translation. The zero-odometer translated by $-a_{p,2}$, $\hat{o}_{0/1} : T_{0/1} \rightarrow \mathbb{Z}$ is given by $\hat{o}_{0/1}(0) = \hat{o}_{0/1}(1) = -1$ and $\hat{o}_{0/1}(i) = \hat{o}_{0/1}(1+i) = 0 = \hat{o}_{0/1}(2i) = \hat{o}_{0/1}(1+2i) = 0$. The one-odometer translated by $-a_{q,2}$, $\hat{o}_{1/1} : T_{1/1} \rightarrow \mathbb{Z}$ is given by $\hat{o}_{1/1}(0) = \hat{o}_{1/1}(i) = \hat{o}_{1/1}(1+i)$ and $\hat{o}_{1/1}(1) = -1$. Similarly, the enlarged one-odometer translated by $-a_{q,2}$, $\hat{o}_{1/1}^d : T_{1/1}^d \rightarrow \mathbb{Z}$ is given by $\hat{o}_{1/1}^d = \hat{o}_{1/1}$ on $T_{1/1}$ and $\hat{o}_{1/1}(1-i) = -2$, $\hat{o}_{1/1}(i-1) = 0$.

Now, let $(\{o_i^-\})\{o_i^+\}$ respect an arbitrary (reversed) horizontal boundary string. If $o_1^+ \in \{o_{0/1}, o_{1/1}\}$, then, $o_i^+ \in \{o_{0/1}, o_{1/1}\}$ depending on the respective letter. Similarly, if $o_1^- \in \{\hat{o}_{0/1}, \hat{o}_{1/1}\}$ then $o_i^- \in \{\hat{o}_{0/1}, \hat{o}_{1/1}\}$.

Proof. This is immediate from the construction above. \square

5.7.2. Vertical boundary strings. The vertical boundary string case involves more computations since the translations involve non-zero affine factors. Fix $k \geq 1$. The following functions, corresponding to the quadratic growth of the hyperbola bases appear, depending on the string:

$$(54) \quad t(j) = -j(j+1)/2 \quad q(j) = \lfloor \frac{j^2}{4} \rfloor$$

In each case, let $(\{o_i^-\})\{o_i^+\}$ respect the indicated (reversed) vertical boundary string.

Case 1: $p^k q$ and its reversal. Suppose $o_1^+ = o_{0/1}$ on $T_{1/1}$, the first tile in $p^k q$. Then, for $1 \leq j \leq k$

$$(55) \quad o_j^+ = \begin{bmatrix} t(j) & t(j) \\ t(j-1) & t(j-1) \\ t(j-2) & t(j-2) \end{bmatrix}$$

and

$$(56) \quad o_{k+1}^+ = \begin{bmatrix} t(k+1) & t(k+1)+1 \\ t(k) & t(k) \end{bmatrix}.$$

If $o_1^- = o_{0/1}$ on $T_{0/1}$, the first tile in $\text{rev}(p^k q)$, then

$$(57) \quad o_j^- = \begin{bmatrix} t(j+1)+2 & t(j+1)+3 \\ t(j)+1 & t(j)+2 \\ t(j-1) & t(j-1)+1 \end{bmatrix}$$

for $2 \leq j \leq k+1$.

Case 2: pq^k and its reversal. Suppose $o_1^+ = o_{0/1}$ on $T_{0/1}$, the first tile in pq^k . Then for $2 \leq j \leq k+1$, $j' = 2(j-1)$

$$(58) \quad o_j^+ = \begin{bmatrix} q(j'+2)+1 & q(j'+1) \\ q(j'+1)+1 & q(j') \end{bmatrix}.$$

If $o_{1/1}^- = o_{1/1}$ on $T_{1/1}$, the first tile in $\text{rev}(pq^k)$ then for $1 \leq j \leq k$

$$(59) \quad o_j^- = \begin{bmatrix} q(2j) & q(2j-1) \\ q(2j-1) & q(2j-2) \end{bmatrix}$$

and

$$(60) \quad o_{k+1}^- = \begin{bmatrix} q(2k+2) & q(2k+1)-1 \\ q(2k+1) & q(2k) \\ q(2k) & q(2k-1) \end{bmatrix}.$$

Case 3: $pq^k pq^{k+1}$ and its reversal. Suppose $o_{1/1}^+ = o_{0/1}$ on $T_{0/1}$, the first tile in $pq^k pq^{k+1}$. Then o_j^+ for $1 \leq j \leq (k+1)$ are as Case 2 above. Then

$$(61) \quad o_{k+2} = \begin{bmatrix} q(2(k+1)+3)+3 & q(2(k+1)+2)+1 \\ q(2(k+1)+2)+3 & q(2(k+1)+1)+1 \\ q(2(k+1)+1) & q(2(k+1))+1 \end{bmatrix}$$

and for $k+3 \leq j \leq 2k+3$, $j'' = 2(j-2)$

$$(62) \quad o_j = \begin{bmatrix} q(j''+4)+3 & q(j''+3)+1 \\ q(j''+3)+3 & q(j''+2)+1 \end{bmatrix}.$$

If $o_{1/1}^- = o_{1/1}$ on $T_{1/1}$, the first tile in $\text{rev}(pq^k pq^{k+1})$ then o_j^- for $1 \leq j \leq (k+2)$ the first $(k+2)$ are as Case 2 above. Then, for $(k+3) \leq j \leq 2k+2$,

$$(63) \quad o_j^- = \begin{bmatrix} q(2(j-1)+2)+1 & q(2(j-1)+1) \\ q(2(j-1)+1)+1 & q(2(j-1)) \end{bmatrix}$$

and for $w = 2(k + 1)$

$$(64) \quad o_{2k+3}^- = \begin{bmatrix} q(2w+2)+1 & q(2w+1) \\ q(2w+1)+1 & q(2w) \\ q(2w)+1 & q(2w-1) \end{bmatrix}.$$

Proof. These are verified directly by induction and the definition of translation. \square

6. BASE CASES

Before we extend the hyperbola recursion to all odometers and tiles, we study a degenerate family and in fact prove Theorem 1.3 for this family. The reader is encouraged to skim or skip this section and come back to it after reading the general recursive algorithm.

The reduced fractions which we analyze here are those in a Farey quadruple where at least one of the two parents is $(0/1)$ or $(1/1)$. Specifically, we prove the following.

Proposition 6.1. *For each Farey quadruple of the form $\mathbf{q}_{(w)} = (p_1, q_1, p_2, q_2)$ where $w = 3^k$ or 2^k for $k \geq 0$ there is a quadruple of standard and alternate tile odometers*

$$(o_{p_1}, o_{q_1}, o_{p_2}, o_{q_2}) \quad \text{and} \quad (\hat{o}_{p_1}, \hat{o}_{q_1}, \hat{o}_{p_2}, \hat{o}_{q_2})$$

with finite domains, $T(o_{n/d}) = T_{n/d}$ and $T(\hat{o}_{n/d}) = \hat{T}_{n/d}$. The tile odometers of each such child Farey pair satisfy the following properties.

- (a) Under the lattice $L'(n/d)$, $T(n/d)$ generates an almost pseudo-square tiling
- (b) $\hat{T}(n/d)$ covers \mathbb{Z}^2 under $L'(n/d)$
- (c) There exist unique, distinct recurrent extensions $o_{n/d} : \mathbb{Z}^2 \rightarrow \mathbb{Z}$ and $\hat{o}_{n/d} : \mathbb{Z}^2 \rightarrow \mathbb{Z}$ satisfying the correct growth dictated by 9.
- (d) $T(n/d)$ is a (w_h, w_v) -pseudo-square which $o_{n/d}$ respects:

Standard case		w_h	w_v
3^k odd, $k \geq 1$	$1/d, d \geq 4$ even	$qp^k qp^{k+1}$	$p^{2k+1}q$
3^k even, $k \geq 0$	$1/d, d \geq 3$ even	qp^{k+1}	$p^{2(k+1)}q$
2^k odd, $k \geq 0$	$\mathcal{R}(1/d)$ $d \geq 3$ even	$q^{2(k+1)}p$	pq^{k+1}
2^k even, $k \geq 1$	$\mathcal{R}(1/d), d \geq 4$ even	$q^{2k+1}p$	$pq^k pq^{k+1}$

The first column denotes a word which selects a degenerate Farey quadruple and the parity of the reduced fraction displayed in the second column.

- (e) $\hat{T}(n/d)$ is a w_h/v -pseudo-square which $\hat{o}_{n/d}$ respects:

Alternate case		w_h	w_v
3^k odd, $k \geq 1$	$1/d, d \geq 4$ even	-	$p^{2k+1}q$
3^k even, $k \geq 0$	$1/d, d \geq 3$ even	qp^{k+1}	-
2^k odd, $k \geq 0$	$\mathcal{R}(1/d)$ $d \geq 3$ even	-	pq^{k+1}
2^k even, $k \geq 1$	$\mathcal{R}(1/d), d \geq 4$ even	$q^{2k+1}p$	-

In particular, the alternates coincide with the standards on one set of parallel boundaries.

- (f) Some later odometers contain exact translations of earlier odometers. To state this succinctly, write $w(p, q)$ for the even and odd reduced fraction in the child Farey pair of $\mathbf{q}_{(w)}$ and let $T(n/d)(v) = T(n/d) \cup (T(n/d) + v)$ for $v \in \mathbb{Z}[i]$ and $n/d \in \{p, q\}$.

The following holds for all $k \geq 1$:

$$(65) \quad \begin{aligned} T(3^k(p)) &\supset T(q, v_{q,1} + v_{p,1} + v_{p,2}) & \text{offset} = 0 \\ \hat{T}(3^k(p)) &\supset T(q, v_{q,1} + v_{p,1} + 2v_{p,2}) & \text{offset} = 0 \\ \hat{T}(3^k(q)) &\supset T(q, -v_{q,1} - v_{p,1}) & \text{offset} = v_{p,2} + v_{p,1} \end{aligned}$$

where $(p, q) = 3^{k-1}(p, q)$ and

$$(66) \quad \begin{aligned} T(2^k(q)) &\supset T(p, v_{p,2} + v_{q,2} - v_{q,1}) & \text{offset} = v_{q,1} \\ \hat{T}(2^k(q)) &\supset T(p, v_{p,2} + v_{q,2} - 2v_{q,1}) & \text{offset} = v_{q,1} \\ \hat{T}(2^k(p)) &\supset T(p, v_{p,2} + v_{q,2}) & \text{offset} = v_{q,1} \end{aligned}$$

where $(p, q) = 2^{k-1}(p, q)$. The third column records $c(T_1) - c(T_2)$ where T_1 is the tile in the second column and T_2 is the tile in the first column.

The tile odometers for $k \geq 1$ have an analogous decomposition with affine factors and translations dictated by (65) and (66). For example, the restriction of $o_{3^k(p)}$ to $T(q, v_{q,1} + v_{p,1} + v_{p,2})$ is exactly equal to translated earlier tile odometers, $o_q^1 \cup o_q^2$ where $c(T(o_q^1)) - c(T_{o_{3^k(p)}}) = 0$, $T(o_q^1) \cup T(o_q^2) = T(q, v_{q,1} + v_{p,1} + v_{p,2})$, $s(o_q^1) - s(o_q^2) = a_{p,2}$, and $s(o_q^2) - s(o_{3^k(p)}) = 0$.

- (g) Some later odometers contain partial translations of earlier odometers. The following holds for all $k \geq 1$ (using the same notation as the previous item):

$$(67) \quad T(3^k(q)) \supset T(q, v_{p,1} + 2v_{p,2}) \quad \text{offset} = 0$$

where $(p, q) = 3^{k-1}(p, q)$ and

$$(68) \quad T(2^k(p)) \supset T(p, -2v_{q,1} + v_{q,2}) \quad \text{offset} = 2v_{q,1}$$

where $(p, q) = 2^{k-1}(p, q)$. The tile odometers for $k \geq 1$ have an analogous decomposition (as in the previous item) but only after removing two corner cells from each of the subtiles on the right-hand-side:

$$(69) \quad T^{sm}(q) = T(q) \setminus \{c_1 \cup c_2\} \quad \text{where } (p, q) = 3^{k-1}(p, q)$$

where $c_1 = c(T(q))$ and $c_2 = c_1 + (v_{q,1} + v_{q,2} - v_{p,2})$ and

$$(70) \quad T^{sm}(p) = T(p) \setminus \{c'_1 \cup c'_2\} \quad \text{where } (p, q) = 2^{k-1}(p, q)$$

where $c'_1 = c(T(p)) + v_{p,1} - i$ and $c'_2 = c(T(p)) + v_{p,2} + 1$.

This family will form a base case for the general recursion in the subsequent section. As noted above, there is a recursive structure here but with some ‘errors’ in the full decomposition. If the tile sizes are reduced to avoid these errors, then later tiles will be too small to cover \mathbb{Z}^2 .

Since these errors are limited to the degenerate family and the odometers for this family are so simple, we take the cumbersome but elementary approach and provide the exact formulas. One could avoid this by adding additional cases to the general recursion, however, a benefit here is that we can easily show these base cases satisfy a slightly stronger recurrence property as specified exactly in the last subsection. We then use this property to show recurrence inductively in the general recursion.

6.1. Base points. We first check that the base points of the hyperbola $0/1$ and $1/1$, are on $\partial\Gamma_F$ via an explicit construction. We recall a criteria for checking recurrence from the sandpile literature. Let $s : \mathbb{Z}^2 \rightarrow \mathbb{Z}$ and let H be a finite induced subgraph of the F -lattice. H is *allowed* for s if there is a vertex v of H where $s(v)$ is at least the in-degree of v in H and otherwise is *forbidden*.

Proposition 6.2. [HLM⁺08] *An integer superharmonic function g is recurrent if and only if every nonempty induced subgraph of the F -lattice is allowed for $s := \Delta g + 1$.*

In particular, Proposition 6.2 reduces verifying recurrence of a function to checking a condition on its Laplacian (which is no surprise given the function s in the statement is usually referred to as a recurrent sandpile [LP10]).

Lemma 6.1. *The functions*

$$g_{0/1}(x) = -\frac{x_2(x_2+1)}{2} \quad g_{1/1}(x) = -\lfloor \frac{(x_2-x_1)^2}{4} \rfloor$$

are odometers for $0/1$ and $1/1$ respectively.

Proof. The growth condition can be checked using the definition (2). Moreover, $\Delta g_{0/1}(x) = \Delta g_{1/1}(x) = -1\{(x_1+x_2)\text{ is even}\}$. By Proposition 6.2 it remains to check that every nonempty induced subgraph H of the F -lattice is allowed for $s = 1\{(x_1+x_2)\text{ is odd}\}$. Let x denote the lower left vertex of H . That is x has minimal x_2 coordinate and of all other $y \in H$ with $y_2 = x_2$, x_1 is minimal. This implies the only possible neighbors of x in H are $x+e_1$ or $x+e_2$. If (x_1+x_2) is odd, then, $s(x) = 1$ so we may suppose otherwise. If $(x+e_1) \in H$, then $s(x+e_1) = 1$ and by the location of x , $(x+e_1-e_2) \notin H$, thus $s(x+e_1)$ is larger than its in-degree in H , completing the proof. \square

6.2. Staircases. The *staircase* fractions are the reduced fractions of the form $\frac{1}{d}$ for d odd and their rotations, $\mathcal{R}(1, d) = (\frac{d-1}{2}, \frac{d+1}{2})$. These fractions are the even child or odd child in Farey quadruples with words 3^k or 2^k for $k \geq 0$ respectively. As the construction will indicate, the tiles and Laplacians of odometers will respect the rotational invariance from Lemma 3.6.

We start with the standard even child of \mathbf{q}_{3^k} for $k \geq 0$.

Lemma 6.2. *For each $d \geq 3$ odd,*

$$T_{1/d} := \{(x_1, x_2) \in [2-d, d] \times [0, d+1] : 1 \leq (x_1+x_2) \leq (d+2)\} \cup \{(0, 0), (2, d+1)\}$$

is a $(qp^{k+1}, p^{2(k+1)}q)$ -pseudo-square which $g_{1/d} : T_{1/d} \rightarrow \mathbb{Z}$, given by,

$$g_{1/d}(x) = -\frac{1}{2}x_2(x_2+1) + (x_2 + \min(x_1-1, 0)) + 1\{(x_1, x_2) \in \{(0, 0), (2, d+1)\}\}$$

respects.

Proof. We start by observing that the bottom boundary of $T_{1/d}$ is qp^{k+1} zero-one horizontal boundary string. Indeed,

$$T_{1/d} \supset A_1 \cup A_2 := \{[0, 1] \times [0, 1]\} \cup \{[2, d] \times [0, 2]\}$$

is a qp^{k+1} horizontal boundary string:

$$A_1 = T_{1/1} \quad A_2 = v_{p,1} + \bigcup_{j=1}^{k+1} (T_{0/1} + jv_{p,1})$$

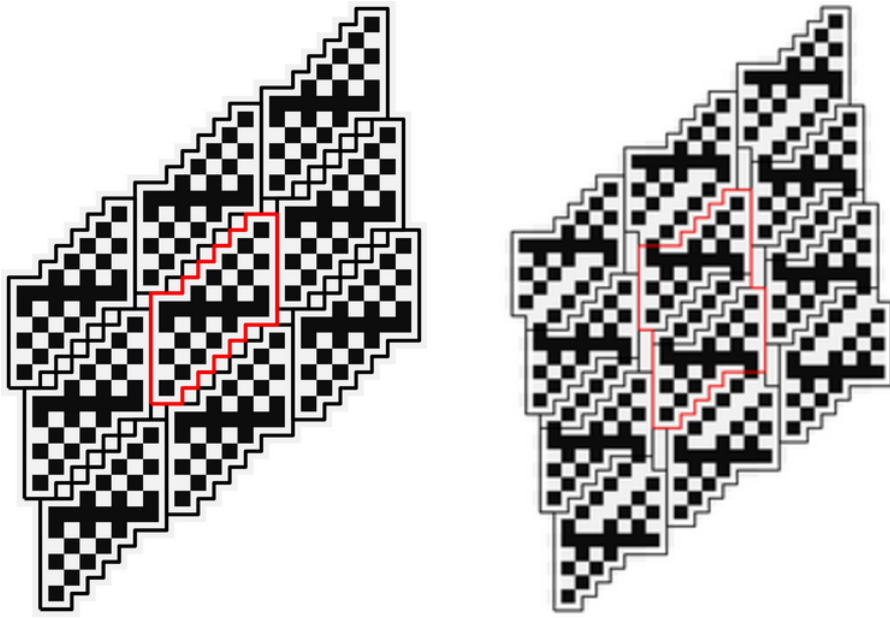


FIGURE 17. A period of the Laplacian of a staircase odometer on the left and its alternate. The string is 22 and the fraction is $3/4$. Each tile is outlined in the dual lattice.

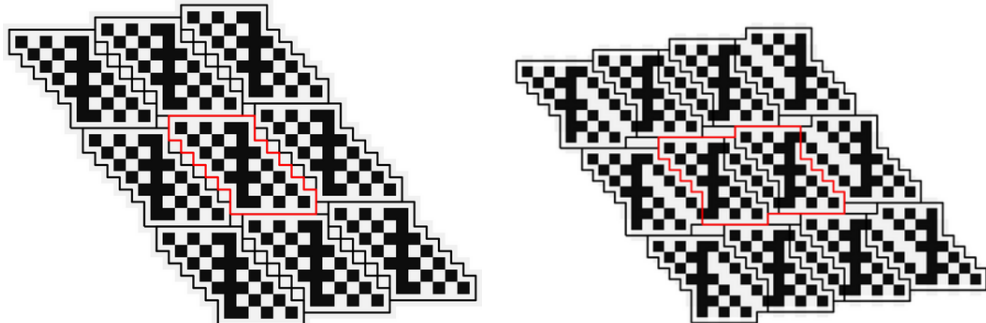


FIGURE 18. The rotated standard and alternate staircase odometers of Figure 17. The string is 33 and the fraction is $1/7$.

Moreover an inspection of the formula shows that $g_{1/d} = o_{1/1}$ on A_1 and $g_{1/d} = o_{0/1}$ on the translations of $T_{0/1}$ which form A_2 .

The top boundary of $T_{1/d}$ is a $\text{rev}(p^{k+1}q)$ zero-one horizontal reversed boundary string. Indeed,

$$T_{1/d} \supset A_2^r \cup A_1^r := \{[2-d, 0] \times [d-1, d+1]\} \cup \{[1, 2] \times [d, d+1]\}$$

is a $p^{k+1}q$ zero-one reversed horizontal boundary string:

$$A_2^r = \bigcup_{j=0}^k \{T_{0/1} + jv_{p,1}\} \quad A_1^r = T_{1/1} + kv_{p,1} + v_{q,1} + 1.$$

To check that $g_{1/d}$ respects the string, it is convenient to consider the translation

$$g_{1/d}^r = g_{1/d} - (1, -d) \cdot x - \frac{1}{2}d(d+1) + 1$$

and recall the translated versions of the zero-one odometers, $\hat{o}_{1/1}$ and $\hat{o}_{0/1}$ defined in Section 5.7.1. Once we make this translation, we can use the formula to compute

$$g_{1/d}^r([1, 2] \times [d, d+1]) = \hat{o}_{1/1} = \begin{bmatrix} 0 & 0 \\ 0 & -1 \end{bmatrix}$$

and $g_{1/d}^r([2-d, 0] \times [d-1, d+1]) = 0$ and $g_{1/d}^r([2-d, 0], d-1) = -1$ which coincides with copies of $\hat{o}_{0/1}$.

The check for the right and left boundaries proceeds by comparing to the explicit formulas for the degenerate zero-one strings given in Section 5.7.2. We use the notation defined there. We first check that the right-boundary is a $p^{2(k+1)}q$ string by observing

$$T_{1/d} - (d-1, 0) \supset A_1 \cup A_2 := \bigcup_{j=0}^{2(k+1)-1} (T_{1/1} + j \cdot v_{p,2}) \cup (T_{0/1} + (2(k+1)-1)v_{p,2} + v_{q,2}).$$

Indeed, the upper right corner of each $v_{p,2}$ translation of $T_{1/1}$ satisfies the equality $x_1 + x_2 = 3$ and the upper right corner of $T_{0/1} + (2(k+1)-1)v_{p,2} + v_{q,2}$ is $(3-d, d+1)$. To check the formula matches (55) observe that on $A_1 \cup A_2 + (d-1, 0)$, $g_{1/d} = -\frac{1}{2}x_2(x_2+1) + x_2$. And so, on each $T_j := T_{1/1} + (j-1) \cdot v_{p,2} + (d-1, 0)$,

$$g_{1/d} \upharpoonright_{T_j} = \begin{bmatrix} t(j+1) & t(j+1) \\ t(j) & t(j) \\ t(j-1) & t(j-1) \end{bmatrix} + \begin{bmatrix} j+1 & j+1 \\ j & j \\ j-1 & j-1 \end{bmatrix} = \begin{bmatrix} t(j) & t(j) \\ t(j-1) & t(j-1) \\ t(j-2) & t(j-2) \end{bmatrix}.$$

The formula also implies it coincides with (56) on A_2 .

The argument for the left boundary is symmetric. Start by observing

$$T_{1/d} \supset A_1 \cup A_2 := T_{0/1} \cup \bigcup_{j=0}^{2(k+1)-1} (T_{1/1} + j \cdot v_{p,2} + i).$$

Since, on the left boundary $g_{1/d} = -\frac{1}{2}x_2(x_2+1) + (x_1 + x_2 - 1)$, $g_{1/d} \upharpoonright_{A_1} = o_{0/1}$. The lower left corner of each $T_j := T_{1/1} + i + (j-2) \cdot v_{p,2}$ for $2 \leq j \leq 2(k+1)+1$ lies on the left boundary, $(x_1 + x_2) = 1$. Hence,

$$g_{1/d} \upharpoonright_{T_j} = \begin{bmatrix} t(j+1) & t(j+1) \\ t(j) & t(j) \\ t(j-1) & t(j-1) \end{bmatrix} + \begin{bmatrix} 2 & 3 \\ 1 & 2 \\ 0 & 1 \end{bmatrix}$$

which is exactly (57). \square

Next is the standard odd child of \mathbf{q}_{2^k} .

Lemma 6.3. *For each $p_1 = \frac{\frac{d-1}{2}}{\frac{d+1}{2}}$, $d \geq 3$ odd,*

$T_{p_1} := \{(x_1, x_2) \in [0, d+1] \times [1, 2d-1] : -1 \leq (x_2 - x_1) \leq d\} \cup \{(0, d+1), (d+1, d-1)\}$ is a $(q^{2(k+1)}p, pq^{(k+1)})$ -pseudo-square which $g_{p_1} : T_{p_1} \rightarrow \mathbb{Z}$, given by,

$$g_{p_1}(x) = -\lfloor \frac{(x_2 - x_1)^2}{4} \rfloor + \min(d - x_2, 0) + 1\{x \in \{(0, d+1), (d+1, d-1)\}\} \quad \text{for } x \in T_{p_1}$$
 respects.

Proof. The computations are identical to that of previous Lemma. In this case, the vertical strings match the formula given by (58), (59), (60). \square

We next construct the alternate staircase odometers. By Lemma 5.6, each of the tile odometers defined in the previous two lemmas have a common extension to \mathbb{Z}^2 under $L'(n/d)$. However, in the next two cases, we require a different argument as the alternate odometers overlap in the tiling. We start with the alternate even child of \mathbf{q}_{3^k}

Lemma 6.4. *For each $d \geq 3$ odd, there is a unique function $\hat{g}_{1/d} : \mathbb{Z}^2 \rightarrow \mathbb{Z}$ with*

$$\begin{aligned}\hat{g}_{1/d}(x) = & -\frac{1}{2}x_2(x_2+1) + \min(0, 2-x_1) + \min(0, d-2+x_1) \quad \text{for } x \in \hat{T}_d \\ & + \max(x_1+x_2-2, 0) + 1_{A \cup B}\end{aligned}$$

where

$$\begin{aligned}A &= \{-(d-1) \times [-1, 0]\} \cup \{3 \times [d, d+1]\} \\ B &= \{(x_1, x_2) : (x_1 + x_2) = 2 \text{ and } 0 < x_2 < d\} \\ C &= \{-1 \times [1-d, 0]\} \cup \{(d+1) \times [4-d, 3]\} \\ D &= \{(x_1, x_2) \in [4-2d, d] \times [0, d] : -d+2 \leq x_1 + x_2 \leq d+2\} \\ \hat{T}_{1/d} &= A \cup B \cup C \cup D\end{aligned}$$

and

$$\hat{g}_{1/d}(x \pm v_{1/d,i}) = \hat{g}_{1/d}(x) \pm a_{1/d,i} \cdot x + k_{1/d,i} \quad \text{for } x \in \mathbb{Z}^2,$$

where $k_{p,\pm i} \in \mathbb{Z}$ is a constant and $i \in \{1, 2\}$ selects the lattice vector. Moreover, $\hat{T}_{1/d}$ is a $w_h = qp^{k+1}$ pseudo-square which $\hat{g}_{1/d}$ respects.

Next is the alternate odd child of \mathbf{q}_{2^k} .

Lemma 6.5. *For each $p = \frac{\frac{d-1}{2}}{\frac{d+1}{2}}$, $d \geq 3$ odd, there is a unique function $\hat{g}_p : \mathbb{Z}^2 \rightarrow \mathbb{Z}$ with*

$$\begin{aligned}\hat{g}_p(x) = & -\lfloor \frac{(x_2-x_1)^2}{4} \rfloor + \min(d-x_2-1, 0) + \min((2d-1)-x_2, 0) \quad \text{for } x \in \hat{T}_p \\ & + \max((x_2-x_1)-d+1, 0) + 1_{A \cup B}\end{aligned}$$

where

$$\begin{aligned}A &= \{[-1, 0] \times 2d\} \cup \{[d, d+1] \times d-2\} \\ B &= \{(x_1, x_2) : (x_2 - x_1) = d-1 \text{ and } 0 < x_1 < d\} \\ C &= \{-1 \times [d+1, 2d]\} \cup \{(d+1) \times [d-2, 2d-3]\} \\ D &= \{(x_1, x_2) \in [0, d] \times [1, 3d-3] : -1 \leq x_2 - x_1 \leq 2d-1\} \\ \hat{T}_p &= A \cup B \cup C \cup D\end{aligned}$$

and

$$\hat{g}_p(x \pm v_{p,i}) = \hat{g}_p(x) \pm a_{p,i} \cdot x + k_{p,i} \quad \text{for } x \in \mathbb{Z}^2,$$

where $k_{p,\pm i} \in \mathbb{Z}$ is a constant and $i \in \{1, 2\}$ selects the lattice vector. The vertical boundary respects a pq^{k+1} boundary string where p is omitted.

We next record the formula for the Laplacians. Recall that $\partial T = \{x \in \mathbb{Z}^2 : \exists y \notin T \text{ such that } |y-x|=1\}$

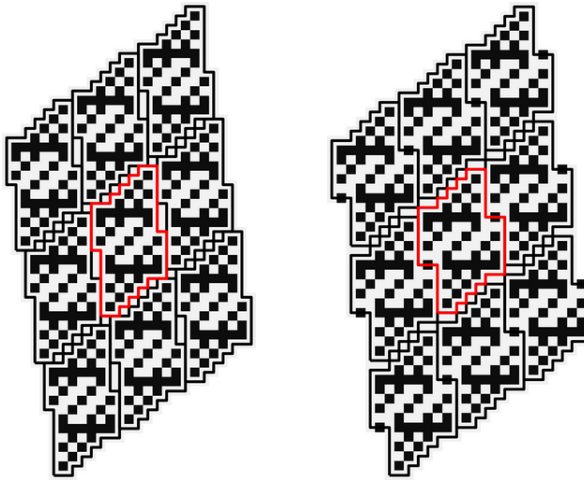


FIGURE 19. A period of the Laplacian of a doubled staircase odometer on the left and its alternate. The string is 22 and the reduced fraction is $5/7$. Each tile is outlined in the dual lattice.

Lemma 6.6. For $d \geq 3$ odd, let $T_{1/d}$, $\hat{T}_{1/d}$ and $g_{1/d}$, $\hat{g}_{1/d}$ be as in Lemmas 6.2 and 6.4. The Laplacian, $\Delta g_{1/d}$, satisfies

$$(71) \quad \begin{aligned} \Delta g_{1/d}(x) &= \Delta g_{1/d}(x \pm v_{1/d,*}) \text{ for all } x \in \mathbb{Z}^2 \\ \Delta g_{1/d}(x) &= -1\{(x_1 + x_2) \text{ is odd}\} - 1\{(x_1 + x_2) \text{ is even and } x_1 = 1\} \\ &\quad + 1_{\{(0,1) \cup (2,d)\}} \quad \text{on } T_d \setminus \partial T_d \\ \Delta g_{1/d}(x) &= 0 \quad \text{on } \partial T_d \end{aligned}$$

The Laplacian of the alternate, $\Delta \hat{g}_{1/d}$ satisfies

$$(72) \quad \begin{aligned} \Delta \hat{g}_{1/d}(x) &= \Delta \hat{g}_{1/d}(x \pm v_{1/d,*}) \text{ for all } x \in \mathbb{Z}^2 \\ \Delta \hat{g}_{1/d}(x) &= -1\{(x_1 + x_2) \text{ is odd}\} \\ &\quad - 1\{(x_1 + x_2) \text{ is even and } x \in \{-(d-2) \times [0, d-1]\} \cup \{2 \times [1, d]\}\} \\ &\quad - 1\{(x_1 + x_2) = 2 \text{ and } 1 \leq x_2 \leq d-1\} \\ &\quad + 1\{(x_1 + x_2) = 1 \text{ and } 1 \leq x_2 \leq d-2\} \\ &\quad + 1\{(x_1 + x_2) = 3 \text{ and } 2 \leq x_2 \leq d-1\} \\ &\quad + 1_{(1-d,1) \cup (3,d-1)} \quad \text{on } T_d \setminus \partial T_d \\ \Delta \hat{g}_{1/d}(x) &= -1_{(1-d,0) \cup (3,d)} \quad \text{on } \partial T_d \end{aligned}$$

6.3. Doubled staircases. The *doubled staircases* are the reduced fractions of the form $\frac{1}{d}$ for $d \geq 4$ even and their rotations $\mathcal{R}(1, d) = (d-1, d+1)$. These are respectively the odd or even child in Farey quadruples with words 3^k and 2^k for $k \geq 1$. They are the sibling of the opposite parity of the staircases.

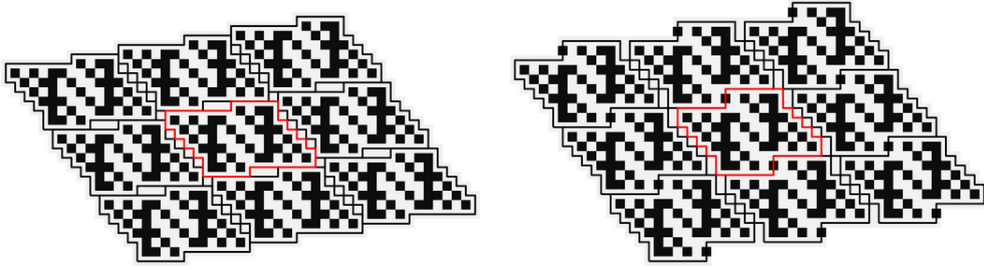


FIGURE 20. The rotated standard and alternate doubled staircase odometers of Figure 19. The string is 33 and the reduced fraction is $1/6$.

Lemma 6.7. *For each $d \geq 4$ even, there is a unique function $g_{1/d} : \mathbb{Z}^2 \rightarrow \mathbb{Z}$ with*

$$\begin{aligned} g_{1/d}(x) = & -\frac{1}{2}x_2(x_2 + 1) + \min(0, x_1 - 1) + \min(0, d + 1 - x_1) \quad \text{for } x \in T_{1/d} \\ & + \max((x_2 + x_1) - d - 1, 0) + 1_{A \cup B} \end{aligned}$$

where

$$\begin{aligned} A &= (0, -1) \cup (d + 2, d + 1) \\ B &= \{(x_1, x_2) : (x_1 + x_2) = (d + 1) \text{ and } 0 < x_2 < d\} \\ C &= \{(x_1, x_2) \in [-d + 2, 2d] \times [-1, d + 1] : 0 \leq (x_1 + x_2) \leq 2d + 2\} \\ D &= \{(x_1, x_2) : x_1 \geq d \text{ and } x_2 = -1 \text{ or } x_1 \leq 2 \text{ and } x_2 = d + 1\} \\ T_{1/d} &:= \{A \cup B \cup C\} \setminus D \end{aligned}$$

and

$$g_{1/d}(x \pm v_{1/d,i}) = g_{1/d}(x) \pm a_{1/d,i} \cdot x + k_{1/d,\pm i} \quad \text{for } x \in \mathbb{Z}^2,$$

where $k_{d,\pm i}$ is a constant and $i \in \{1, 2\}$ selects the lattice vectors.

Moreover, $g_{1/d}$ respects a $qp^k qp^{k+1}$ horizontal boundary string and a $p^{(2k+1)}q$ vertical boundary string.

Lemma 6.8. *For each $q = \frac{d-1}{d+1}$ $d \geq 4$ even, there is a unique function $g_q : \mathbb{Z}^2 \rightarrow \mathbb{Z}$ with*

$$\begin{aligned} g_q(x) = & -\lfloor \frac{(x_2 - x_1)^2}{4} \rfloor + \min(0, d - x_2) + \min(0, 2d - x_2) \quad \text{for } x \in T_q \\ & + \max((x_2 - x_1) - d, 0) + 1_{A \cup B} \end{aligned}$$

where

$$\begin{aligned} A &= (-1, 2d + 1) \cup (d + 1, d - 1) \\ B &= \{(x_1, x_2) : (x_2 - x_1) = d \text{ and } 0 < x_1 < d\} \\ C &= \{(x_1, x_2) \in [-1, d + 1] \times [1, 3d - 1] : -1 \leq (x_2 - x_1) \leq 2d + 1\} \\ D &= \{(x_1, x_2) : x_1 = -1 \text{ and } x_2 \leq d + 1 \text{ or } x_1 = d + 1 \text{ and } x_2 \geq 2d - 1\} \\ T_q &:= \{A \cup B \cup C\} \setminus D \end{aligned}$$

and

$$g_q(x \pm v_{q,i}) = g_q(x) \pm a_{q,i} \cdot x + k_{q,\pm i} \quad \text{for } x \in \mathbb{Z}^2,$$

where $k_{d,\pm i}$ is a constant and $i \in \{1, 2\}$ selects the lattice vectors.

Moreover, g_q respects a zero-one $q^{(2k+1)}p$ horizontal boundary string and a $pq^kpq^{(k+1)}$ vertical boundary string.

We next construct the alternates.

Lemma 6.9. *For each $d \geq 4$ even, there is a unique function $\hat{g}_{1/d} : \mathbb{Z}^2 \rightarrow \mathbb{Z}$ with*

$$\begin{aligned}\hat{g}_{1/d}(x) = & -\frac{1}{2}x_2(x_2 + 1) + \min(0, x_1) + \min(0, d - x_1 - 1) \quad \text{for } x \in \hat{T}_{1/d} \\ & + \max((x_2 + x_1) - d, 0) + 1_{A \cup B}\end{aligned}$$

where

$$\begin{aligned}A &= (-1, -1) \cup (d, d + 2) \\ B &= \{(x_1, x_2) : (x_1 + x_2) = (d) \text{ and } 0 < x_1 < d - 1\} \\ C &= \{(x_1, x_2) \in [-d + 1, 2d - 2] \times [-1, d + 2] : -1 \leq (x_1 + x_2) \leq 2d + 1\} \\ D &= \{(x_1, x_2) : x_1 \geq d \text{ and } x_2 \in [-1, 0] \text{ or } x_1 \leq -1 \text{ and } x_2 \in [d + 1, d + 2]\} \\ \hat{T}_{1/d} &:= \{A \cup B \cup C\} \setminus D\end{aligned}$$

and

$$\hat{g}_{1/d}(x \pm v_{1/d,i}) = \hat{g}_{1/d}(x) \pm a_{1/d,i} \cdot x + \hat{k}_{1/d,\pm i} \quad \text{for } x \in \mathbb{Z}^2,$$

where $\hat{k}_{d,\pm i}$ is a constant and $i \in \{1, 2\}$ selects the lattice vectors.

Moreover, $\hat{g}_{1/d}$ respects a horizontal zero-one $p^{(2k+1)}q$ boundary string and its reversal.

Lemma 6.10. *For each $q = \frac{d-1}{d+1}$, $d \geq 4$ even, there is a unique function $\hat{g}_q : \mathbb{Z}^2 \rightarrow \mathbb{Z}$ with*

$$\begin{aligned}\hat{g}_q(x) = & -\lfloor \frac{(x_2 - x_1)^2}{4} \rfloor + \min(0, d - x_2) + \min(0, 2d - 1 - x_2) \quad \text{for } x \in T_q \\ & + \max(0, x_2 - x_1 - d) + 1_{A \cup B}\end{aligned}$$

where

$$\begin{aligned}A &= (-2, 2d) \cup (d + 1, d - 1) \\ B &= \{(x_1, x_2) : (x_2 - x_1) = d \text{ and } 0 < x_1 < d\} \\ C &= \{(x_1, x_2) \in [-2, d + 1] \times [1, 3d - 2] : -1 \leq (x_2 - x_1) \leq 2d + 1\} \\ D &= \{(x_1, x_2) : x_1 \leq -1 \text{ and } x_2 \leq d + 1 \text{ or } x_1 \geq d \text{ and } x_2 \geq 2d\} \\ T_q &:= \{A \cup B \cup C\} \setminus D\end{aligned}$$

and

$$\hat{g}_q(x \pm v_{q,i}) = g_q(x) \pm a_{q,i} \cdot x + k_{q,\pm i} \quad \text{for } x \in \mathbb{Z}^2,$$

where $\hat{k}_{d,\pm i}$ is a constant and $i \in \{1, 2\}$ selects the lattice vectors.

Moreover, \hat{g}_q respects a zero-one $q^{(2k+1)}p$ horizontal boundary string and its reversal.

Lemma 6.11. *The Laplacians are rotations of each other and have the following formulas:*

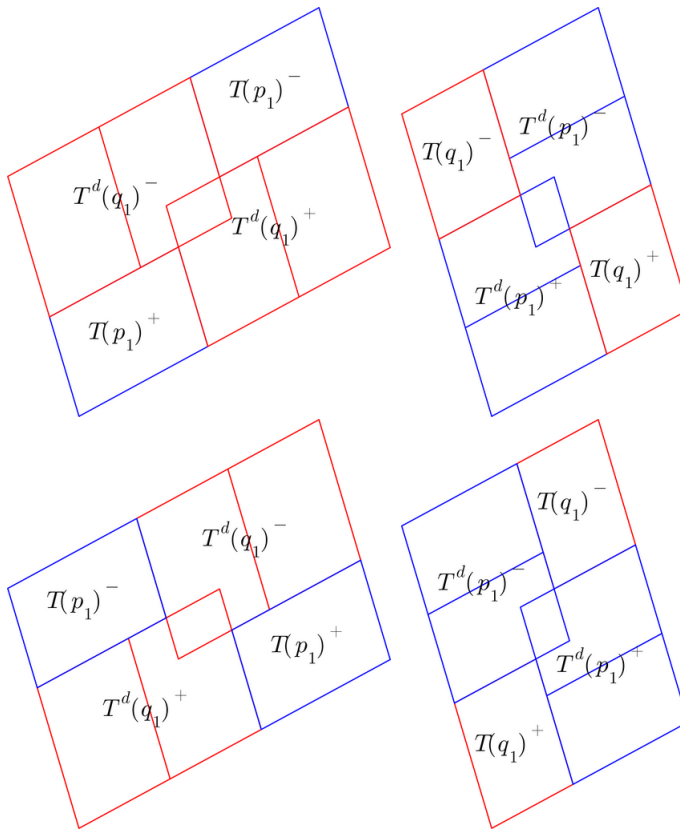


FIGURE 21. The two possible orientations for a standard tile pair from Definition 3. The left column is the odd child and the right column is the even child. The first row is the odd-first orientation and the second is the even-first orientation. Only one type of overlap between parents (corresponding to Type 1 children) is displayed - see Figure 22 for the other types of overlaps.

6.4. One-sided recurrence. In this section we prove that the staircase odometers and their doubles are recurrent. In fact, we prove something slightly stronger which we will use to prove incurrence inductively.

Lemma 6.12. *The staircases are recurrent.*

Proof. Slide a horizontal plane or vertical plane till it touches a side of the boundary and then check cases. \square

7. ODOMETERS AND TILES

This section extends the hyperbola recursion of Section 3 to odometers and tiles. That is, we associate to each rational in a Farey quadruple a pair of tiles and odometers. For continuity of the literature, the formality which we use to define the recursion is similar to [LPS16].

7.1. Standard tiles. Let $(p_0, q_0) = \mathcal{C}(p_1, q_1)$ form a Farey quadruple labeled by a recursion word $w \in F_3^*$. Let \mathcal{W}_1 count the number of 1s in w .

Definition 3. A pair of tiles $(T(p_0), T(q_0)) \subset \mathbb{Z}^2$ are standard tiles for (p_0, q_0) if they appear in Proposition 6.1, are $(T_{0/1}, T_{1/1})$ from Section 5.4, or have the standard tile decomposition:

$$(73) \quad \begin{aligned} T(p_0) &= T(p_1)^+ \cup T(p_1)^- \cup T^d(q_1)^+ \cup T^d(q_1)^- \\ T(q_0) &= T^d(p_1)^+ \cup T^d(p_1)^- \cup T(q_1)^+ \cup T(q_1)^- \end{aligned}$$

where $T^d(n/d)^\pm$ denote doubled tiles,

$$(74) \quad \begin{aligned} T^d(p)^\pm &= T(p)^{\pm,1} \cup T(p)^{\pm,2} := T(p) \cup (T(p) + v_{p,2}) \\ T^d(q)^\pm &= T(q)^{\pm,1} \cup T(q)^{\pm,2} := T(q) \cup (T(q) + v_{q,1}) \end{aligned}$$

and $(T(p_1), T(q_1))$, with or without superscripts, are standard tiles for (p_1, q_1) . The tile positions in (73) depend on the parity of \mathcal{W}_1 : if \mathcal{W}_1 is odd

$$(75) \quad \begin{aligned} c(T) - c(T(p_0)) &= \begin{cases} 0 & \text{if } T = T(p_1)^+ \\ 2v_{q_1,1} + v_{q_1,2} & \text{if } T = T(p_1)^- \\ 2v_{p_1,1} & \text{if } T = T^d(q_1)^+ \\ v_{p_1,2} & \text{if } T = T^d(q_1)^- \end{cases} \\ c(T) - c(T(q_0)) &= \begin{cases} 0 & \text{if } T = T^d(p_1)^+ \\ v_{q_1,1} + v_{q_1,2} & \text{if } T = T^d(p_1)^- \\ 2v_{p_1,1} & \text{if } T = T(q_1)^+ \\ 2v_{p_1,2} & \text{if } T = T(q_1)^- \end{cases} \end{aligned}$$

otherwise

$$(76) \quad \begin{aligned} c(T) - c(T(p_0)) &= \begin{cases} 0 & \text{if } T = T^d(q_1)^+ \\ 2v_{p_1,1} + v_{p_1,2} & \text{if } T = T^d(q_1)^- \\ 2v_{q_1,1} & \text{if } T = T(p_1)^+ \\ v_{q_1,2} & \text{if } T = T(p_1)^- \end{cases} \\ c(T) - c(T(q_0)) &= \begin{cases} 0 & \text{if } T = T(q_1)^+ \\ 2v_{p_1,1} + v_{p_1,2} & \text{if } T = T(q_1)^- \\ v_{q_1,1} & \text{if } T = T^d(p_1)^+ \\ v_{q_1,2} & \text{if } T = T^d(p_1)^- \end{cases} \end{aligned}$$

see Figure 21.

The tiles in the standard tile decomposition of $T(n/d)$ will be called subtiles of $T(n/d)$. The tile orientations in (75) and (76) will be referred to as the odd-first and even-first orientations respectively. A single tile in a pair of standard tiles is a standard tile.

Before proving general existence of standard tiles, we derive an extension of rotation invariance, Lemma 3.6, to tiles and a tiling property, assuming existence up to a certain depth.

Lemma 7.1. Suppose standard tiles exist for all $n/d \in \mathcal{T}_m$, for $m \leq m_0$, some $m_0 \geq 1$. Then, the following properties are satisfied for each such $0 < n/d < 1$.

- (1) Rotation invariance: $\mathcal{R}(T(n/d)) = T(\mathcal{R}(n/d))$

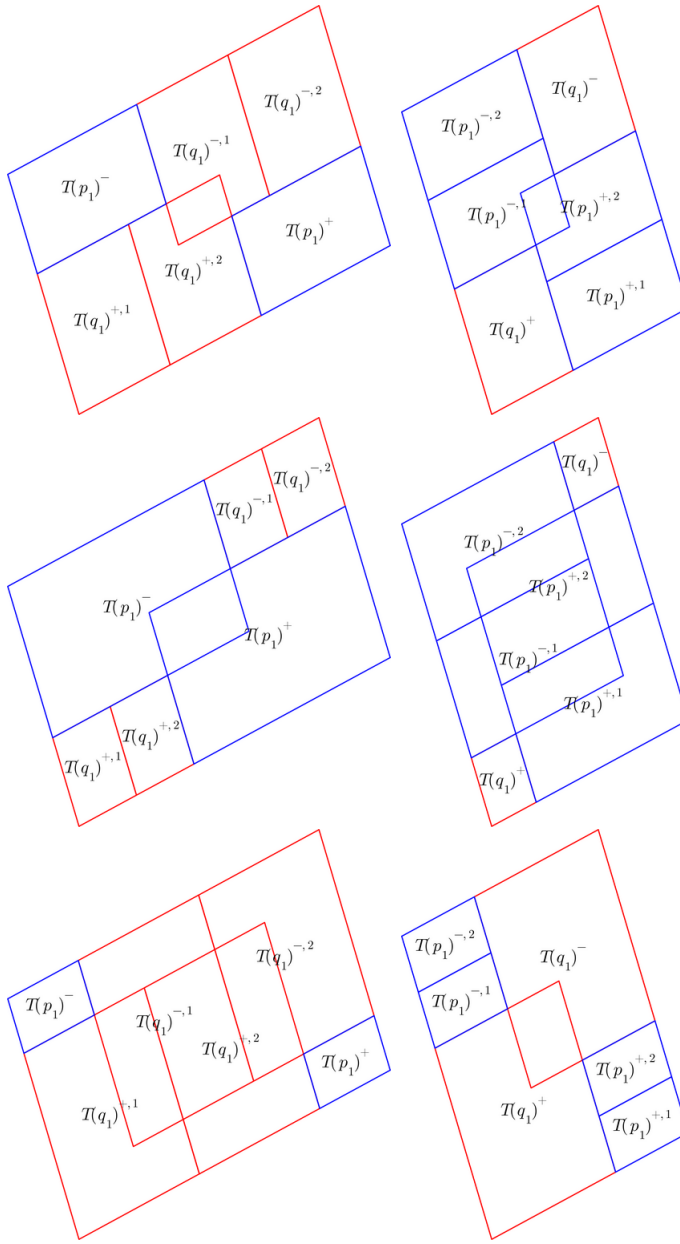


FIGURE 22. All possible overlaps between parents in a standard tile. The left column denotes the odd child and the right column is the even child. The rows from top to bottom correspond to Type 1, 2, then 3 children. The parent tiles are labeled in their centers with notation from Definition 3. The orientation is the even-first orientation.

(2) *Boundary tiling:* starting at $c(T(n/d))$ the boundary word of $T(n/d)$ can be written as $w = w_1 * \widehat{w_2} * \text{rev}(\widehat{w_1}) * \text{rev}(\widehat{w_2})$ where w_1, w_2 satisfy the hypotheses in Lemma 4.1 and $\sum w_1 + i = v_{n/d,1}$ and $\sum w_2 - 1 = v_{n/d,2}$.

Proof. Both properties are true by Proposition 6.1 if $T(n/d)$ does not have a standard tile decomposition. Thus, we may assume $T(n/d)$ has a standard tile decomposition and that both properties are satisfied for the parent tiles of $T(n/d)$.

Step 1: Rotation invariance

If (n/d) is even, then its parent tiles are $T^d(p_1)^\pm$ and $T(q_1)$. By Lemma 3.7 and the inductive hypothesis, $\mathcal{R}(T^d(p_1)^\pm) = T^d(\mathcal{R}(p_1))$ and $\mathcal{R}(T(q_1)) = T(\mathcal{R}(q_1))$. By Lemma 3.6, these are the parent tiles of $T(\mathcal{R}(n/d))$. This together with the standard decomposition and Lemma 3.7 again implies $T(\mathcal{R}(n/d)) = \mathcal{R}(T(n/d))$. The proof applies to (n/d) odd after observing \mathcal{R} on the parent tiles is an involution. Indeed, the second hypothesis implies 180-degree symmetry.

Step 2: Boundary tiling

Every base case tile, $T(n/d)$ has a (w_1, w_2) -boundary word of the form $w_1 * w_2 * \widehat{\text{rev}}(w_1) \widehat{\text{rev}}(w_2)$ and $T(\mathcal{R}(n/d))$ has a $(-iw_2, -iw_1)$ boundary word both of which start at $c(T)$. Moreover, each such w_1 and w_2 satisfy the desired properties. By induction and the standard decomposition every subsequent standard tile has a boundary word decomposition. Thus, by Step 1, it suffices to show that the *bottom edges*, the w_1 in the boundary word decompositions satisfy the conditions in Lemma 4.1.

We start by rewriting the standard tile recursion to produce just the two bottom edges for each odd-even tile pair for each child Farey pair in a Farey quadruple: $(w_t, v_t) \in F_2 \times F_2$. The base cases are quadruples \mathbf{q}_{2^k} for $k \geq 0$ and \mathbf{q}_{3^k} for $k > 0$ for which we have explicit formulas from Section 6 for the odd-even pair of edges (w_0, v_0) :

$$\begin{pmatrix} w_0 \\ v_0 \end{pmatrix} = \begin{cases} \begin{pmatrix} 1 * (1 * i)^{2k+1} * (1 * 1) \\ 1 * (1 * i)^{2k} (1 * 1) \end{pmatrix} & \mathbf{q}_{2^k} \text{ for } k \geq 0 \\ \begin{pmatrix} (1 * 1)^k (1 * i) * (1 * 1)^{k+1} * 1 \\ 1 * (1 * 1)^{k+1} \end{pmatrix} & \mathbf{q}_{3^k} \text{ for } k > 0 \end{cases}$$

Now, given a recursion word $str \in F_3^*$ describing a quadruple \mathbf{q}_{str} the standard tile decomposition implies

$$(77) \quad \begin{pmatrix} w_{t+1} \\ v_{t+1} \end{pmatrix} = \begin{cases} \begin{pmatrix} w_t * i * v_t * i * v_t \\ w_t * i * v_t \end{pmatrix} & \text{if } \sum(str[i] = 1) \text{ is odd} \\ \begin{pmatrix} v_t * i * v_t * w_t \\ v_t * i * w_t \end{pmatrix} & \text{if } \sum(str[i] = 1) \text{ is even} \end{cases},$$

where w_t, v_t are the edges of the odd-even parent Farey pair in \mathbf{q}_{str} .

It will be convenient to augment the recursion so that it generates the bottom edge concatenated with an extra i . The augmented recursion has as base cases

$$\begin{pmatrix} \tilde{w}_0 \\ \tilde{v}_0 \end{pmatrix} = \begin{cases} \begin{pmatrix} 1 * (1 * i)^{2k+1} * (1 * 1 * i) \\ 1 * (1 * i)^{2k} (1 * 1 * i) \end{pmatrix} & \text{if } str = 2^k \text{ for } k \geq 0 \\ \begin{pmatrix} (1 * 1)^k (1 * i) * (1 * 1)^{k+1} * (1 * i) \\ (1 * 1)^{k+1} * (1 * i) \end{pmatrix} & \text{if } str = 3^k \text{ for } k > 0 \end{cases}$$

and the recursive step is

$$(78) \quad \begin{pmatrix} \tilde{w}_{t+1} \\ \tilde{v}_{t+1} \end{pmatrix} = \begin{cases} \begin{pmatrix} \tilde{w}_t * \tilde{v}_t * \tilde{w}_t \\ \tilde{w}_t * \tilde{v}_t \end{pmatrix} & \text{if } \sum(str[i] = 1) \text{ is odd} \\ \begin{pmatrix} \tilde{v}_t * \tilde{v}_t * \tilde{w}_t \\ \tilde{v}_t * \tilde{w}_t \end{pmatrix} & \text{if } \sum(str[i] = 1) \text{ is even} \end{cases},$$

where similarly \tilde{w}_t, \tilde{v}_t are the augmented edges of the odd-even parents of str . Use induction and compute using (78) to show that the augmented words sum to the desired lattice vectors. It remains to verify the rest of the hypotheses for which we use (78) and the forms of the base cases. We split into cases based on the structure of the recursion word \mathbf{q}_{str} .

*Case 1: $str = 2^k * s * str'$ for $k \geq 0, s \in \{1, 3\}$ and $|str'| \geq 0$*

If $k = 0$ and $s = 3$ then proceed to Case 2. Otherwise, write

$$\begin{pmatrix} p_k \\ q_k \end{pmatrix} = \begin{pmatrix} 1 * (1 * i)^{2k+1} * (1 * 1 * i) \\ 1 * (1 * i)^{2k} (1 * 1 * i) \end{pmatrix}.$$

By Lemma 5.1 both w_t and v_t are of the form $p * \tilde{w} * q$ where \tilde{w} is a palindrome in the letters p, q where

$$(p, q) = \begin{cases} (p_k, q_k) & \text{if } s = 1 \\ (q_k, p_{k-1}) & \text{if } s = 3. \end{cases}$$

An inspection of the formula shows that

$$(79) \quad \mathbf{rev}(b) * i = i * b \quad \text{for } b \in \{p, q\}$$

as words in the letters $\{1, i\}$. We claim this implies that case (b) of Lemma 4.1 holds. First take $s = 1$ and write in the letters $\{1, i\}$,

$$\begin{aligned} p_k \tilde{w} q_k &= (1 * 1 * i) * (1 * i)^{2k} * (1 * 1 * i) * \tilde{w} * 1 * (1 * i)^{2k} * (1 * 1 * i) \\ &= (1 * 1 * i) * ((1 * i)^{2k} * (1 * 1 * i) * \tilde{w} * 1 * (1 * i)^{2k} * 1) * 1 * i \\ &=: (1 * 1 * i) * \tilde{v} * 1 * i. \end{aligned}$$

As we have augmented a trailing i , it suffices to show \tilde{v} is a palindrome in the letters $\{1, i\}$:

$$\begin{aligned}\mathbf{rev}(\tilde{v}) &= 1 * (i * 1)^{2k} * 1 * \mathbf{rev} \tilde{w} * (i * 1 * 1) * (i * 1)^{2k} \\ &= (1 * i)^{2k} * 1 * 1 * (\mathbf{rev} \tilde{w} * i) * 1 * (1 * i)^{2k} * 1 \\ &= (1 * i)^{2k} * (1 * 1 * i) * \tilde{w} * 1 * (1 * i)^{2k} * 1 \\ &= \tilde{v},\end{aligned}$$

where in the second to last step we used (79). The argument when $s = 3$ and $k \geq 1$ proceeds in the same fashion using (79).

*Case 2: $str = 3^k * s * str'$ for $k > 0$, $s \in \{1, 2\}$ and $|str'| \geq 0$*

The argument is similar to Case 1, however, the letters in this case are:

$$\binom{p_k}{q_k} = \binom{h_k * h_{k+1}}{h_{k+1}} := \binom{(1 * 1)^k * (1 * i) * (1 * 1)^{k+1} * (1 * i)}{(1 * 1)^{k+1}(1 * i)}.$$

By Lemma 5.1 both w_t and v_t are of the form $p * \tilde{w} * q$ where \tilde{w} is a palindrome in the letters p, q where

$$(p, q) = \begin{cases} (p_k, q_k) & \text{if } s = 1 \\ (q_{k-1}, p_k) & \text{if } s = 2. \end{cases}$$

Compute to see that

$$\begin{aligned}(80) \quad \mathbf{rev}(b) * \mathbf{rev}(h_{k+1}) * i &= (\mathbf{rev}(h_{k+1}) * i) * b \\ &= i * h_{k+1} * b \quad \text{for } b \in \{p_k, q_k\}.\end{aligned}$$

and

$$(81) \quad 1 * (1 * 1)^k * \mathbf{rev}(b) = b * 1 * (1 * 1)^k \quad \text{for } b \in \{p_k, q_{k-1}\}.$$

The rest of the argument is similar to Case 1: when $s = 1$ use (80) and when $s = 2$ use (81). \square

The next lemma uses the abstract recursion on binary words in (31) as well as the pseudo-square boundary decomposition. For notational convenience, write $w_h(n/d)$ for the binary word associated to the reduced fraction in (31) with initial seed $w_0 = \{\}$ and $\mathbf{Q}_{\{\}} = (qqp, qp, p, q)$. Also write $w_v(n/d) = \mathcal{F}(w_h(\mathcal{R}(n/d)))$.

Lemma 7.2. *A standard tile, $T(n/d)$ exists for every reduced rational $0 \leq \frac{n}{d} \leq 1$. Moreover, when $0 < n/d < 1$, the tile has the following properties.*

- (a) $T(n/d)$ generates a $(v_{n/d,1}, v_{n/d,2})$ -regular almost pseudo-square tiling.
- (b) Each $T(n/d)$ is a $(w_h(n/d), w_v(n/d))$ -pseudo-square with offsets respecting the tiling:
 - (a) $c(T) - c(T(n/d)) = v_{n/d,1} - (i + 1)$ where T is the last tile of $w_h(n/d)$
 - (b) $c(T') - c(T(n/d)) = v_{n/d,2} - (2i - 1)$ where T' is the last tile of $\mathbf{rev}(w_v(n/d))$
- (c) The surrounding of $T(n/d)$ with respect to $(v_{n/d,1}, v_{n/d,2})$ consists of two stacked zero-one horizontal and two vertical boundary strings.
- (d) When $T(n/d)$ has a standard decomposition, the shared boundary between neighboring subtiles is part of or is a stacked horizontal or vertical zero-one boundary string.

Proof. In light of Proposition 6.1, we may assume $T(n/d)$ has a standard decomposition and the statements are true for its parents, $T(p_1)$ and $T(q_1)$. Also, by Lemma 7.1 to prove part (a) it suffices to show that $T(n/d)$ is a topological disk, *i.e.*, does not have any internal holes.

This however follows from part (c) and Lemma 5.4, hence it remains to prove (b) and (c). We assume that the decomposition given is in the even-first orientation, otherwise flip the subsequent statements.

Step 1: (b)

By the inductive hypothesis, $T(p_1)$ and $T(q_1)$ are $(w_h(p_1), w_v(p_1))$ and $(w_h(q_1), w_v(q_1))$ pseudo-squares. By rotation, we may assume $T(n/d)$ is odd. Let T be the last tile in $T(q_1)^{+,1}$ and T' the first tile in $T(q_1)^{+,2}$. By definition T is a translation of $T(0/1)$ and T' a translation of $T(1/1)$. Moreover, by the definition of the standard decomposition and the inductive hypothesis on the offsets, $c(T') - c(T) = (1 + i)$, in particular, we can glue the two boundary strings together. A similar argument applies to the interface between $T(q_1)^{+,2}$ and $T(p_1)$. This shows if (n/d) is odd, then $T(n/d)$ respects $w_h(q_1)w_h(q_1)w_h(p_1)$ otherwise it respects $w_h(q_1)w_h(p_1)$. A symmetric argument applies to the vertical boundary strings and a computation shows that the offsets respect the tiling.

Step 2: (c)

Let A be the horizontal string for $T(n/d)$ and B the reversed horizontal string for $T(n/d) - v_{n/d,2}$. Set $c(T(n/d)) = 0$. By part (b), the first tile in B is located at $c(T(n/d)) - v_{n/d,2} + v_{n/d,2} - (2i - 1)$. Thus, the offset between the first tile in B and the first tile in A is $2i - 1 = v_{0/1,2} + i$, the correct initial offset for a stacked string.

Similarly if C is the vertical string for $T(n/d)$ and D the reversed vertical string for $T(n/d) + v_{n/d,1}$, then the offsets between the first tiles is $(i + 1) = -v_{1/1,1}$. The other two sides are stacked strings by the above arguments for $T(n/d) - v_{n/d,1}$ and $T(n/d) + v_{n/d,2}$.

Step 3: (d)

We state the arguments with the aid of Figure 22. First consider the three possible boundaries between $T(q_1)^{+,1/2}$ and $T(p_1)^-$ when $T(n/d)$ is odd. By the inductive hypothesis, the offset between the first tile in the reversed zero-one horizontal boundary string for $T(q_1)^{+,1}$ and the first tile for the zero-one horizontal string in $T(p_1)^-$ is $v_{0/1,2} + i$. Since the initial offset is correct, the rest of the interface forms part of a stacked horizontal zero-one boundary string by part (3) of Lemma 5.1. Indeed, every letter other than the first matches across the interface. Reversing p_1 and q_1 above shows the three possible interfaces between $T(p_1)^+$ and $T(q_1)^{-,1/2}$ also form part of a stacked horizontal boundary string. When $T(n/d)$ is even, the interface between $T(p_1)^{+,1}$ and $T(p_1)^{+,2}$ is exactly a stacked horizontal boundary string by the inductive hypothesis part (c). By rotation, the above arguments apply to the vertical interfaces.

□

7.2. Weak standard odometers. Our current goal is to extend the standard tile decomposition to odometers. In order to do so, we must define the operation of doubling a partial odometer. However, in the course of the recursion, doubled odometers may need to be corrected in the interior of the tile so we need a notion of tile that only depends on the boundary in the pseudo-square decomposition.

Definition 4. Let $T(n/d)$ be a $(w_h(n/d), w_v(n/d))$ pseudo-square. A partial tile $T^{h^\pm/v^\pm}(n/d)$ is a tile which coincides with $T(n/d)$ on one of the four sides:

$$(82) \quad T^{h^\pm/v^\pm}(n/d) \cap T(n/d) \supset \begin{cases} w_h(n/d) & \text{case } h^+ \\ \mathbf{rev}(w_h(n/d)) & \text{case } h^- \\ w_v(n/d) & \text{case } v^+ \\ \mathbf{rev}(w_v(n/d)) & \text{case } v^-. \end{cases}$$

A boundary tile $T^b(n/d)$ coincides with $T(n/d)$ on every side:

$$(83) \quad T^b(n/d) \cap T(n/d) \supset w_h(n/d) \cup \mathbf{rev}(w_h(n/d)) \cup w_v(n/d) \cup \mathbf{rev}(w_v(n/d)).$$

We now define the notion of a doubled odometer using partial tiles. But before we do so, we define an operation, for convenience, which will allow us to quickly pass from a tile decomposition to an odometer decomposition. Say $T(n/d)$ and $T(n/d')$ are two tiles with $c(T(n/d')) - c(T(n/d)) = v_{n/d,i}$. Then, two partial odometers $o(n/d)$ and $o(n/d')$ respect the tile translations if $s(o(n/d')) - s(o(n/d)) = a_{n/d,i}$ and the domains of $o(n/d)$ and $o(n/d')$ are $T(n/d)$ and $T(n/d')$ respectively.

Definition 5. For $(n/d) \in \{p_0, q_0\}$ let $T(n/d)$ be a standard tile and $T^{h^\pm/v^\pm}(n/d)$ a partial tile. Denote by

$$(84) \quad T^{d,p,\pm}(n/d) = T^b(n/d)^1 \cup T^{h^\pm/v^\pm}(n/d)^2 := T^b(n/d) \cup (T^{h^\pm/v^\pm}(n/d) + v_{n/d})$$

a partial doubled tile where $v_{n/d} = v_{p_0,2}$ or $v_{n/d} = v_{q_0,1}$ for $n/d = p_0$ or q_0 respectively.

The weak doubling of a partial odometer $o_{n/d}$ with domain $T^b(n/d)$ is a partial odometer $d(o)_{n/d}^\pm : T^{d,p}(n/d) \rightarrow \mathbb{Z}$ with the decomposition

$$(85) \quad d(o)_{n/d}^\pm = o_{n/d} \cup o_{n/d}^*$$

where $T(o_{n/d}) = T^b(n/d)^1$ and $T(o_{n/d}^*) = T^{h^\pm/v^\pm}(n/d)^2$ and, after being restricted to the relevant zero-one boundary strings from Definition 4, $o_{n/d}^*$ and $o_{n/d}$ respect the tile translations.

We now use these to partially define the standard recursion. The full recursion requires alternate tiles odometers which are defined in the next two subsections.

Definition 6. A pair of partial odometers $o_{p_0} : T^b(p_0) \rightarrow \mathbb{Z}$ and $o_{q_0} : T^b(q_0) \rightarrow \mathbb{Z}$ are weak standard tile odometers for (p_0, q_0) if they appear in Proposition 6.1, are $(o_{0/1}, o_{1/1})$ from Section 5.4 or if $(T(p_0), T(q_0))$ are standard tiles with standard decompositions for (p_0, q_0) and the partial odometers have the standard decompositions:

$$(86) \quad \begin{aligned} o_{p_0} &= o_{p_1}^+ \cup o_{p_1}^- \cup d(o)_{q_1}^+ \cup d(o)_{q_1}^- \\ o_{q_0} &= d(o)_{p_1}^+ \cup d(o)_{p_1}^- \cup o_{q_1}^+ \cup o_{q_1}^- \end{aligned}$$

where each $o_{n/d}$ is a weak standard tile odometer for (n/d) and the offsets are specified by requiring the odometers to respect the tile translations in Definition 3. The weak standard tile odometers on the right-hand-side of (86) will be called weak subodometers of o_{p_0} or o_{q_0} respectively.

We say weak standard tile odometers $o_{n/d}$ and $o'_{n/d}$ are *lattice adjacent* if

$$\begin{aligned} c(T(o_{n/d})) - c(T(o_{n/d})') &= v_{n/d,i} \\ s(o_{n/d}) - s(o'_{n/d}) &= \pm a_{n/d,i}, \end{aligned}$$

for $i \in \{1, 2\}$. We now prove an analogue of Lemma 7.2 for weak standard odometers.

Lemma 7.3. *A weak standard odometer, $o(n/d)$ exists for every reduced rational $0 \leq \frac{n}{d} \leq 1$. Moreover, when $0 < n/d < 1$, the odometer has the following properties.*

- (a) $o(n/d)$ respects $(w_h(n/d), w_v(n/d))$
- (b) Let A, B, C, D denote the first and last tiles of $w_h(n/d)$ and the last and first tiles of $\text{rev}(w_h)(n/d)$ respectively (geometrically a counter-clockwise walk around the tile). Let o_Z be the restriction of $o(n/d)$ to $Z \in \{A, B, C, D\}$. Then, $s(o_B) - s(o_A) = 0$, $s(o_C) - s(o_D) = a_{0/1,2} - a_{1/1,2}$ and $s(o_C) - s(o_B) = a_{n/d,2} - a_{1/1,2}$.
- (c) Lattice adjacent $o'_{n/d}$ and $o_{n/d}$ are compatible.

Proof. By Proposition 6.1, we may assume the tile $T(n/d)$ has a standard decomposition and hence the subodometers of $o(n/d)$ exist and satisfy (a),(b), and (c) of the inductive hypotheses.

Step 1: Existence

Since subodometers exist, it suffices to show that the odometer decomposition is well-defined *i.e.*, the subodometers have a common extension on their overlaps. By possibly deleting parts of the subodometers, we may assume that the only overlaps are on the internal zero-one stacked boundary strings specified in part (d) of Lemma. By an inductive application of (a) and (b) the subodometers respect the corresponding stacked boundary strings and therefore by Lemma 5.5 have a common extension to $T^b(n/d)$.

Step 2. Inductive hypotheses

We copy the proof of parts (b) and (c) of Lemma 7.2. To check that the affine offsets are the ones required in Lemma 5.5, we use the fact that the subodometers respect the tiling together with an inductive application of (b).

□

7.3. Alternate tiles. We now construct alternate tiles. In this case, the decomposition depends on the last letter of the recursion word, in particular, the parents of the parents. If the last letter of the recursion word is i , we say that we are in the Type i case. (The initial quadruple is one of the base cases.)

Definition 7. *A pair of tiles $(\hat{T}(p_0), \hat{T}(q_0)) \subset \mathbb{Z}^2$ are alternate tiles for (p_0, q_0) if they appear in Proposition 6.1, are $(T(0/1), T(1/1))$ from Section 5.4 or if they have the alternate tile decomposition*

$$(87) \quad \begin{aligned} \hat{T}(p_0) &= T^{ds}(p_1)^+ \cup T^{ds}(p_1)^- \cup T(q_1)^+ \cup T(q_1)^- \cup \hat{T}(q_1) \\ \hat{T}(q_0) &= T(p_1)^+ \cup T(p_1)^- \cup T^{ds}(q_1)^+ \cup T^{ds}(q_1)^- \cup \hat{T}(p_1) \end{aligned}$$

where $T^{ds}(n/d)^\pm$ denote doubled tiles where the doubling is different depending on the orientation:

$$(88) \quad \begin{aligned} T^{ds}(p)^\pm &= T(p)^{\pm,1} \cup T(p)^{\pm,2} := T(p) \cup (T(p) + S_p) \\ T^{ds}(q)^\pm &= T(q)^{\pm,1} \cup T(q)^{\pm,2} := T(q) \cup (T(q) + S_q), \end{aligned}$$

where

$$(89) \quad (S_p, S_q) = \begin{cases} (v_{q,1} + v_{p,2}, -v_{q,1} + v_{p,2}) & \text{if } \mathcal{W}_1 \text{ is even} \\ (-v_{q,1} + v_{p,2}, v_{q,1} + v_{p,2}) & \text{otherwise} \end{cases}$$

and $(T(p_1), T(q_1))$ with or without superscripts are standard tiles for (p_1, q_1) and $\hat{T}(n/d)$ is an alternate tile for n/d .

The standard tile positions in (87) depend on the parity of \mathcal{W}_1 : if \mathcal{W}_1 is odd

$$(90) \quad \begin{aligned} c(T) - c(\hat{T}(p_0)) &= \begin{cases} 2v_{p_1,1} & \text{if } T = T(q_1)^+ \\ 2v_{p_1,2} - v_{q_1,1} & \text{if } T = T(q_1)^- \\ 0 & \text{if } T = T^{ds}(p_1)^+ \\ v_{q_1,1} + v_{q_1,2} & \text{if } T = T^{ds}(p_1)^- \end{cases} \\ c(T) - c(\hat{T}(q_0)) &= \begin{cases} 2v_{p_1,1} & \text{if } T = T^{ds}(q_1)^+ \\ v_{p_1,2} & \text{if } T = T^{ds}(q_1)^- \\ 0 & \text{if } T = T(p_1)^+ \\ v_{p_1,2} + v_{q_1,2} + 2v_{q_1,1} & \text{if } T = T(p_1)^- \end{cases} \end{aligned}$$

otherwise

$$(91) \quad \begin{aligned} c(T) - c(\hat{T}(p_0)) &= \begin{cases} 0 & \text{if } T = T(q_1)^+ \\ 2v_{p_1,1} + 2v_{p_1,2} + v_{q_1,1} & \text{if } T = T(q_1)^- \\ v_{q_1,1} & \text{if } T = T^{ds}(p_1)^+ \\ v_{q_1,2} & \text{if } T = T^{ds}(p_1)^- \end{cases} \\ c(T) - c(\hat{T}(q_0)) &= \begin{cases} 0 & \text{if } T = T^{ds}(q_1)^+ \\ 2v_{p_1,1} + v_{p_1,2} & \text{if } T = T^{ds}(q_1)^- \\ v_{q_1,1} & \text{if } T = T(p_1)^+ \\ v_{p_1,2} + v_{q_1,2} - v_{q_1,1} & \text{if } T = T(p_1)^- \end{cases} \end{aligned}$$

The alternate tile positions in (87) may depend on both the parity of \mathcal{W}_1 , (even-first/odd-first) and the type of the child:

$$(92) \quad c(\hat{T}(q_1)) - c(\hat{T}(p_0)) = \begin{cases} v_{p_1,2} + 2v_{p_1,1} - v_{q_1,1} & \text{odd-first and Type 1 or 3} \\ *(v_{p_1,2}) & \text{odd-first and Type 2} \\ v_{q_1,1} + v_{p_1,2} & \text{even-first and Type 1 or 3} \\ *(v_{p_1,2} + v_{q_1,1}) & \text{even-first and Type 2} \end{cases}$$

$$(93) \quad c(\hat{T}(p_1)) - c(\hat{T}(q_0)) = \begin{cases} v_{p_1,2} + v_{q_1,1} & \text{odd-first and Type 1} \\ 2v_{q_1,1} + v_{q_1,2} & \text{odd-first and Type 2} \\ *(v_{q_1,1} + v_{p_1,2}) & \text{odd-first and Type 3} \\ v_{p_1,2} + 2v_{p_1,1} - v_{q_1,1} & \text{even-first and Type 1} \\ v_{q_1,2} & \text{even-first and Type 2} \\ *(v_{p_1,2} + v_{q_1,1} - 2(v_{q_1,1} - 2v_{p_1,1})) & \text{even-first and Type 3} \end{cases}$$

where in the cases indicated by *, the alternate tile may be omitted.

We now make an important exception in the definition of $c(\cdot)$ for alternate tiles. If $\hat{T}(n/d)$ has an alternate decomposition, then let

$$(94) \quad c(\hat{T}(n/d)) = \begin{cases} c(T(q_1)^{+,1}) & \text{even-first and } n/d \text{ even} \\ c(T(q_1)^+) & \text{even-first and } n/d \text{ odd} \\ c(T(p_1)^+) & \text{odd-first and } n/d \text{ even} \\ c(T(p_1)^{+,1}) & \text{odd-first and } n/d \text{ odd} \end{cases}$$

Lemma 7.4. *An alternate tile, $\hat{T}(n/d)$ exists for every reduced rational $0 \leq \frac{n}{d} \leq 1$. Moreover, when $0 < n/d < 1$, the alternate tile has the following properties.*

- (1) *Symmetry and rotation invariance: $\hat{T}(n/d)$ is 180-degree symmetric and $\mathcal{R}(\hat{T}(n/d)) = \hat{T}(\mathcal{R}(n/d))$*
- (2) *$\hat{T}(n/d)$ covers space under the lattice $L'(n/d)$*
- (3) *If n/d is even $\hat{T}(n/d)$ is a $w_h(n/d)$ -pseudo-square, otherwise a $w_v(n/d)$ pseudo-square with offsets respecting the tiling:*
 - (a) *Even case: $c(T_1) = c(\hat{T}(n/d))$ where T_1 is first tile of $w_h(n/d)$*
 - (b) *Odd case: $c(T'_1) = c(\hat{T}(n/d)) + s$ where T'_1 is the first tile of $\text{rev}(w_v(n/d))$ where $s = 0$ in the even-first orientation, otherwise $s = -v_{q_1,1} + v_{p_1,2}$.*
- (4) *The surrounding of $\hat{T}(n/d)$ with respect to $(v_{n/d,1}, v_{n/d,2})$ consists of either part of a stacked zero-one boundary string or a complete overlap on a subtile.*
- (5) *When $\hat{T}(n/d)$ has an alternate decomposition, the shared boundary between neighboring subtiles is part of or is a stacked horizontal or vertical zero-one boundary string.*

Proof. We may assume by Proposition 6.1 that $\hat{T}(n/d)$ has an alternate decomposition. The proof of (1) is identical to that of Lemma 7.1.

Step 1: (2)

By (1), we may assume $\hat{T}(n/d)$ is even. We also suppose $\hat{T}(n/d)$ is in the even-first orientation, as the odd-first argument is repetitive. Let $w_{n/d,i}$ denote the boundary words of the standard subtiles as specified by Lemma 7.1. Consider the enlarged tile, $T^e(n/d)$ with boundary word $w_1 = w_{q_1,1}w_{q_1,1}w_{p_1,1}$ and $w_2 = w_{p_1,2}w_{q_1,2}w_{p_1,2}$. Translate the enlarged tile so that $c(T^e(n/d)) - c(\hat{T}(n/d)) = -v_{q_1,1}$.

By Lemma 4.1, $T^e(n/d)$ generates a regular $(\sum v_{n/d,1} + v_{q_1,1}, \sum v_{n/d,2})$ almost pseudo-square tiling. We use this to show there are no gaps in the $(\sum v_{n/d,1} + v_{q_1,1}, \sum v_{n/d,2})$ -regular tiling of $\hat{T}(n/d)$ and the only sub-tiles which overlap are $T(q_1)^{-,1}$ and $T(q_1)^{+,2}$. The proof proceeds along the lines of Figure 25.

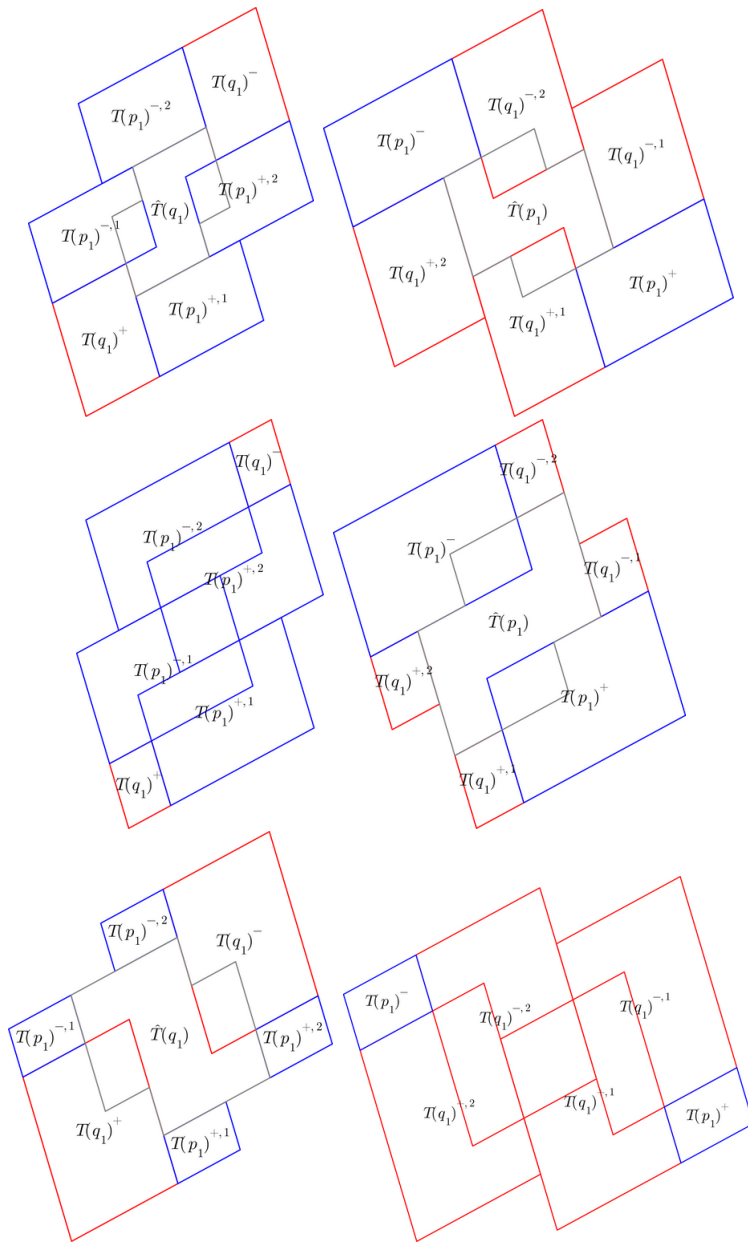


FIGURE 23. As Figure 22 (even-first) but for alternate tiles with labels from Definition 7.

By 180-degree symmetry and regularity of the tiling, it suffices to analyze the lower-left corner of a surrounding. Take the shifted tiling of $\hat{T}(n/d)$ with respect to $(\sum v_{n/d,1} + v_{q,1}, \sum v_{n/d,2})$ and compare the lower-left surrounding:

$$S^s := \hat{T}(n/d) \cup (\hat{T}(n/d) + v_{n/d,1} + v_{q,1,1}) \cup (\hat{T}(n/d) - v_{n/d,2}) \cup (\hat{T}(n/d) + v_{n/d,1} + v_{q,1,1})$$

to the corresponding corner of the non-shifted tiling

$$S := \hat{T}(n/d) \cup (\hat{T}(n/d) + v_{n/d,1}) \cup (\hat{T}(n/d) - v_{n/d,2}) \cup (\hat{T}(n/d) - v_{n/d,2} + v_{n/d,1})$$

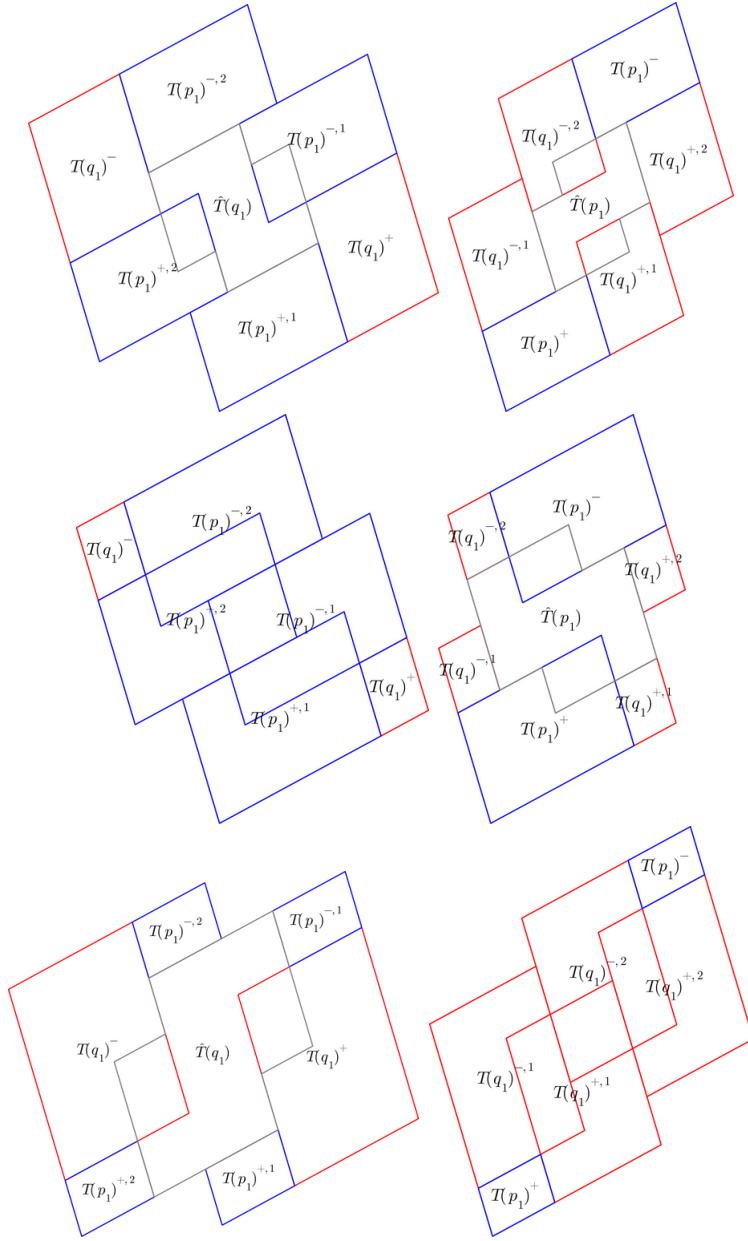


FIGURE 24. As Figure 23 but in the odd-first orientation

Since $T^e(n/d)$ generates a $(\sum v_{n/d,1} + v_{q,1}, \sum v_{n/d,2})$ almost pseudo-square tiling, each pair of tiles in S^s can only overlap on their boundaries, and by definition of $T^e(n/d)$, there are only two gaps in S^s both of which are squares with a $(w_{q_1,1}, w_{p_1,2})$ boundary word. Using the alternate decomposition, these two gaps are filled in the non-shifted tiling and $T(q_1)^{-1}$ and $T(q_1)^{+2}$ overlap completely, concluding the proof of this step.

Step 2: (3) (4) and (5)

Given Step 1, the proof is similar to that of Lemma 7.1. Indeed, we can use the alternate decomposition to concatenate boundary strings of the standard subtiles which make up the boundary of $\hat{T}(n/d)$. See Figures 23 and 24. To see that the external and internal

surroundings consists of stacked strings we refer to the right of Figure 25 and the proof of (d) in Lemma 7.1.

1

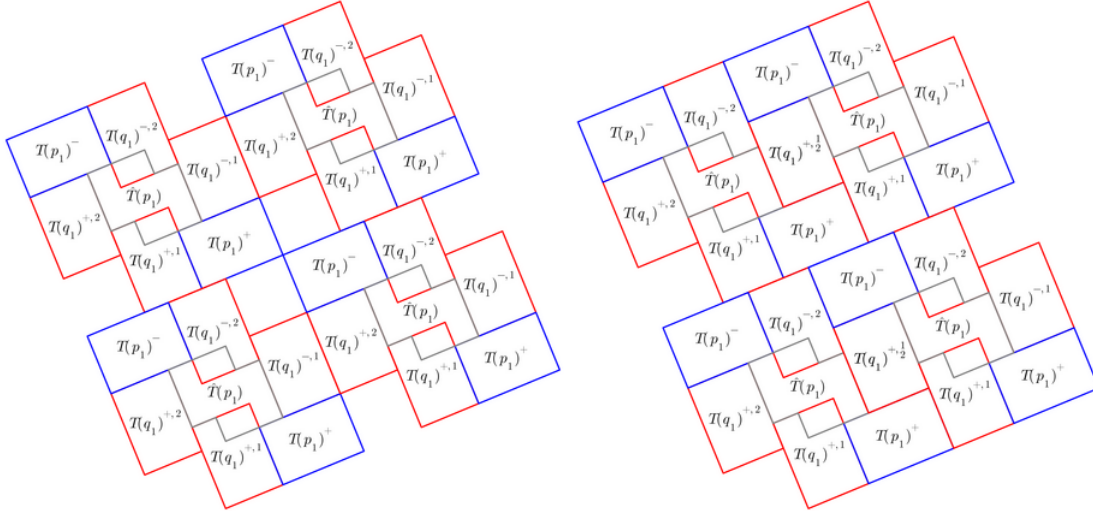


FIGURE 25. A visual explanation of the proof of Lemma 7.4. On the left is a lower-left surrounding of shifted tiling and on the right is a lower-left surrounding of the non-shifted tiling.

7.4. Weak alternate odometers. The recursion for alternate odometers given the subtle placement is similar to the standard ones. To that end, we first extend the notion of boundary tile and doubled odometers to this shifted case.

Definition 8. When $\hat{T}(n/d)$ has an alternate decomposition, an alternate boundary tile, $\hat{T}^b(n/d)$ coincides with the standard boundary subtiles in its decomposition

(95) $\hat{T}^b(n/d) \cap \hat{T}(n/d) = \bigcup T^b(n/d')$ where $T(n/d')$ ranges over the standard subtiles

Let $T^{ds,h/v,\pm}(n/d) = T^b(n/d) \cup (T^{h/v,\pm}(n/d) + S_{n/d})$ denote the shifted doubling of $T(n/d)$ where $S_{n/d}$ is from (88). As in Definition 5 extend the weak doubled odometer $ds(o)_{n/d} : T^{ds,h/v,\pm}(n/d) \rightarrow \mathbb{Z}$ to this case.

We are now ready to state a weak version of the alternate odometer recursion, analogous to the standard one from before.

Definition 9. A pair of partial odometers $\hat{o}_{p_0} : T(p_0) \rightarrow \mathbb{Z}$ and $\hat{o}_{q_0} : T(q_0) \rightarrow \mathbb{Z}$ are weak alternate tile odometers for (p_0, q_0) if they appear in Proposition 6.1, are $(o_{0/1}, o_{1/1})$ from Section 5.4 or $(\hat{T}(p_0), \hat{T}(q_0))$ are alternate tiles for (p_0, q_0) and the partial odometers have the alternate decompositions:

$$(96) \quad \begin{aligned} \hat{o}_{p_0} &= ds(o)_{p_1}^+ \cup ds(o)_{p_1}^- \cup o_{q_1}^+ \cup o_{q_1}^- \cup \hat{o}(q_1) \\ \hat{o}_{q_0} &= o_{p_1}^+ \cup o_{p_1}^- \cup ds(o)_{q_1}^+ \cup ds(o)_{q_1}^- \cup \hat{o}(p_1) \end{aligned}$$

where $ds(o)_{n/d}^\pm$ and $\hat{o}(n/d)$ are the respective weak shifted doublings and weak alternate parent odometers respecting the tile translations in Definition 6. In the indicated cases in Definition 7, we omit the alternate parent odometers.

Lemma 7.5. *A weak alternate odometer, $\hat{o}(n/d)$ exists for every reduced rational $0 \leq \frac{n}{d} \leq 1$. Moreover, when $0 < n/d < 1$, the odometer has the following properties.*

- (a) $\hat{o}(n/d)$ respects $w_h(n/d)$ or $w_v(n/d)$ if (n/d) is even or odd respectively.
- (b) Lattice adjacent $\hat{o}'_{n/d}$ and $\hat{o}_{n/d}$ are compatible.

Proof. Given Lemma 7.4 the proof is identical to the proof of Lemma 7.3. \square

8. CORRECTING THE RECURSION

In this section we complete the weak recursion defined in the previous section. This step requires us to possibly ‘correct’ doubled odometers which overlap. This is done by either a chain of ancestors or by checking that immediate parents overlap on immediate grandparents. We start by developing the machinery to chain together ancestors and then use that to fully define the recursion.

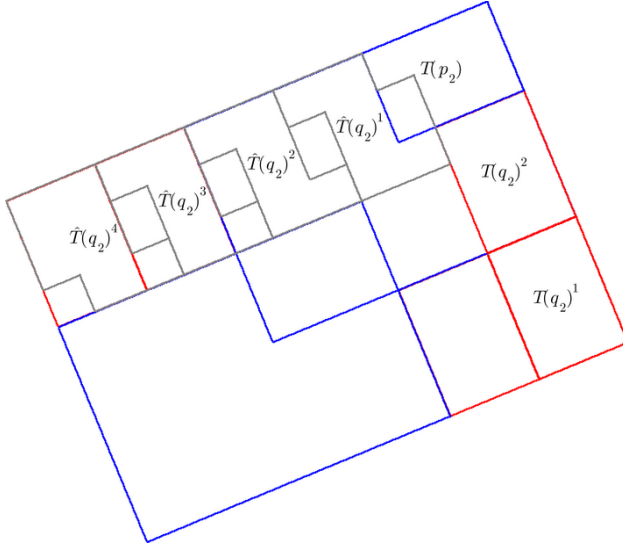


FIGURE 26. An odd L -correction with labels as in Definition 10 overlaid on its standard tile.

8.1. Corrected partial tiles. In this section we define a partial tile, Definition 4, for every standard tile which will allow us to fill in doubled weak odometers which don’t overlap on a common ancestor. The construction of this partial tile will involve a chain of ancestor tiles. Let $(p_0, q_0) = \mathcal{C}(p_1, q_1)$ with recursion word $w \in F_3^*$ and recall the standard tile decomposition from Definition 3.

Definition 10 (Odd L -correction). *Suppose $w = w_1 * s * 2^k$ where $|w_1| \geq 0$, $s \in \{1, 3\}$, and $k \geq 0$. Let (p_2, q_2) be the parent Farey pair corresponding to the string $w = w_1 * s$ and let $(T(p_2), T(q_2))$ be standard tiles for (p_2, q_2) and $\hat{T}(q_2)$ an alternate tile for q_2 .*

An L -correction for $T(p_0)$, $T^{L,\pm}(p_0)$ is a partial tile, $T^{v,\pm}(p_0)$ with the following decomposition

$$(97) \quad T^{L,\pm}(p_0) = \bigcup_{j=0}^k (T(q_2) + K_1 \cdot j) \cup (T(p_2) + K_2) \cup \left(K_3 + \bigcup_{i=1}^{2(k+1)-z} (\hat{T}(q_2) + K_4 \cdot i) \right)$$

where the initial offset is specified by requiring $T(q_2)$ match an outer $T(q_1)$ tile in the standard decomposition of $T(p_0)$:

$$\begin{cases} T(q_1)^{+,2} & 10 \\ T(q_1)^{-,1} & 11 \\ T(q_1)^{+,1} & 00 \\ T(q_1)^{-,2} & 01 \end{cases}$$

and the subsequent offsets are

$$[K_1, K_2] = \begin{cases} [v_{q_2,2}, v_{q_2,2} + (v_{q_2,1} - 2v_{p_2,1})] & 10 \\ [v_{q_2,2}, -v_{p_2,2}] & 11 \\ [v_{q_2,2}, v_{q_2,2}] & 00 \\ [-v_{q_2,2}, -v_{p_2,2} - (2v_{p_2,1} - v_{q_2,1})] & 01 \end{cases}$$

and

$$[K_3, K_4] = \begin{cases} [(-v_{q_2,2} + v_{p_2,2}) + (2v_{p_2,1} - v_{q_2,1}), -v_{q_2,1}] & 10 \\ [2v_{p_2,1} - v_{q_2,1}, v_{q_2,1}] & 11 \\ [-(v_{q_2,2} + v_{p_2,2}), v_{q_2,1}] & 00 \\ [0, -v_{q_2,1}] & 01, \end{cases}$$

where the right-hand side columns denote the case:

$$(98) \quad \begin{aligned} 10 &= \mathcal{W}_1 \text{ is odd and } + \\ 11 &= \mathcal{W}_1 \text{ is odd and } - \\ 00 &= \mathcal{W}_1 \text{ is even and } + \\ 01 &= \mathcal{W}_1 \text{ is even and } -. \end{aligned}$$

The term, z in (97) is either 0 or 1 and if $z = 0$, we say the L -correction is elongated.

The correction in the even-case is similar but the offsets are slightly different due to the lack of rotational symmetry in the parameterization.

Definition 11 (Even L -correction). Suppose $w = w_1 * s * 3^k$ where $|w_1| \geq 0$, $s \in \{1, 2\}$, and $k \geq 0$. Let (p_2, q_2) be the parent Farey pair corresponding to the string $w = w_1 * s$ and let $(T(p_2), T(q_2))$ be standard tiles for (p_2, q_2) and $\hat{T}(p_2)$ an alternate tile for p_2 .

An L -correction for $T(q_0)$, $T^{L,\pm}(q_0)$ is a partial tile $T^{h,\pm}(q_0)$ with the following decomposition.

$$(99) \quad T^{L,\pm}(q_0) = \bigcup_{j=0}^k (T(p_2) + K_1 \cdot j) \cup (T(q_2) + K_2) \cup \left(K_3 + \bigcup_{i=1}^{2(k+1)-z} (\hat{T}(p_2) + K_4 \cdot i) \right)$$

where the initial offset is specified by requiring $T(p_2)$ match an outer $T(p_1)$ tile in the standard decomposition of $T(p_0)$:

$$\begin{cases} T(p_1)^{+,1} & \{0 \text{ or } 1\}0 \\ T(p_1)^{-,2} & \{0 \text{ or } 1\}1 \end{cases}$$

and

$$[K_1, K_2, K_4] = \begin{cases} [2v_{p_2,1}, 2v_{p_2,1}, v_{p_2,2}] & 10 \\ [-2v_{p_2,1}, -v_{q_2,1}, v_{p_2,2}] & 00 \\ [-2v_{p_2,1}, -v_{q_2,1} + v_{p_2,1} - v_{q_2,1}, -v_{p_2,2}] & 11 \\ [2v_{p_2,1}, 2v_{p_2,1} + v_{p_2,2} - v_{q_2,2}, -v_{p_2,2}] & 01 \end{cases}$$

and

$$K_3 = \begin{cases} v_{q_2,1} - 2v_{p_2,1} + (v_{q_2,2} - v_{p_2,2} + v_{q_2,1}) & 10 \text{ and } s = 2 \\ v_{q_2,1} - 2v_{p_2,1} & 10 \text{ and } s = 1 \\ v_{q_2,2} - v_{p_2,2} & 00 \text{ and } s = 2 \\ 2v_{p_2,1} - v_{q_2,1} & 00 \text{ and } s = 1 \\ v_{q_2,2} - v_{p_2,2} + v_{q_2,1} & 11 \text{ and } s = 2 \\ 0 & 11 \text{ and } s = 1 \\ v_{q_2,2} - v_{p_2,2} - 2v_{p_2,1} + v_{q_2,1} & 01 \text{ and } s = 2 \\ 0 & 01 \text{ and } s = 2, \end{cases}$$

where the cases on the right are described by (98). The term, z in (99) is either 0 or 1 and if $z = 0$, we say the L -correction is elongated.

Note that the initial offset requirement assumes that $T(p_2) = T(p_1)$ in the odd case and $T(q_2) = T(q_1)$ in the even case but this follows the standard tile decomposition or Proposition 6.1. We assert a final exception to the definition of $c(\cdot)$:

$$(100) \quad c(T^{L,\pm}(n/d)) = c(T(n/d)).$$

We next verify existence of L -corrections.

Lemma 8.1. For every $n/d \in \{p_0, q_0\}$ from Definition 11 or 10. an L -correction exists and has the following properties.

(1) *Rotation invariance:*

$$\begin{aligned} \mathcal{R}^1(T^{L,+}(q_0)) &= T^{L,-}(\mathcal{R}(q_0)) \\ \mathcal{R}^2(T^{L,+}(q_0)) &= T^{L,-}(q_0) \\ \mathcal{R}^3(T^{L,+}(q_0)) &= T^{L,+}(\mathcal{R}(q_0)) \\ \mathcal{R}^4(T^{L,+}(q_0)) &= T^{L,+}(q_0) \end{aligned}$$

(2) *The elongated $T^{L,\pm}(q_0)$ coincides with $T(q_0)$ on two sides*

$$T^{L,\pm}(q_0) \cap T(q_0) \supset \begin{cases} w_h(q_0) \cup w_v(q_0) & 10 \\ w_h(q_0) \cup \mathbf{rev}(w_v(q_0)) & 00 \\ \mathbf{rev}(w_h(q_0)) \cup \mathbf{rev}(w_v(q_0)) & 11 \\ \mathbf{rev}(w_h(q_0)) \cup w_v(q_0) & 01 \end{cases}$$

where the cases on the right are described by (98).

Proof. The stated rotation invariance follows from the decomposition and rotation invariance of standard and alternate tiles. To prove the second claim, we rotate and flip to assume we are in case ‘10’ and $w = w_1 * s * 3^k$ from Definition (11). We then proceed by induction on $k \geq 0$

If $k = 0$, the claim follows by the standard decomposition of $T(q_0)$ and the definition of the L -corection. Indeed, the elongated $T^{L,+}(q_0) \cap T(q_0) \supseteq T(p_1)^{+,1} \cup T(q_1)^+$ which shows $T^{L,\pm}(q_0) \cap T(q_0) \supseteq w_h(q_0)$. For the vertical direction, since $\hat{T}(p_1)$ is a $w_v(p_1)$ -pseudo-square, it agrees with $T(p_1)$ on the vertical boundaries.

Now, suppose $k \geq 1$ is given and let q'_0 be the even child in $\mathbf{q}_{w[1:w|-1]}$. By the inductive hypothesis, the elongated $T^{L,+}(q'_0)$ coincides with $T(q'_0)$ on the bottom and left boundaries. Also, by definition, we may write the elongated correction for q_0 as

$$\begin{aligned} T^{+,L}(q_0) &= T(p_1) \cup (T^{+,L}(q'_0) + 2v_{p_1,1}) \\ &\cup (\hat{T}(p_1) \cup \hat{T}(p_1) + v_{p_1,2}) + (v_{q_1,1} + v_{q_0,1} + v_{q_0,2}). \end{aligned}$$

We can then conclude using the standard decomposition for $T(q_0)$. \square

8.2. Tile odometers. We are now ready to fully define the recursion. Roughly, the full recursion proceeds by taking the weak recursion and filling in the interior. The difficulty occurs whenever there is overlap that is not on a boundary string. Whenever the doubled odometers overlap on a common ancestor or do not overlap at all, the doubled odometers may be taken to be usual standard odometers. Otherwise, the overlap is *corrected* by a pair of complementary, $\pm L$ -corrections.

Definition 12. A weak standard (alternate) tile odometer is a standard (alternate) tile odometer if it is one of the base cases or in the decompositions (86) ((96)), weak subodometers are replaced by respective tile subodometers. Further, depending on the recursion word and parity, each weak doubled subodometer is either two standard tile subodometers or a standard tile subodometer and an odometer which respects an L -correction.

Specifically, let n/d be a child in \mathbf{q}_w and let (p_1, q_1) denote the parent Farey pair. In the standard case, if n/d is odd, then in (86), each doubled term is replaced by

$$d(o)_{q_1}^\pm \rightarrow \begin{cases} o_{q_1}^{\pm,1} \cup o_{q_1}^{\pm,2} & \text{if } w = *\{1 \text{ or } 2\} \\ o_{q_1}^\pm \cup o_{q_1}^{L,\pm} & \text{if } w = *3 \end{cases}$$

where $o_{q_1,\pm i}$ are standard tile odometers for $T(q_1)^{\pm,i}$. In the even-first orientation, $o^\pm(q_1)$ is a tile odometer for $T(q_1)^{+,1}$ or $T(q_1)^{-,2}$ and $o_{q_1}^{L,\pm}$ is a partial odometer with decomposition that respects the L -corrections for $T(q_1)^{-,1}$ or $T(q_1)^{+,2}$. In the odd-first orientation, 1 and 2 are flipped. If n/d is even, the decomposition is defined by rotating the decomposition for $\mathcal{R}(n/d)$.

Similarly, in the alternate case, if n/d is even, then each weak shifted doubled term is replaced in the exact same way as the standard odd case except the L correction is taken to be the elongated L correction. Rotate to complete the definition.

Before proving existence of tile odometers, we prove that L -corrected odometers exist, assuming existence up to a certain depth. An important tool in the remaining proofs will be

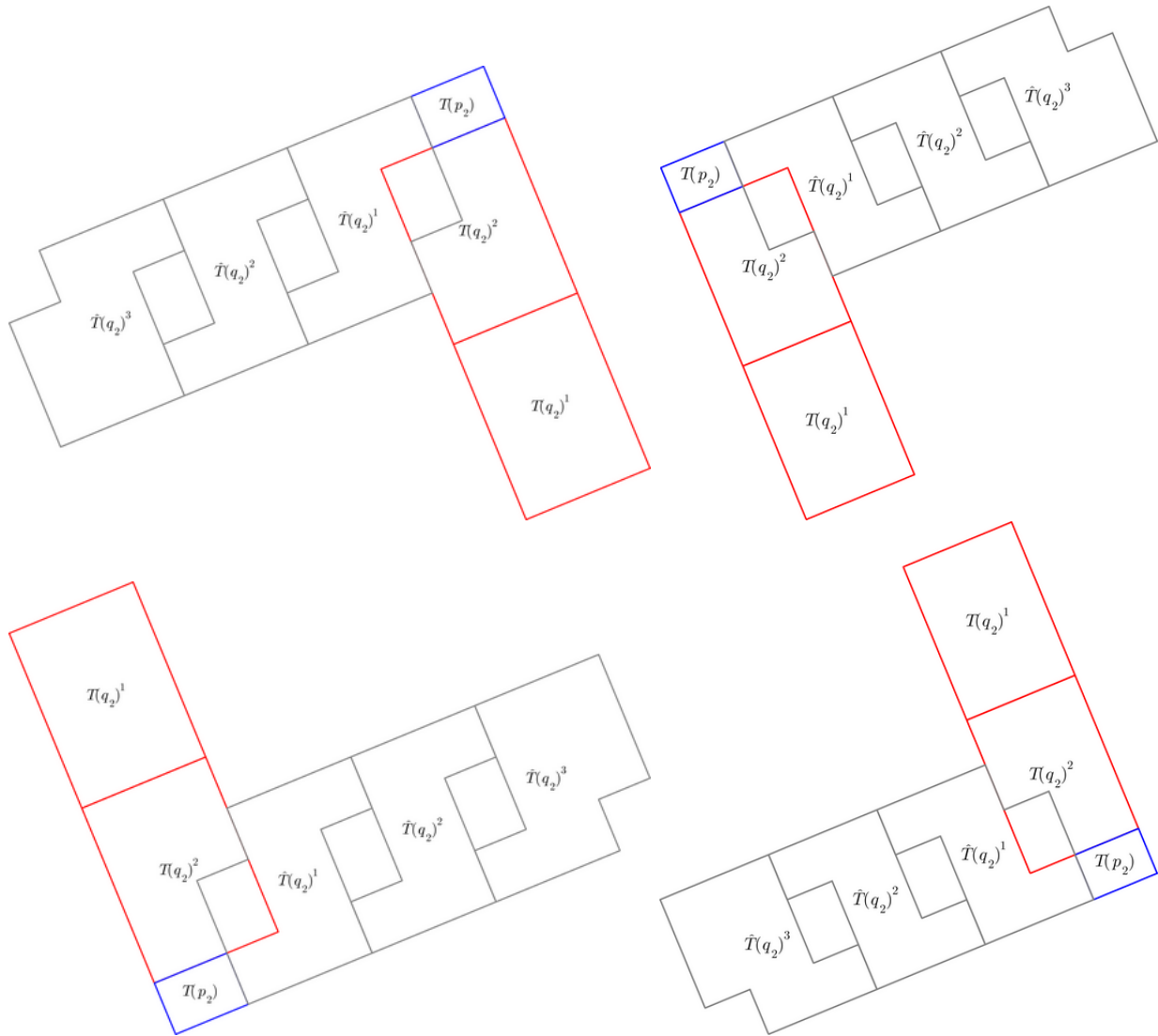


FIGURE 27. The four possible orientations for an odd L -correction as described in Definition 10. From top left to bottom right, 10, 00, 11 then 01.

the *double decomposition*, a decomposition of all or select subtiles in the standard or alternate decomposition. In the figures, grandparent subtiles are indicated with a 2 subscript.

Lemma 8.2. *Suppose tile odometers exist for all $n/d \in \mathcal{T}_m$, for $m \leq m_0$, some $m_0 \geq 1$, then partial odometers which respect the L -correction $\sigma_{n/d}^{L,\pm}$ exist for all $n/d \in \mathcal{T}_{m_0+1}$ and respect the appropriate zero-one boundary string from Lemma 8.1.*

Proof. We show that the L -corrected odometer, $\sigma_{n/d}^{L,\pm}$ exist by showing each pair of overlapping subodometers in the L -correction are compatible. The decomposition of $\sigma_{n/d}^{L,\pm}$ consists of lattice adjacent tile odometers and one of two possible new types of intersection seen in Figure 29. Since we have shown lattice adjacent odometers to be compatible (and that there are no gaps between lattice adjacent odometers), it suffices deal with the new intersection. This can be dealt with by the double decomposition see Figure 30. In particular, in the

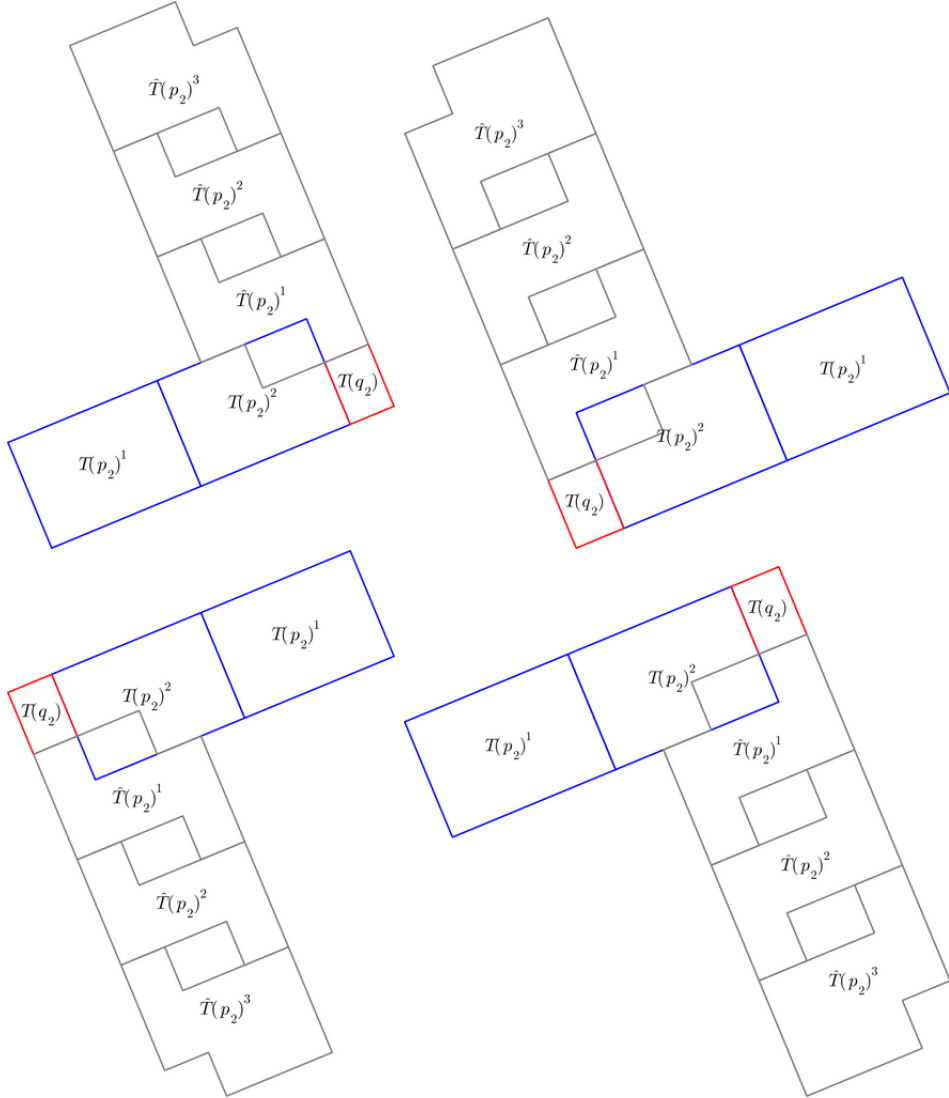


FIGURE 28. The four possible orientations for an even L -correction as described in Definition 11. From top left to bottom right, 10, 00, 11 then 01.

double decomposition, every pair of interfaces between the triple are part of or are a complete stacked zero-one boundary string. In case the triple comes from the base cases, compatibility is a consequence of Proposition 6.1.

To see that $o_{n/d}^{L,\pm}$ coincides with the standard odometer on the appropriate zero-one boundary strings, we induct on $k \geq 0$ from Definitions (11) or (10) as in the proof of Lemma 8.1. \square

We finally prove existence of tile odometers. Figures 31, 32, 33, 34 will be a visual aid throughout the proof.

Lemma 8.3. *Tile odometers exist.*

Proof. We proceed by induction. Start by using Lemma 8.2 to see that tile odometers are indeed weak tile odometers. It remains to verify the internal odometer decomposition is well-defined. That is, we check that each pair of overlapping subodometers is pairwise

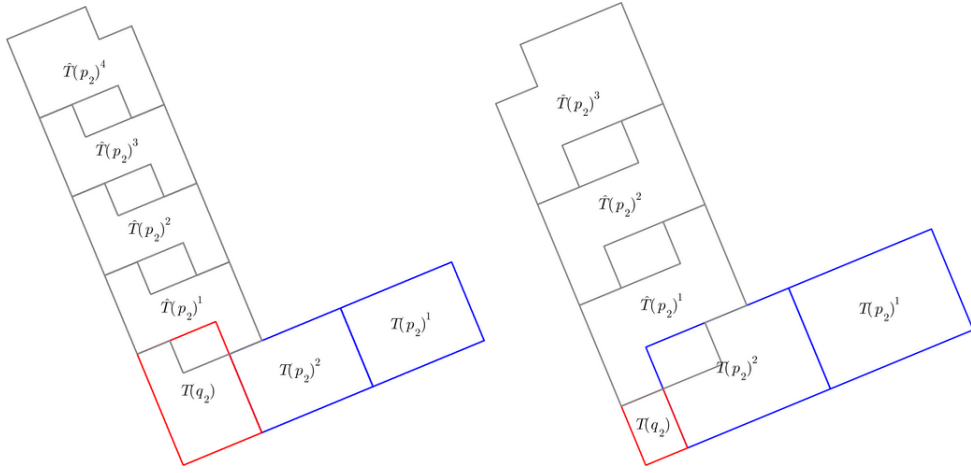


FIGURE 29. The two possible odd-even overlaps for an even L -correction as described in Definition 11: $s = 1$ on the left (elongated) and $s = 2$ on the right.

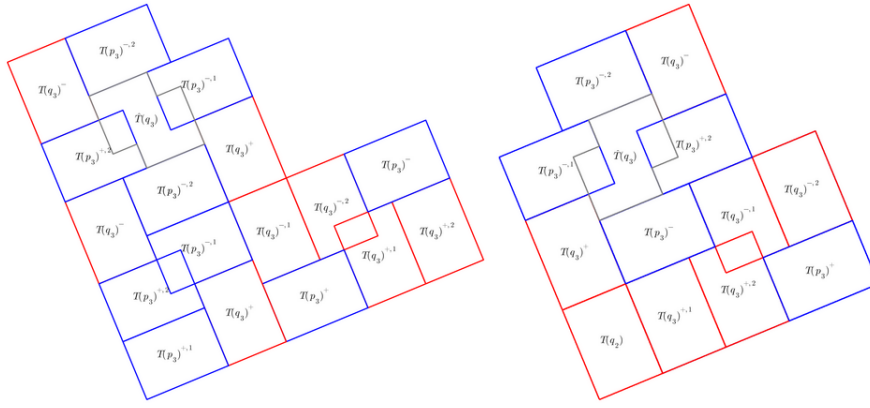


FIGURE 30. Decompositions of the triple $(\hat{T}(p_2)^1, T(q_2), T(p_2)^2)$, in Figure 29: $s = 1$ on the left and $s = 2$ on the right.

consistent. As compatibility is affine invariant, and the decompositions are, up to affine factors, rotationally invariant, it suffices to show compatibility for either n/d or $\mathcal{R}(n/d)$. Let \mathbf{q}_w denote the quadruple for which n/d is a child. We split the remainder of proof into cases. In each case, we use the double decomposition displayed in the indicated Figure to show that the subodometers either overlap on stacked boundary strings or on grandparent tiles. Also, assume the even-first orientation, otherwise flip the subsequent arguments.

*Case 1: Odd standard odometer: $w = * \{1 \text{ or } 2\}$; Figure 31*

The interfaces between every non-overlapping tile consists of stacked zero-one boundary strings therefore those odometers are compatible. If $w = *1$, the tiles $T(q_1)^{+,2}$ and $T(q_1)^{-,1}$ overlap, by the double decomposition, exactly on $T(p_2)^{+,1/2}$, and therefore those subodometers are compatible. Similarly, if $w = *2$, $T(p_1)^-$ and $T(p_1)^+$ overlap on $T(p_2)^{+,1/2}$ and so those subodometers are compatible.

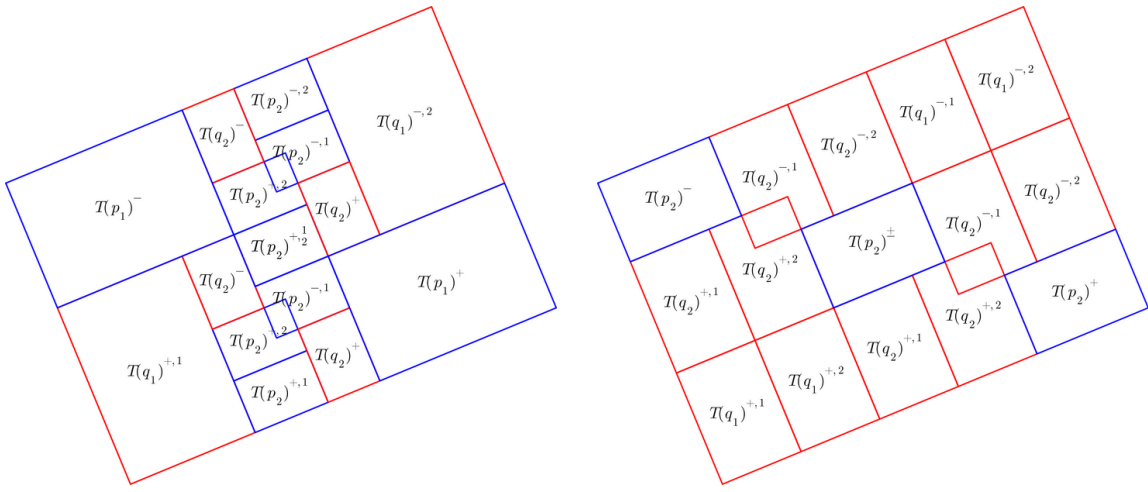


FIGURE 31. Double decomposition of $T(p_0)$ in the even-first orientation for recursion words $w = *1$ and $w = *2$ respectively.



FIGURE 32. Decomposition and then double decomposition of corrected $T(p_0)$ in the even-first orientation. The first row is $w = *13$ and the second is $w = *23$

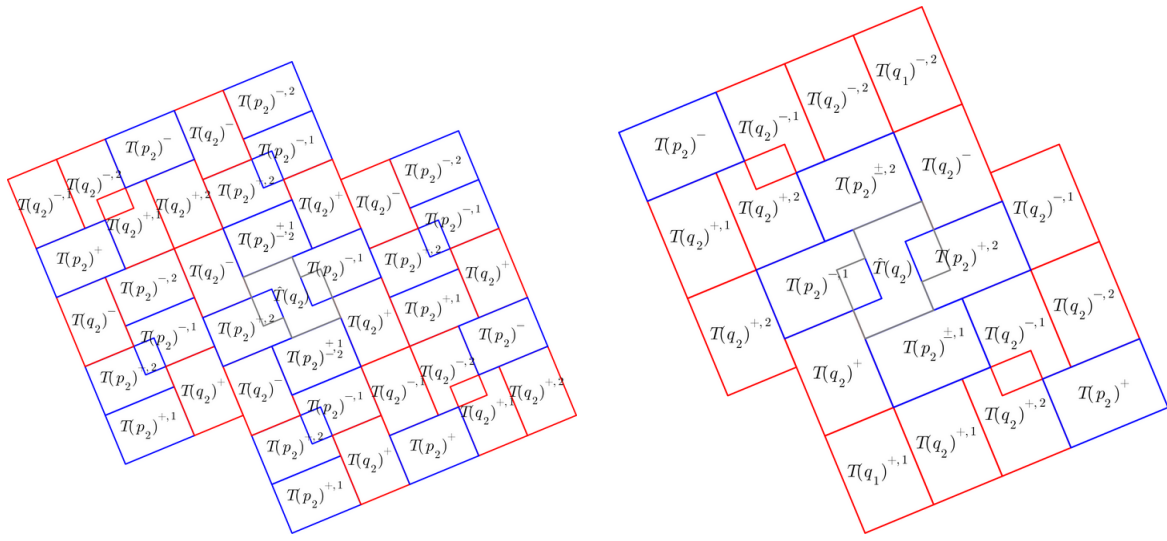


FIGURE 33. Double decomposition of $\hat{T}(q_0)$ in the even-first orientation for recursion words $w = *1$ and $w = *2$ respectively.

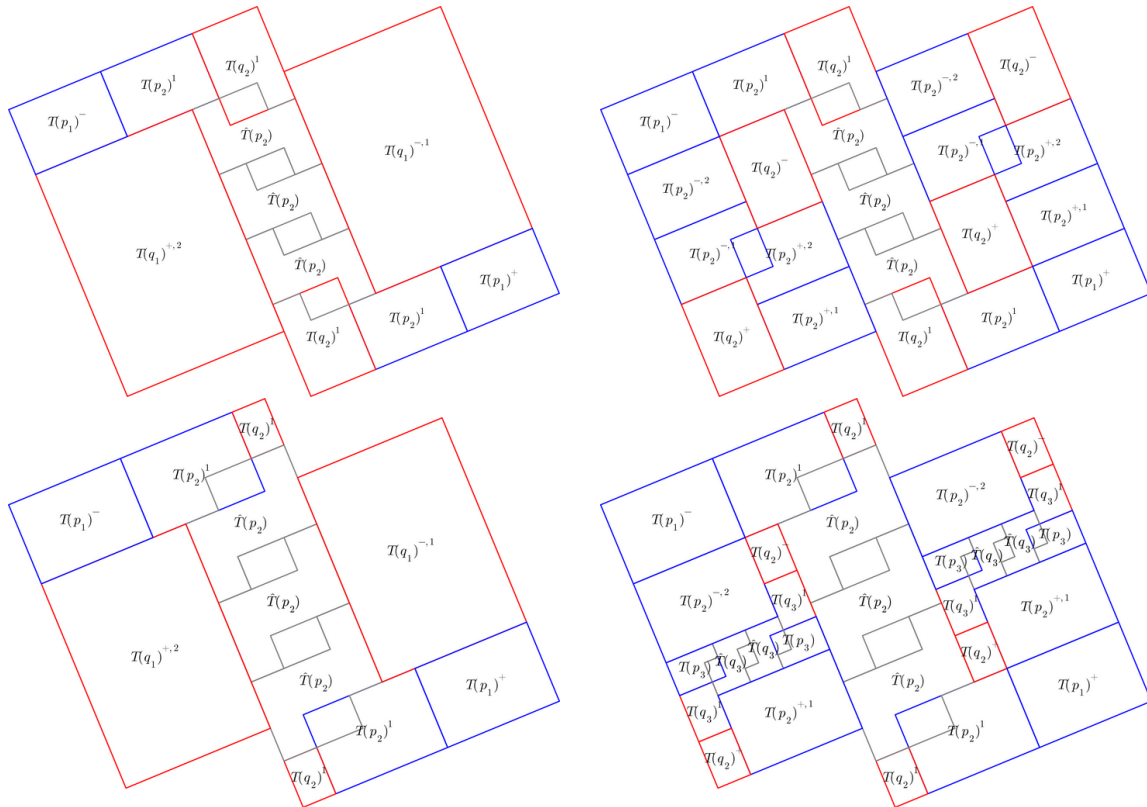


FIGURE 34. Decomposition and then double decomposition of corrected $\hat{T}(q_0)$ in the even-first orientation. The first row is $w = *13$ and the second is $w = *23$

*Case 2: Odd standard odometer: $w = *3$; Figure 32*

In this case, due to the L -correction, the only overlap is that of lattice adjacent $\hat{T}(p_2)$ (subsubtile). The rest of the interfaces are part of or is a stacked zero-one boundary string. By previous arguments, the $(T(q_1)^{+,1}, T(p_1)^{-})$ and $T(q_1)^{-,2}$ interfaces are parts of stacked boundary strings. The interface between $T(p_1)^{\pm}$ and $T^{L,\pm}(q_1)$ corresponds to a full stacked vertical boundary string (lattice adjacent standard tile $T(p_1)$).

It remains to analyze the interface between $T^{L,\pm}(q_1)$ and $T(q_1)^{+,1}, T(q_1)^{-,2}$. By Lemma 8.2 $(T^{L,+}(q_1), T(q_1)^{+,1})$ each intersect on a $w_v(q_1)$ stacked boundary string. By induction on k in the recursion word for the L correction, similar to the proof of Lemma 8.2, the interface between $(T^{L,+}(q_1), T(q_1)^{-,2})$ and $(T^{L,-}(q_1), T(q_1)^{+,1})$ consists of a sequence of lattice adjacent standard odometers for $T(p_1)^+$ followed by a (q_2, p_2) interface which is an almost palindrome by the word Lemma.

*Case 3: Even alternate odometer: $w = *\{1 \text{ or } 2\}$; Figure 33*

The overlap argument is similar to Case 1. If $w = *1$, $T(q_1)^{+,1}$ and $T(q_1)^{-,2}$ overlap $\hat{T}(p_1)$ on $T(p_2)^{\pm,1/2}$. The interfaces between $(T(p_1)^+, T(q_1)^{-,1})$, $(T(p_1)^-, T(q_1)^{+,2})$, $(T(p_1)^+, T(q_1)^{+,1})$, $(T(p_1)^-, T(q_1)^{-,2})$ are part of stacked zero-one boundary strings by the same argument as given previously in the weak standard case.

The new interfaces are $(T(q_1)^{\pm,1}, T(q_1)^{\pm,2}, \hat{T}(p_1))$ and $(T(p_1) \cdot \hat{T}(p_1))$. In the latter case, by the double decomposition, $(T(p_1) \cdot \hat{T}(p_1))$ intersect on the boundary of lattice adjacent standard tile odometers for $T(q_2)$. In the former case, the interface between $(T(q_1)^{+,1}, T(q_1)^{+,2}, \hat{T}(p_1))$ is part of a stacked vertical zero-one boundary string. Indeed, augment the vertical boundary string of $T(q_1)^{+,2}$ by adding $w_v(p_1)$ to the start. Then, since $\hat{T}(p_1)$ is a $w_v(p_1)$ pseudo-square, the augmented interface is exactly $w_v(p_1) \cup w_v(q_1)$ and $\text{rev}(w_v(q_1)) \cup \text{rev}(w_v(p_1))$. This is exactly stacked boundary string for p_0 and therefore, the odometer there is compatible. The argument for $w = *2$ is identical.

*Case 4: Even alternate odometer: $w = *3$; Figure 34*

This is almost identical to Case 2. The only difference is in the overlaps $(T^{L,+}(q_1), T(q_1)^{+,2})$ and $(T^{L,-}(q_1), T(q_1)^{-,1})$. In this case, we need to augment the vertical boundary strings as in Case 3 for $T(q_1)$. Once augmented, those interfaces then become exactly stacked vertical boundary string for p_0 .

□

9. GLOBAL ODOMETERS

We now observe that both weak and alternate tile odometers can be extended to global odometers with the correct growth.

Lemma 9.1. *For every reduced fraction $0 < n/d < 1$, there are two functions, g, \hat{g} on \mathbb{Z}^2 whose restriction to a standard or alternate tile are alternate and standard tile odometers for which the periodicity condition 9 holds and for which*

$$(101) \quad x \rightarrow f(x) - \frac{1}{2}x^t M(n, d)x - b \cdot x$$

is $L'(n/d)$ -periodic for some $b \in \mathbb{R}^2$, for each $f \in \{g, \hat{g}\}$.

Proof. Given that we have proved standard and alternate tile odometers which are lattice adjacent are compatible, the proof is identical to Lemma 10.1 in [LPS16]. □

It remains to check that the functions which we have constructed are recurrent.

Lemma 9.2. *For each $0 < n/d < 1$, g and \hat{g} are recurrent.*

Proof. Let $s, \hat{s} = \Delta g, \Delta \hat{g}$. Depending on whether the distant ancestor is 2^k or 3^k , slide a vertical or horizontal plane till it touches the configuration then use the Lemma 6.12. \square

REFERENCES

- [BN91] Daniele Beauquier and Maurice Nivat. On translating one polyomino to tile the plane. *Discrete & Computational Geometry*, 6(4):575–592, 1991.
- [BTW87] Per Bak, Chao Tang, and Kurt Wiesenfeld. Self-organized criticality: An explanation of the 1/f noise. *Physical review letters*, 59(4):381, 1987.
- [CP18] Scott Corry and David Perkinson. *Divisors and sandpiles*, volume 114. American Mathematical Soc., 2018.
- [CPS08] Sergio Caracciolo, Guglielmo Paoletti, and Andrea Sportiello. Explicit characterization of the identity configuration in an abelian sandpile model. *Journal of physics A: mathematical and theoretical*, 41(49):495003, 2008.
- [Dha90] Deepak Dhar. Self-organized critical state of sandpile automaton models. *Physical Review Letters*, 64(14):1613–1616, 1990.
- [DS10] Deepak Dhar and Tridib Sadhu. Pattern formation in growing sandpiles with multiple sources or sinks. *Journal of Statistical Physics*, 138(4-5):815–837, 2010.
- [DS11] Deepak Dhar and Tridib Sadhu. The effect of noise on patterns formed by growing sandpiles. *Journal of Statistical Mechanics: Theory and Experiment*, 2011(03):P03001, 2011.
- [DS13] Deepak Dhar and Tridib Sadhu. A sandpile model for proportionate growth. *Journal of Statistical Mechanics: Theory and Experiment*, 2013(11):P11006, 2013.
- [DSC09] Deepak Dhar, Tridib Sadhu, and Samarth Chandra. Pattern formation in growing sandpiles. *EPL (Europhysics Letters)*, 85(4):48002, 2009.
- [GLM⁺05] Ronald L Graham, Jeffrey C Lagarias, Colin L Mallows, Allan R Wilks, and Catherine H Yan. Apollonian circle packings: geometry and group theory i. the apollonian group. *Discrete & Computational Geometry*, 34(4):547–585, 2005.
- [HLM⁺08] Alexander E Holroyd, Lionel Levine, Karola Mészáros, Yuyal Peres, James Propp, and David B Wilson. Chip-firing and rotor-routing on directed graphs. In *In and out of equilibrium 2*, pages 331–364. Springer, 2008.
- [Jár18] Antal A Jarai. Sandpile models. *Probability surveys*, 15:243–306, 2018.
- [KK21] Michael Kapovich and Alex Kontorovich. On superintegral kleinian sphere packings, bugs, and arithmetic groups. *arXiv preprint arXiv:2104.13838*, 2021.
- [Kli18] Caroline J Klivans. *The mathematics of chip-firing*. CRC Press, 2018.
- [LBR02] Yvan Le Borgne and Dominique Rossin. On the identity of the sandpile group. *Discrete mathematics*, 256(3):775–790, 2002.
- [LKG90] SH Liu, Theodore Kaplan, and LJ Gray. Geometry and dynamics of deterministic sand piles. *Physical Review A*, 42(6):3207, 1990.
- [LP10] Lionel Levine and James Propp. What is... a sandpile. In *Notices Amer. Math. Soc*, 2010.
- [LPS16] Lionel Levine, Wesley Pegden, and Charles K Smart. Apollonian structure in the abelian sandpile. *Geometric and Functional Analysis*, 26(1):306–336, 2016.
- [LPS17] Lionel Levine, Wesley Pegden, and Charles K Smart. The apollonian structure of integer superharmonic matrices. *Annals of Mathematics*, pages 1–67, 2017.
- [Mel20] Andrew Melchionna. The sandpile identity element on an ellipse. *arXiv preprint arXiv:2007.05792*, 2020.
- [Ost03] Srdjan Ostojic. Patterns formed by addition of grains to only one site of an abelian sandpile. *Physica A: Statistical Mechanics and its Applications*, 318(1-2):187–199, 2003.
- [Pao12] Guglielmo Paoletti. Deterministic abelian sandpile models and patterns. 2012.
- [Peg] Wesley Pegden. Sandpile galleries. <http://www.math.cmu.edu/~wes/sandgallery.html>.

- [PS13] Wesley Pegden and Charles Smart. Convergence of the abelian sandpile. *Duke mathematical journal*, 162(4):627–642, 2013.
- [PS20] Wesley Pegden and Charles K Smart. Stability of patterns in the abelian sandpile. In *Annales Henri Poincaré*, volume 21, pages 1383–1399. Springer, 2020.
- [Red05] Frank Redig. Mathematical aspects of the abelian sandpile model. *Les Houches lecture notes*, 83:657–659, 2005.
- [Sma13] Charles K Smart. Aim chip firing 2013: The f -lattice. 2013. <https://www.aimath.org/WWN/chipfiring/flattice.pdf>.
- [Tan96] Lin Tan. The group of rational points on the unit circle. *Mathematics Magazine*, 69(3):163–171, 1996.